Boson stars efficiently nucleate vacuum phase transitions
by Thomas John Brueckner

A thesis submitted in partial fulfillment of the requirements for the degree of Doctor of Philosophy in Physics
Montana State University

Abstract:
In the hot dense early universe, first order phase transitions were possible through the tunnelling of a scalar field. When studying the formation of true vacuum bubbles in the semi-classical approximation, the tunnelling rate depends primarily on the Euclidean action of the bubble configuration. Others have shown that bubble nucleation by compact objects (neutron stars, black holes) proceeds more rapidly than in Coleman's process of bubble formation in empty space. In this paper, I consider nucleation by another kind of astrophysical object, a boson star, the ground state of a self-gravitating scalar field. I model a boson star in a self-interacting potential that also has a term cubic in the scalar field, the so-called 2-3-4 potential. In the limiting case of a "small" star nucleating a "large" bubble, I compare its Euclidean action, S_E^{Bubble} to the empty space bubble action of Coleman, $S_E^{Coleman}$, and I find that the action ratio $S_E^{Bubble}/S_E^{Coleman}$ decreases significantly from unity as the energy difference between the vacua increases. This decrease from unity enhances the nucleation rate.

BOSON STARS EFFICIENTLY NUCLEATE VACUUM PHASE TRANSITIONS

by

Thomas John Brueckner

A thesis submitted in partial fulfillment
of the requirements for the degree

of

Doctor of Philosophy

in

Physics

MONTANA STATE UNIVERSITY-BOZEMAN
Bozeman, Montana

April 1997

APPROVAL

of a thesis submitted by

Thomas John Brueckner

This thesis has been read by each member of the thesis committee and has been found to be satisfactory regarding content, English usage, format, citations, bibliographic style, and consistency, and is ready for submission to the College of Graduate Studies.

William A. Hiscock _____ (Signature) April 15, 1997 (Date)

Approved for the Department of Physics

John C. Hermanson _____ (Signature) 4-15-97 (Date)

Approved for the College of Graduate Studies

Robert Brown _____ (Signature) 5/8/97 (Date)

STATEMENT OF PERMISSION TO USE

In presenting this thesis, in partial fulfillment of the requirements for a doctoral degree at Montana State University-Bozeman, I agree that the Library shall make it available to borrowers under the rules of the Library. I further agree that copying of this thesis is allowable only for scholarly purposes, consistent with "fair use" as prescribed in the U.S. Copyright Law. Requests for extensive copying or reproduction of this thesis should be referred to University Microfilms International, 300 North Zeeb Road, Ann Arbor, Michigan 48106, to whom I have granted "the exclusive right to reproduce and distribute my dissertation in and from microform along with the non-exclusive right to reproduce and distribute my abstract in any format in whole or in part."

Signature Thomas J. Brueckner

Date May 6, 1997

TABLE OF CONTENTS

LIST OF TABLES

LIST OF FIGURES

LIST OF FIGURES (continued)

Abstract

In the hot dense early universe, first order phase transitions were possible through the tunnelling of a scalar field. When studying the formation of true vacuum bubbles in the semi-classical approximation, the tunnelling rate depends primarily on the Euclidean action of the bubble configuration. Others have shown that bubble nucleation by compact objects (neutron stars, black holes) proceeds more rapidly than in Coleman's process of bubble formation in empty space. In this paper, I consider nucleation by another kind of astrophysical object, a boson star, the ground state of a self-gravitating scalar field. I model a boson star in a self-interacting potential that also has a term cubic in the scalar field, the so-called 2-3-4 potential. In the limiting case of a "small" star nucleating a "large" bubble, I compare its Euclidean action, S_E^{Bubble}, to the empty space bubble action of Coleman, $S_E^{Coleman}$, and I find that the action ratio $S_E^{Bubble}/S_E^{Coleman}$ decreases significantly from unity as the energy difference between the vacua increases. This decrease from unity enhances the nucleation rate.

CHAPTER 1

WHY SHOULD ONE STUDY BOSON STARS AS SEEDS FOR VACUUM PHASE TRANSITIONS?

In the beginning, the universe was hot and dense, and a variety of unusual processes and objects existed. One of the more unusual processes is that of a first order vacuum phase transition in a quantum field. Of particular interest is the theory of a scalar field that undergoes a vacuum phase transition, since the scalar Higgs field is a crucial part of larger theories, like electroweak theory, that unify some of the fundamental forces of nature.

In the early universe's menagerie of exotic objects are boson stars, a self-gravitating configuration of a quantum field. Each boson in the star is in the same quantum state. These stars, prevented from collapsing by the Heisenberg uncertainty principle, can range in mass from a few thousand kilograms up to astrophysical size, depending upon the boson's mass. Some scientists view bosonic matter as a possible part of the dark matter content of the universe.

It is logical to ask whether boson stars affect first order phase transitions in the scalar field. The most basic model of a first order vacuum phase transition is one in which a region of empty spacetime spontaneously changes

phase,[1] much like drops of rain form spontaneously in a pure water vapor. This region of the new phase is called a vacuum bubble. The scalar field, which I shall call φ, tunnels from its initial state at a local minimum of the potential, through the barrier in the potential $V(\varphi)$, to the true vacuum at the global minimum. Figure 1 shows the tunnelling process for spontaneous bubble formation in empty space.

A second process, induced nucleation, can also generate first order phase transitions. Induced nucleation is like the mundane process of using silver iodide crystals to seed clouds and form precipitation over arid regions of land. Using a boson star to seed a phase transition has a notable advantage over the spontaneous formation process. The boson star is a configuration of the scalar field, $\varphi(r)$, that starts out with a positive central value, $\varphi(0) > 0$. The field in the ground state decreases gradually in size as it extends out from the center of the star, asymptotically approaching zero as radial distance r approaches infinity. In terms of the potential in figure 1, the central value of the star is high up on the "bump" in the potential. According to quantum theory, the barrier is more easily penetrable when the initial value of φ is high up on the potential barrier. It is therefore reasonable to conjecture that, in comparison to spontaneous bubble formation in empty space, a

---

[1]S. Coleman, "Fate of the false vacuum: Semiclassical theory," Physical Review D, 15, 2929 (1977).

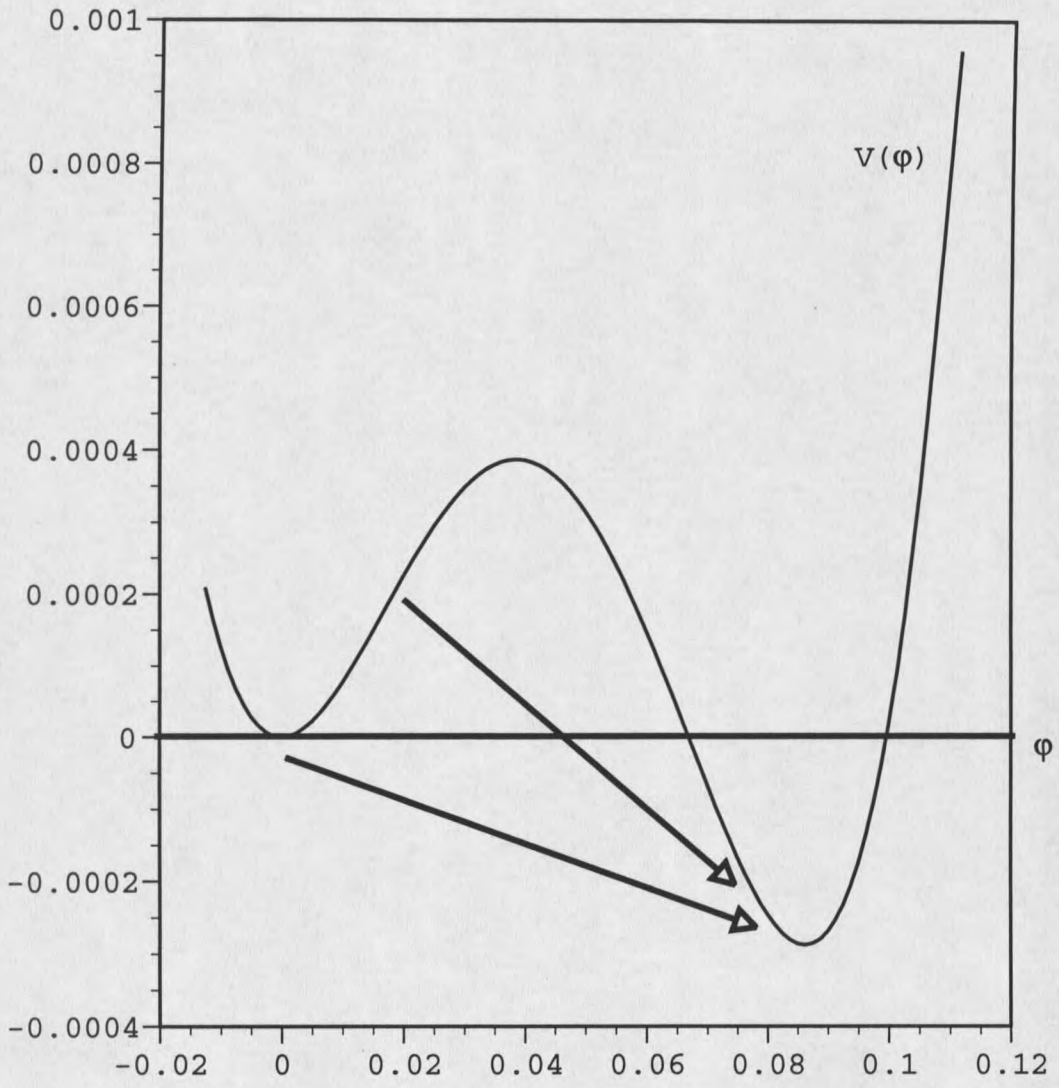

Figure 1. Tunnelling events for first order vacuum phase transitions. The lower arrow shows the tunnelling event corresponding to spontaneous formation of vacuum bubbles in empty space. The upper arrow shows the tunnelling event for a first order phase transition that a boson star has nucleated. The potential barrier is more easily penetrated in the latter case.

boson star might more readily initiate a tunnelling event in the vacuum field. The verification of that conjecture is the subject of this thesis. I compared the two processes, and I found that a boson star has a significantly greater efficiency at nucleating first order phase transitions in the case of a small star nucleating a large bubble of the new phase.

I shall provide greater detail on what makes a boson star small in relation to a large bubble, how to construct a model boson star, and other aspects of this nucleation process. Specifically, in chapter 2, I will discuss the time evolution of the temperature of the universe in the Robertson-Walker cosmological model. Also, I will discuss the temperature dependence of effective potentials that allow vacuum phase transitions. In chapter 3, I review some of the foundational concepts of boson stars, and I discuss the calculation of boson star models for later use in the bubble nucleation process. In chapter 4, I review the theory of spontaneous formation of vacuum bubbles, and I introduce the "small star-large bubble" limit. I discuss the details of the calculation of a nucleation rate, and I conclude chapter 4 with results confirming that boson stars are quite efficient at nucleating phase transitions. The thesis ends with a brief chapter 5 in which I discuss the prospects for future work.

CHAPTER 2

WHAT WAS THE EARLY UNIVERSE LIKE?

The Early Universe Was Hot and Dense.

The early universe was hot and dense in comparison to the present.[1] This idea has convincing observational support, principally in the observation of nearly perfect isotropy of the remnant 2.7 K cosmic background radiation. To understand the significance of the cosmic background radiation (CBR), one needs to examine the big bang theory of the early universe. In 1948, George Gamow, Ralph Alpher and Robert Herman constructed a big bang model to study nucleo-synthesis. They envisioned a cosmic fireball of neutrons that cooled adiabatically and eventually synthesized the lighter nuclei hydrogen, helium, lithium, beryllium, and boron. This nuclear "soup," consisting of a hot, dense neutron gas,[2] that filled the universe was in thermal equilibrium with all the radiation. Eventually, though, the nuclear soup cooled enough that the individual nuclei began to capture and hold their ration of electrons. When this

[1]The discussions in this section are due mainly to P.J.E. Peebles, Principles of Physical Cosmology (Princeton University Press, Princeton, 1993) and to R.M. Wald, General Relativity (University of Chicago Press, Chicago, 1984.

[2]G. Gamow, "The Evolution of the Universe," Nature, 162, 680 (1948).

happened, the density of free electrons, which had hitherto efficiently scattered radiation, decreased dramatically. Scattering of radiation became less frequent, and thermal equilibrium broke down. The radiation began to stream freely, without further significant interaction with the matter. This decoupling of matter and radiation occurred over a period of time, not all at one instant, but one refers to this period as the "decoupling time." One may also say that, at decoupling, the universe became transparent. The light then was mainly in the visible and near infrared, with a blackbody spectrum at a temperature of a few thousand Kelvins. Alpher and Herman predicted[3] in 1948 that the radiation, like a gas of photons in an enclosed space, should have expanded with the universe and cooled to a temperature today of roughly 5 K. After 1948, other scientists in Britain, the US and the Soviet Union refined the estimate of the present temperature of the CBR. In 1965 Arno Penzias and Robert Wilson discovered an isotropic source of "excess antenna temperature" of approximately 3.5 K.[4] Robert Dicke, P.J.E. Peebles and their collaborators gave the immediate

---

[3]R.A. Alpher and R. Herman, "Evolution of the Universe," Nature, 162, 774 (1948).

[4]A.A. Penzias and R.W. Wilson, "A Measurement of Excess Antenna Temperature at 4080 Mc/s," Astrophysical Journal, 142, 419 (1965).

interpretation[5] that this "excess antenna temperature" was actually the red-shifted primordial radiation that Gamow and his collaborators had predicted 17 years earlier. This discovery implied the hot, dense nature of the big bang:

> "A temperature in excess of 10^{10} °K during the highly contracted phase of the universe is strongly implied by a present temperature of 3.5°K for blackbody radiation....If the cosmological solution has a singularity, the temperature would rise much higher than 10^{10} °K in approaching the singularity."[6]

Since 1965, very fine measurements[7] of the cosmic background radiation have yielded a temperature $T = 2.736 \pm 0.017$°K. These observations have fully vindicated the prediction of Gamow and his collaborators.

Gamow built his big bang theory of nucleosynthesis upon the theory of the expanding universe. I shall now review the calculation of the scale, density, and temperature in the early universe based upon the Robertson-Walker model of an expanding universe.

---

[5]R.H. Dicke, et al., "Cosmic Black-body Radiation," Astrophysical Journal, 142, 414 (1965).

[6]Ibid.

[7]Peebles, Physical Cosmology, 131.

Most cosmological models assume that the universe is homogeneous and isotropic -- the so-called cosmological principle. This assumption is a reasonable one, for astronomical observations, especially of the CBR, record a homogeneous and isotropic distribution of radiation and matter in the universe.[8]

In the Robertson-Walker model, one envisions the four dimensional spacetime manifold as a foliation of spacelike hypersurfaces. A parameter, t, labels each spacelike hypersurface of the foliation. The 3-geometry of each hypersurface is homogeneous and isotropic.

Each isotropic observer in the spatial leaf moves upon a world line that is orthogonal to each leaf. This allows one to call t the proper time that an isotropic observer would measure. It also allows one to synchronize all clocks on each spatial leaf.

The imposition of isotropy forces the geometry of each leaf to be that of a space of constant curvature. Such homogeneous spaces are of three kinds: spherical, flat, and hyperbolic. It is customary to refer to the former as a "closed" space-time, to the latter as an "open" spacetime.

To get an intuitive grasp of how spherical and hyperbolic geometries compare to flat space, one might examine a circle. In a spherical geometry, the circumference of a

---

[8]One must understand this homogeneity and isotropy to be evident on some suitably large scale, certainly larger than galactic.

circle is less than $2\pi r$. One can understand this by considering this circle and its radii to be confined to the surface of an ordinary sphere. In a flat geometry, the circumference is exactly $2\pi r$. In a hyperbolic geometry, the circumference is more than $2\pi r$. One can understand this by considering the circle and its radii to be confined to the surface of a saddle of hyperboloidal shape.

Physically, one can say that a closed spacetime contains matter which is dense enough to close the universe back on itself. The open and flat spacetimes have sparse matter density, so that they do not close back in on themselves.

The assumptions of homogeneity and isotropy yield significant simplifications of the metric. The metric on a four dimensional manifold will in general have ten arbitrary functions of the four-dimensional position. The assumption of homogeneity implies the presence of an isometry, spatial translation, at each point on the manifold. The further assumption of isotropy implies another isometry, spatial rotations. In addition, the isometries reduce the number of independent functions from ten down to only one function, $a(t)$. The most convenient form of the Robertson-Walker line element is

$$ds^2 = -dt^2 + d\ell^2 \ ,$$

with

$$d\ell^2 = a(t)^2 \begin{cases} d\psi^2 + \sin^2\psi\left(d\theta^2 + \sin^2\theta\, d\phi^2\right) & \text{(closed)} \\ d\psi^2 + \psi^2\left(d\theta^2 + \sin^2\theta\, d\phi^2\right) & \text{(flat)} \\ d\psi^2 + \sinh^2\psi\left(d\theta^2 + \sin^2\theta\, d\phi^2\right) & \text{(open)} \end{cases} . \qquad (2.1)$$

In this metric,[9] the function a(t) is the cosmic scale parameter; in the case of a closed spacetime, one interprets it as the size of the universe. For example, if two galaxies are a proper distance L_0 apart at present, then at some earlier time t, they were a distance $L_0 \cdot a(t)$ apart, setting the present value of the scale factor to unity for convenience. Therefore, it is imperative to know the behavior of a(t) over time: does it get smaller or larger with time?

In order to determine the behavior of a(t), one must solve the Einstein field equations for these metrics. In general, the Einstein field equations relate the distribution and motion of matter and radiation to the geometry of the spacetime. One uses a stress-energy tensor, T_{ab}, to mathematically represent the matter and radiation. The Einstein tensor, G_{ab}, represents the curvature of the spacetime. These two tensors form the Einstein equations:

$$G_{ab} = 8\pi T_{ab} . \qquad (2.2)$$

---

[9]Throughout most of this thesis, I use natural units: c = 1, G = 1, k_B = 1 and h = 1. I employ a metric signature -+++ and follow the sign conventions of C.W. Misner, K.S. Thorne, and J.A. Wheeler, Gravitation (San Francisco: Freeman, 1973). I use abstract index notation; cf. R.M. Wald, General Relativity, 24.

The matter of the universe, on the cosmic scale, at least, is described by the stress-energy tensor of a perfect fluid.

$$T_{ab} = \rho\, u_a u_b + (\rho + P) g_{ab} \ . \qquad (2.3)$$

The metric tensor of the spacetime is g_{ab}. In fact, the stress-energy tensor of a perfect fluid is the most general form compatible with the homogeneity and isotropy of the Robertson-Walker model. The quantity ρ de-notes the energy density of the fluid, P denotes its pressure, and u^a is the fluid's four-velocity. Focussing on only the matter, one approximates it as "dust," with P = 0, while for radiation, ρ = P/3.

To understand the evolution of the scale factor, a(t), and the density, ρ, one must solve the Einstein field equations. The two equations relating a(t) with ρ and P are

$$\frac{3\dot{a}^2}{a^2} = 8\pi\rho - \frac{3k}{a^2} \ , \qquad (2.4)$$

$$\frac{3\ddot{a}}{a} = -4\pi(\rho + 3p) \ . \qquad (2.5)$$

Overdots denote differentiation with respect to time; k = +1 for closed geometry, k = 0 for flat geometry, and k = -1 for open geometry.

The first mathematical implication one can draw from

these equations is that a(t) is not constant. When ρ and P have realistic values $\rho > 0$ and $P \geq 0$, the second time derivative of a(t), its "acceleration," will be negative. This in turn shows that the universe *must* be either expanding or contracting. Indeed, astronomers beginning with Edwin Hubble have observed[10] that the universe is everywhere expanding. Hubble's famous law, V = HD, relates the recessional velocity, V, of a galaxy to its distance, D, with a constant of proportionality H. Since speed is distance divided by time, one may state that the H is the inverse of some time interval, H = 1/T. One can interpret T as the total expansion time, which should be an estimate of the age of the universe. By convention, H is called the Hubble constant, and T is called the Hubble time.

It is now important to return to the earlier example of the distance between two galaxies, $L(t) = L_0 \cdot a(t)$. Differentiation with respect to time gives

$$\dot{L} = L_0 \cdot \dot{a} \text{ and } L_0 = \frac{L(t)}{a(t)} \Rightarrow \dot{L} = \left[\frac{\dot{a}(t)}{a(t)}\right] \cdot L(t) \ . \qquad (2.6)$$

Now, if one dubs the quantity in brackets as H, one has the essential form of the Hubble law, $V = H \cdot D$, except that, in general, H can be a function of time, i.e., H(t). Thus 1/H

---

[10]E.P. Hubble, "A Relation between Radial Distance and Velocity among Extra-Galactic Nebulae," Proceedings of the National Academy of Sciences, 15, 168 (1929).

is not really the exact age of the universe. Moreover, if one assumes that the universe has been expanding such that its "acceleration" has always been negative, as shown in figure 2, then the Hubble "constant" was larger in the past. Thus, the Hubble time can overestimate the age of an expanding universe.

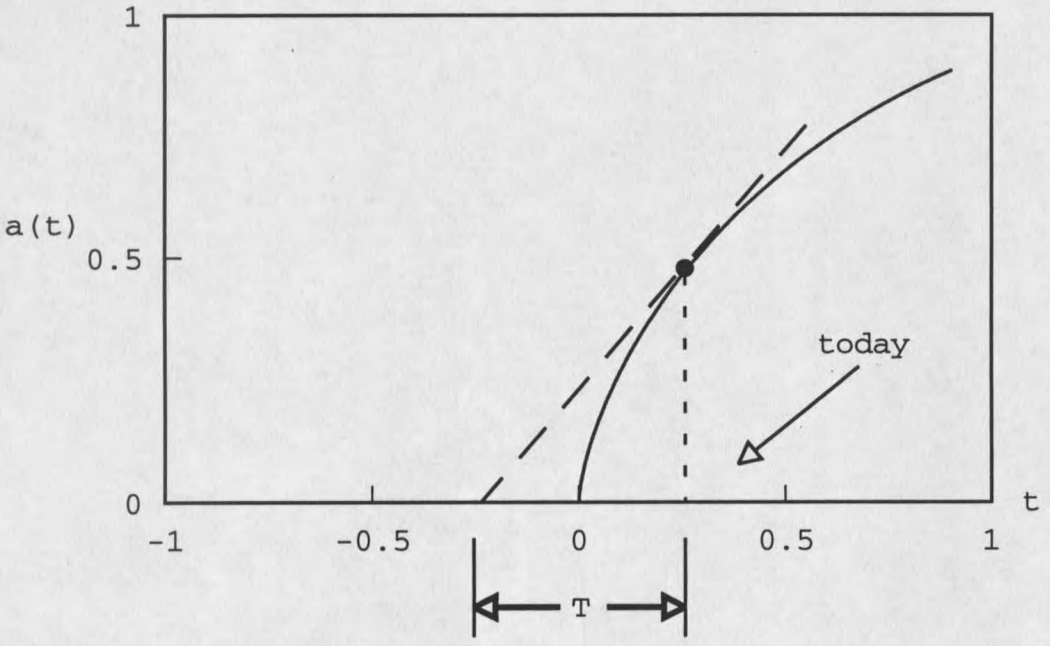

Figure 2. Sample solution for a(t) showing overestimation of the present age of the universe. The diagonal dotted line shows the overestimating effect of extrapolating Hubble's law back in time.

Was the scale factor zero at t = 0? To get an answer, one must combine the two Einstein field equations. With an

algebraic combination of the two equations --

$$\dot{\rho} + 3(\rho + P)\frac{\dot{a}}{a} = 0 \qquad (2.7)$$

-- one can form a pair of conserved quantities. For the galactic "dust" of matter, P = 0, hence

$$\partial_t\left(\rho_{matter}\, a^3\right) = 0 \ . \qquad (2.8)$$

The quantity ρa^3 is a constant. Thus the density of matter varies as the inverse cube of the scale factor:

$$\rho_{matter} \sim \frac{1}{a^3} \ . \qquad (2.9)$$

For radiation, $P = \rho/3$, so

$$\partial_t\left(\rho_{rad}\, a^4\right) = 0 \ . \qquad (2.10)$$

The quantity $\rho \cdot a^4$ is a constant over time. Therefore the density of radiation energy varies with the inverse fourth power of the scale factor.

$$\rho_{rad} \sim \frac{1}{a^4} \ . \qquad (2.11)$$

In the Robertson-Walker model containing both matter and radiation, for sufficiently small values of the scale factor, the energy density of radiation will be larger than the energy density of matter. Later, as a(t) increases, the energy density of matter will approach and eventually exceed the energy density of radiation.

During the radiation-dominated period one can determine the behavior of a(t). Multiplying (2.4) by a^4 and replacing the quantity $\rho \cdot a^4$ with a constant of integration C, one obtains a nonlinear differential equation for a(t):

$$\dot{a}^2 - \frac{\left(\frac{8\pi C}{3}\right)}{a^2} + 3k = 0 \ . \qquad (2.12)$$

It is easy to determine the behavior of a(t) when a(t) becomes relatively small. Specifically, when $a^2 << 8\pi C/9|k|$, the differential equation becomes

$$\dot{a}^2 - \frac{\left(\frac{8\pi C}{3}\right)}{a^2} \approx 0 \ . \qquad (2.13)$$

The approximate solution for small a(t) is $a(t) \doteq A_0 t^{1/2}$, with A_0 being a constant that incorporates the previous constant C. This thime dependence shows that at some finite time in the past, the scale factor a(t) was tending toward zero as the

square root of the time.[11] The energy density of the radiation, proportional to the inverse fourth power of the scale factor, must have been correspondingly large.

To show that the early universe was very hot, it is sufficient to state that for a radiation gas, ρ is proportional to the fourth power of the temperature, T.

$$\rho \sim T^4 \quad . \tag{2.14}$$

Since the energy density varies with the inverse fourth power of the scale factor, the temperature varies inversely with the scale factor.

$$T \sim \frac{1}{a(t)} \quad . \tag{2.15}$$

As a(t) tends toward zero, the temperature T increases, and we know indeed that the scale factor was smaller in the past. Therefore, we can say that, during the radiation-dominated period, the temperature was much higher than it is today.

In summary, the implications of homogeneity and isotropy, and the focus on the radiation-dominated period, lead to the prediction of a hot, dense, compact early

---

[11]Whether one may extend this cosmological model all the way back to a singularity at t = 0 is a matter of current debate. When the energy density of the universe approaches the Planck density, approximately 10^{93} grams/cm^3, one must apply a quantum theory for the gravitational field. This theory is not currently complete. Thus, one may not presume to describe a time when a(t) = 0. For the purposes of this thesis, however, we will not need to resolve this question beyond saying the universe was very compact and dense in its early stage.

universe. This is the exact picture for which Penzias and Wilson found observational evidence in 1965 when they discovered the cosmic background radiation.

Matter Fields Are Effectively Massless at High Temperature.

Quantum theory has been spectacularly successful in describing the behavior of matter in many physical situations, from very low temperatures in a superconducting quantum interference device (SQUID) to very high energies in a large particle collider. When the temperature of the universe is significantly larger than the rest mass of a species of particle,

$$T >> mc^2 \ , \tag{2.16}$$

then the relativistic form of the energy, ε, for a single particle,

$$\varepsilon = \sqrt{(pc)^2 + (mc^2)^2} \ , \tag{2.17}$$

can be approximated with its ultrarelativistic form, $\varepsilon = pc$. (For this section, I briefly reintroduce explicit constants c and $\hbar$.)

Consider a degenerate relativistic electron gas.[12] The number density of electrons in a region of phase space Γ is

$$dn_p = \frac{V\,d^3p}{h^3}\cdot 2 = \frac{4\pi V p^2\,dp}{h^3}\cdot 2\ , \qquad (2.18)$$

where V is the volume, and Planck's constant h represents the "cell-size" in phase space. The final factor of 2 accounts for the multiplicity of states for spin = 1/2 electrons. To find the energy of the gas, one simply integrates the product of $\varepsilon(p)$ and dn_p over all momenta up to the Fermi limit, p_F. The limiting momentum, p_F, depends on the number, N, of electrons one can pack in the given volume, V, in the following way:

$$N = \frac{V\cdot\frac{4\pi}{3}p_F^{\,3}}{h^3} = \frac{V}{\pi^2\hbar^3}\cdot\frac{1}{3}p_F^{\,3}\ . \qquad (2.19)$$

The total energy, E, is

$$E = \int_\Gamma \varepsilon\,dn$$
$$= \int_0^{p_F}(pc)dn_p = \frac{cV}{\pi^2\hbar^3}\int_0^{p_F}p^3dp = \frac{c}{4\pi^2\hbar^3}p_F^{\,4}V = \tfrac{3}{4}\hbar c\,N\left[\frac{3\pi^2N}{V}\right]^{1/3}\ . \qquad (2.20)$$

Now, making use of standard thermodynamic relationships

---

[12] L.D. Landau and E.M. Lifshitz, Statistical Physics (Part I). trans. J.B. Sykes and M.J. Kearsley, 3rd ed., (Oxford: Pergamon Press, 1980), 178.

relating energy, pressure and volume,

$$-\left.\frac{\partial E}{\partial V}\right)_S = P = \tfrac{1}{4}\left(3\pi^2\right)^{1/3}\hbar c\left[\frac{N}{V}\right]^{4/3} = \tfrac{1}{3}\frac{E}{V} \ , \qquad (2.21)$$

one sees that, for high temperature, the electron pressure, P, and energy density, ρ, form a particularly simple equation of state, $P = \rho/3$. This is exactly the same equation of state as a photon gas, as mentioned above. In addition, one can derive the same equation of state for systems of other relativistic particles.

At some early time, when the temperature was significantly greater than the rest mass of the heaviest elementary particle (assuming one exists), the equation of state for all species of particles was that of radiation. As the temperature decreased, the radiation-like description for different species of particles began to fail. The first to lose their radiation-like behavior were the quarks; their equation of state changed gradually to that of "dust," $P = 0$. Then successive species of elementary particle lost their photon-like behavior until finally the electrons left the relativistic regime. The time of dominance for radiation was at an end and the time of matter dominance began.

* * * * * * *

Cooling of the Universe Leads to the Possibility of Phase Transitions in the Vacuum.

In finite temperature quantum field theory, phase transitions in the vacuum becomes possible. What is "the vacuum?" This refers to the ground state of the quantized fields in the absence of sources. Consider a simple φ^4 field theory in flat space. Its Lagrangian density is

$$\mathcal{L} = -\left(\nabla\varphi\right)^2 - \tfrac{1}{2}m^2\varphi^2 - \tfrac{\lambda}{4}\varphi^4 \ . \qquad (2.22)$$

The potential is $V(\varphi) = (1/2)m^2\varphi^2 + (\lambda/4)\varphi^4$. If $m^2 > 0$, there is a minimum at $\varphi = 0$. In terms of quantum field theory, one must instead work with the effective potential, which one derives from a Legendre transformation of the classical action.[13]

To understand the kinds of phase transitions that are possible, one must contrast a quantum field theory at zero temperature with one at non-zero or "finite" temperature, both with quantum corrections to leading order in $\hbar$, the so-called one-loop order. Incorporating the corrections for one-loop quantum fluctuations results in an effective

---

[13]In this section, I follow R.J. Rivers, Path Integral Methods in Quantum Field Theory (Cambridge: Cambridge University Press, 1987), 37, 86.

potential that may have a different number and location of the extrema, compared to the zero-temperature effective potential. For instance, one might consider the φ^4 theory of (2.22). If $\lambda > 0$ and $m^2 < 0$, there will be a second extremum; I discuss this situation below.

Although exact details about the location, etc. of the extrema depend upon which field theory one is studying, there are a few ideas that are relatively simple to express: the temperature dependent mass term, spontaneous breaking of an internal "hidden" symmetry, and a critical temperature. These are the areas in which the differences between zero-temperature and finite-temperature field theories become most important.

The effective mass of the quantum field can acquire a temperature dependence in a finite temperature field theory. Normally, one interprets the mass of the field via the coefficient of the term in the Lagrangian which is quadratic in the field: the square of the mass is twice that coefficient. For the Lagrangian of (2.22), the φ field has mass m. With quantum corrections at finite temperature, however, the mass becomes a function of the temperature, $m^2(T)$. If $m^2(T)$ becomes negative, two real-valued extrema occur at $\varphi = 0$ and the global minimum, $\varphi = (-m^2/\lambda)^{1/2}$, as figure 3 shows.

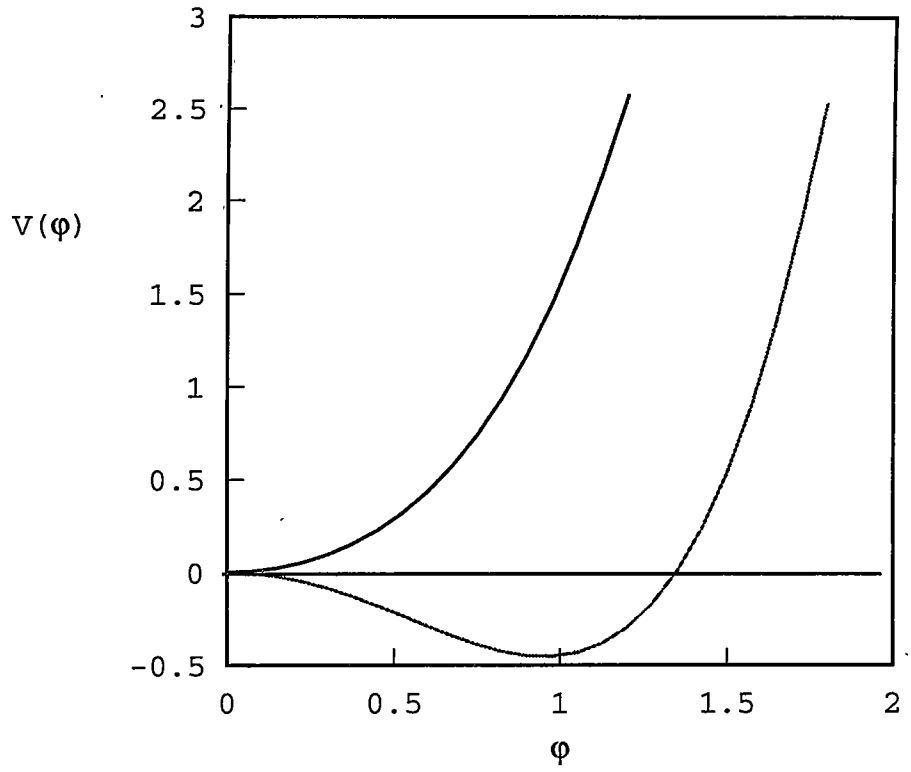

Figure 3. Shape of an effective potential for the two cases $m^2 > 0$ (upper curve) and $m^2 < 0$ (lower curve).

The vacuum expectation value of the scalar field is precisely that value of the field which extremizes the potential. In the first case, that value is $\varphi = 0$. In the second case, however, there are two values for the vacuum , one at $\varphi = 0$ and the other at $\varphi_0 = (-m^2/\lambda)^{1/2}$.

In the theory of spontaneous symmetry breaking, one must first expand the potential about the minimum at φ_0. Using the transformation

$$\varphi \rightarrow u = \varphi - \varphi_0 \ , \tag{2.23}$$

the potential acquires terms cubic in the field u.

$$V(\varphi) \rightarrow V(u) = -m^2u^2 + \lambda\varphi_0 u^3 + \tfrac{\lambda}{4}u^4 + \tfrac{1}{4}m^2{\varphi_0}^2 \ . \tag{2.24}$$

The u field also acquires a new mass: $(-2m^2)^{1/2}$. The discrete symmetry,

$$\varphi \rightarrow -\varphi \ , \tag{2.25}$$

which was manifest in the original Lagrangian does not appear in V(u); it is a hidden symmetry. However, the new ground state, $u = 0$, is asymmetric with respect to the original form of the field theory; the original symmetry is broken.

It is possible to express the temperature dependence of

m^2 with the concept of a critical temperature, T_c. Above T_c, m^2 is positive and the potential has but one extremum, $\varphi = 0$. Below T_c, m^2 is negative and the potential has two extrema. The typical form of the temperature dependence is

$$m^2(T) = m^2\left(1 - \frac{T^2}{T_c^2}\right), \tag{2.26}$$

with the exact form of T_c depending on the details of the field theory in question.

In the simple φ^4 theory above, the field φ can "roll" down into the well at $\varphi = \varphi_0$ from an initial state at $\varphi = 0$, a continuous change in the vacuum expectation value. This continuous change from one value to the other is a second-order phase transition. In electroweak theory, for example, it is possible to have a configuration of coupling constants for the gauge and scalar fields such that a second-order phase transition in the scalar field occurs.

Another kind of phase transition is possible, one in which there is a <u>discontinuous</u> change in the expectation value of the scalar field. This is a first-order phase transition. Figure 4 shows an effective potential in which a first order phase transition may occur. In the electroweak example, a first-order phase transition is possible under another configuration of the coupling constants, a relatively strong gauge coupling constant. As the temperature decreases

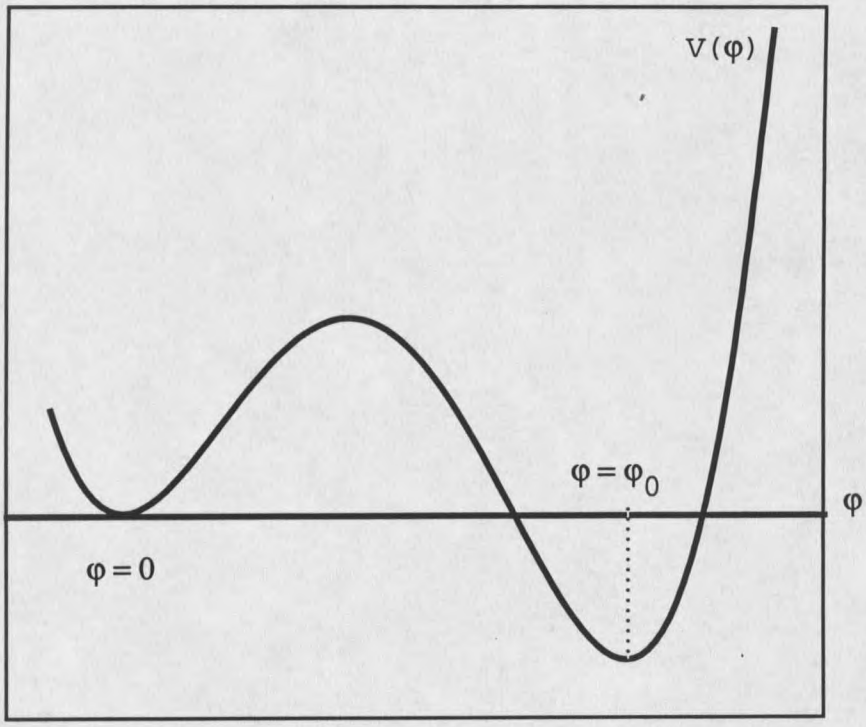

Figure 4. An effective potential in which a first order phase transition may occur.

toward the critical temperature, two wells may appear in the effective potential, as in figure 4. Although the field might originally be located at the quasi-stable minimum at $\varphi = 0$, that state is unstable in quantum field theory. The field may tunnel through the potential barrier to φ_0, a much different process from a second-order phase transition.

First-order phase transitions in quantized scalar fields are the main topic of this thesis. One kind of bubble formation process is of special interest: nucleation by a non-vacuum field configuration, a boson star. This exotic astrophysical object is the topic in chapter 3.

CHAPTER 3

WHAT ARE THE PROPERTIES AND CHARACTERISTICS OF BOSON STARS?

Background Concepts for Calculating Boson Star Models

The idea of a boson star can trace its ancestry back forty years or more to the geometric-electromagnetic entity that John A. Wheeler dubbed a "geon." In German, its name is *Kugelblitz*, the sphere of light. Wheeler suggested the geon as a "self-consistent solution to the problem of coupled electromagnetic and gravitational fields."[1] His most basic geon model was just a stable standing wave beam of light bent into a toroidal shape. Wheeler saw this as a generalization for the concept of material body that was possible within the framework of general relativity.

The idea of a self-gravitating field configuration is a fruitful one. For example, one can model neutron stars in this way, as a self-gravitating spin-1/2 fermionic field configuration. However, one must remember the current idea that neutron stars might not be simply a huge concentration only of neutrons; they might have a shell-like interior structure of exotic meson condensates and a crust of regular baryonic matter. Nonetheless, a neutron star is a well-known

---

[1]J.A. Wheeler, "Geons," Physical Review, 97, 511 (1955).

example of a self-gravitating configuration of a quantum field.

Boson stars also fall into this class of exotic objects, and they have been the object of extensive study recently.[2] The most common model is that of a complex scalar field in gravitational equilibrium, with only the uncertainty principle supporting it against gravitational collapse.

Before going on to review some of the previous research on different kinds of boson stars, it is important to distinguish the self-gravitating field method for constructing a star model, from the "traditional" Oppenheimer-Volkoff method. The distinguishing feature is the use of an implicit equation of state in the former method versus the use of an explicit equation of state in the latter.

In the Oppenheimer-Volkoff approach[3], one assumes that the star has spherical symmetry and that there is no time dependence in the solution. Oppenheimer and Volkoff used the Schwarzschild coordinate system. Their method also assumes that the matter has the stress tensor of a perfect fluid, symbolized in the equations below as $T_{\alpha\beta}$. One must also adopt some equation of state $\rho=\rho(P)$ in order to obtain a solution for the system. Thus, one solves the system (3.1): the

---

[2]See recent reviews in P. Jetzer, "Boson stars," Physics Report, 220, 163 (1992), and T.D. Lee and Y. Pang, "Nontopological solitons," Physics Reports, 221, 251 (1992).

[3]J.R. Oppenheimer and G.M. Volkoff, "On Massive Neutron Cores," Physical Review, 55, 374 (1939).

Einstein field equations, the equation of motion for the fluid, and the equation of state, viz.

$$G_{\alpha\beta} = 8\pi T_{\alpha\beta} \ ,$$

$$\nabla^{\alpha} T_{\alpha\beta} = 0 \ , \qquad (3.1)$$

$$\rho = \rho(P) \ ,$$

for $\rho(r)$, $P(r)$, and for the metric functions $g_{tt}(r)$ and $g_{rr}(r)$, where t denotes the time and r the Schwarzschild radial coordinate. The physical dimensions of the object are constructed from these functions. For example, the radius of the object, R, is the radius at which the pressure vanishes, $P(R) = 0$.

The self-gravitating field method, which I shall use, is one which employs the scalar wave equation as the implicit substitute for the concept of an equation of state.[4] Beginning with the same assumptions about symmetry, and using the same coordinate system, one considers a scalar field φ with an Euler-Lagrange equation of motion given by $\Box\varphi + dV/d\varphi = 0$. One still uses the Einstein field equations, except that now, $T_{\alpha\beta}$ is the stress-energy tensor for the scalar field φ. The stress-energy tensor is a construction not of pressure and

---

[4]R. Ruffini and S. Bonazzola, "Systems of Self-Gravitating Particles in General Relativity and the Concept of an Equation of State," Physical Review, 187, 1767 (1969).

density (as with the perfect fluid) but of the Lagrangian of the scalar field. Therefore, for the self-gravitating field method, the system of equations one must solve is just a bit simpler, one less equation than for the Oppenheimer-Volkoff method. For the self-gravitating field method, the system of equations is

$$\Box\varphi = -\frac{dV}{d\varphi} \ , \qquad (3.2)$$

$$G_{\alpha\beta} = 8\pi T_{\alpha\beta} \ .$$

One solves (3.2) for $\varphi(t,r)$, $g_{tt}(t,r)$ and $g_{rr}(t,r)$. From those functions, one calculates various quantitative properties of the star. For example, one might find the size of the object by looking not for vanishing pressure but for the radial distance R at which the field φ has decreased to 1% of the central field value.

In the self-gravitating field method, the solutions will depend significantly upon the type of scalar potential one studies. Using different potentials in the self-gravitating field method is akin to working with different equations of state in the Oppenheimer-Volkoff method.

The first boson star models were calculated by D. J. Kaup in 1968 using the free particle potential for a classical complex scalar field,

$$V(\varphi) = \tfrac{1}{2} m^2 |\varphi|^2 \ . \qquad (3.3)$$

The corresponding Euler-Lagrange equation is the familiar Klein-Gordon equation:

$$\Box\varphi \equiv \nabla^\alpha \nabla_\alpha \varphi = - m^2 \varphi \ . \qquad (3.4)$$

Kaup calculated size, mass and several thermodynamic quantities from his solutions for the Klein-Gordon geon.[5]

In 1969, Remo Ruffini and Silvano Bonazzola extended the analysis to a quantized scalar field of self-gravitating free bosons, as well as to a quantized spinor field of free fermions. In their examination of the concept of an equation of state,[6] they constructed star models and were able to calculate the size, mass and thermodynamic quantities of boson stars and neutron stars.

The case of the complex scalar field with a quartic self-interaction potential, came under the investigative eye of Monica Colpi, Stuart Shapiro and Ira Wasserman in 1986. In their paper on the gravitational equilibria of self-interacting scalar fields (hereafter, CSW),[7] they used a

---

[5]D.J. Kaup, "Klein-Gordon Geon," Physical Review, 172, 1331 (1968).

[6]Ruffini and Bonazzola, "Self-Gravitating Systems," 1768.

[7]M. Colpi, S.L. Shapiro, I. Wasserman, "Boson Stars: Gravitational Equilibria of Self-Interacting Scalar Fields," Physical Review Letters, 57, 2485 (1986). Hereafter, I shall refer to this paper as CSW.

potential of the form

$$V(\varphi) = \tfrac{1}{2} m^2 |\varphi|^2 + \tfrac{\lambda}{4} |\varphi|^4 \ . \qquad (3.5)$$

They calculated the size and masses of boson star models with this potential. Depending on the mass of the scalar boson in question and on the relative strength of the interaction, boson stars of mass comparable to main sequence stars are possible. They even put together an effective equation of state for the case of relatively strong self-interaction.

What other kind of potentials might one use to model new varieties of boson stars? In chapter 2, I discussed some early universe models that call for a scalar potential in which phase transitions are possible. An example from electroweak theory is the Coleman-Weinberg mechanism.[8] The effective potential is of the following form:

$$V_{CW}(\varphi) = A|\varphi|^2 + |\varphi|^4 \left[\ln\left(\frac{|\varphi|^2}{B^2} \right) - \tfrac{1}{2} \right] \ . \qquad (3.6)$$

One sets its parameters A and B using the masses of the W and Z particles and with the value of the field at the global minimum of the potential. In this potential are a pair of potential wells between which a first-order phase transition may proceed. Figure 5 shows an example of this potential.

---

[8]R.J. Rivers, Path Integral Methods, 243.

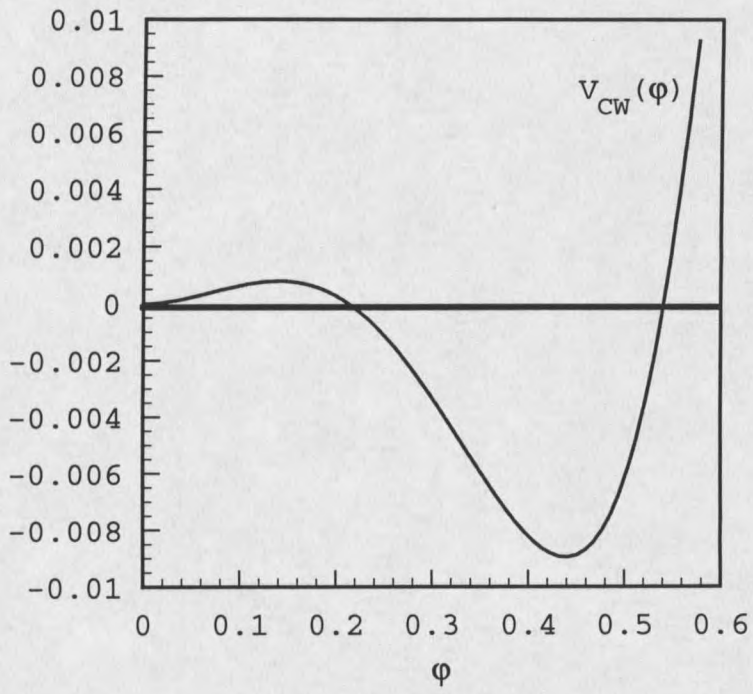

Figure 5. The effective potential in the Coleman-Weinberg process. A = 0.1, B = 0.5.

Another possibility is to use a potential that has terms quadratic, cubic and quartic in the scalar field, the so-called 2-3-4 potential.[9] This potential,

$$V(\varphi) = \tfrac{1}{2}m^2|\varphi|^2 - \eta|\varphi|^3 + \tfrac{\lambda}{4}|\varphi|^4 \ , \qquad (3.7)$$

is easy to work with and one can force it to have two minima by setting the three parameters, boson mass, m, coupling constant for self-interaction, λ, and a temperature-related coefficient η. In fact, the 2-3-4 potential will be my tool in studying the boson stars that nucleate early universe vacuum phase transitions, which is the topic of the next chapter.

Details of Calculating Boson Star Models with the Self-Gravitating Field Method.

To construct boson star models, I will use the self-gravitating field method, closely following the procedures in CSW. Once I have constructed the models, I will use them to calculate a nucleation rate for vacuum phase transitions.

To begin, I take the 2-3-4 potential as the model potential for the boson field φ. I ignore momentarily any

[9]D. Samuel and W.A. Hiscock, "'Thin-wall' approximations to vacuum decay rates," Physics Letters B, 261, 251 (1991); A. Linde, Particle Physics and Inflationary Cosmology (New York: Harwood Academic Publishers, 1990), 120.

coupling of φ to other fields, even possible gauge fields coupled to φ in the spontaneous symmetry breaking process. The Lagrangian density for the complex scalar field φ is

$$\mathcal{L} = -\tfrac{1}{2} g^{ab} \nabla_a \varphi^* \nabla_b \varphi - V(\varphi) \ . \tag{3.8}$$

The Euler-Lagrange equation for φ is

$$\nabla_a \left[\frac{\partial \mathcal{L}}{\partial \left(\nabla_a \varphi^* \right)} \right] - \frac{\partial \mathcal{L}}{\partial \varphi^*} = 0 \ . \tag{3.9}$$

From the Lagrangian one also constructs the stress energy tensor of the scalar field, which is

$$\begin{aligned} T^a_b = {} & \tfrac{1}{2} g^{ac} \left[\nabla_c \varphi^* \nabla_b \varphi + \nabla_b \varphi^* \nabla_c \varphi \right] \\ & - \tfrac{1}{2} \delta^a_b \left[g^{cd} \nabla_c \varphi^* \nabla_d \varphi + m^2 |\varphi|^2 - 2\eta |\varphi|^3 + \tfrac{1}{2} \lambda |\varphi|^4 \right] \ . \end{aligned} \tag{3.10}$$

For solution of the scalar wave equation and the Einstein field equations, it is necessary to make several decisions about the nature of the solutions for the field and about the coordinate system which has so far remained unspecified.

The first decision about the type of boson star solution concerns its functional dependence upon time. For a star with fixed number of bosons, N, the time dependence for the

ground state must be of the form $\exp[-i\omega t]$.[10] At this point in the discussion, ω is the unspecified Lagrange multiplier with which one minimizes the energy of the system under the constraint of fixed N.

A requirement specifically for the ground state is that there must be no nodes in the ground state solution. Later I will make use of this requirement to determine a specific value of ω. I also require that the solution be "localized" in a finite volume of space. In practice, this will happen because the ground state solution will have a decaying exponential dependence, so that it asymptotically approaches zero far from the center of the star.

Another specification of solutions is that they be spherically symmetric. This further simplifies the system of equations, in that the φ solutions depend only on time and the radial coordinate r. Overall, then, the solutions φ will be of the form $\varphi(t,r) = \varphi(r)\exp[i\omega t]$. This time dependence will simplify the system of equations in that all time derivatives are replaced with factors of $\pm i\omega$.

The requirement of spherical symmetry applies to the metric. In addition, since I am looking for equilibrium solutions for φ, the metric must be static, with no time dependence. In the (t, r, θ, ϕ) coordinate system, the form for the line element is

---

[10]T.D. Lee and Y. Pang, "Nontopological solitons," 255.

$$ds^2 = -B(r)\,dt^2 + A(r)\,dr^2 + r^2\,d\Omega^2 \ , \qquad (3.11)$$

where

$$d\Omega^2 = d\theta^2 + \sin^2\theta\,d\phi^2 \ .$$

In this equation, ϕ stands for the azimuthal angle; θ stands for the co-latitudinal angle. Far from the star, where gravitational effects have diminished, the spacetime should become flat. In the limit of large r, both metric functions B(r) and A(r) must approach unity. Later, I will use this asymptotic condition on the metric to scale the metric function B(r).

Now that I have chosen a specific coordinate system, it is possible to write down the explicit form of the scalar wave equation and the Einstein field equations. Before doing that, however, I will rescale the field, the potential and the coordinate system so that they are all dimensionless, for convenience in calculation.

In the first rescaling, I replace the field $\varphi(r)$ with a dimensionless scalar field $\sigma(r)$ such that

$$\sigma = \frac{\sqrt{4\pi}}{M_{Planck}}\,\varphi \ . \qquad (3.12)$$

Then, I change to a dimensionless potential such that

$$V(\varphi) \rightarrow \tilde{V}(\sigma) = \frac{8\pi}{m^2 M_{Planck}^2} V(\varphi) = \sigma^2 - 2\eta^* \sigma^3 + \tfrac{1}{2}\Lambda\sigma^4 \ . \qquad (3.13)$$

The rescaled, dimensionless parameters η^* and Λ are

$$\eta^* = \frac{M_{Planck}}{4\pi m^2}\eta \ , \qquad (3.14)$$

$$\Lambda = \frac{\lambda M_{Planck}^2}{4\pi m^2} \ . \qquad (3.15)$$

Hereafter I will drop the tilde and use $V(\sigma)$ to refer to the rescaled potential.

CSW found that, as far as boson stars are concerned, Λ is actually a better measure of the importance of the self-interaction than λ; if m is much smaller than the Planck mass, then Λ can be large even if λ is small. In studying the 2-3-4 potential for first order phase transitions, the important parameter is actually a combination of both η^* and Λ. This parameter is $\xi = \eta^{*2}/\Lambda$. To grasp the importance of ξ consider the extrema of $V(\sigma)$. One extremum is at $\sigma = 0$; the other two extrema σ_1 and σ_2 are

$$\sigma_{2,1} = \frac{3\eta^*}{2\Lambda}\left(1 \pm \sqrt{1 - \frac{4\Lambda}{9\eta^{*2}}}\right) \ . \qquad (3.16)$$

The latter two extrema will have real values when $\xi > 4/9$; σ_1 is the location of the top of the "bump" in the potential,

and σ_2 is the location of the bottom of the second well. When $\xi = 1/2$, the potential is degenèrate: $V(0) = 0$ and $V(\sigma_2) = 0$. When $\xi > 1/2$, the extremum at σ_2 will be a global minimum; the true vacuum is at σ_2, as figure 6 shows.

At the end of chapter 2, I discussed the concept of a critical temperature for vacuum phase transitions. The parameter ξ is something like an inverse temperature for the following reasons. Consider the shapes of the potential curves in figure 6. When $\xi < 1/2$, the curve looks like an effective potential above the critical temperature. When $\xi = 1/2$, the curve looks like an effective potential at the critical temperature. When $\xi > 1/2$, the curve looks like an effective potential below the critical temperature.

The analogy breaks down when one considers negative values for ξ. One is left to interpret a complex-valued potential. Nonetheless, the parameter ξ will be useful as a restricted indicator of temperature.

The final two rescalings concern the Lagrange multiplier ω and the radial coordinate r. It is convenient to switch to a dimensionless Lagrange multiplier, $\Omega = \omega/m$. Also, a dimensionless radial coordinate $x = mr$ will be helpful.

After these rescalings, I can write down the system of equations. The scalar wave equation in the 2-3-4 potential is

$$\sigma'' = A\left[\left(1 - \frac{\Omega^2}{B}\right)\sigma - 3\eta^*\sigma^2 + \Lambda\sigma^3\right] + \left(\frac{A'}{2A} - \frac{B'}{2B} - \frac{2}{x}\right)\sigma' \ . \qquad (3.17)$$

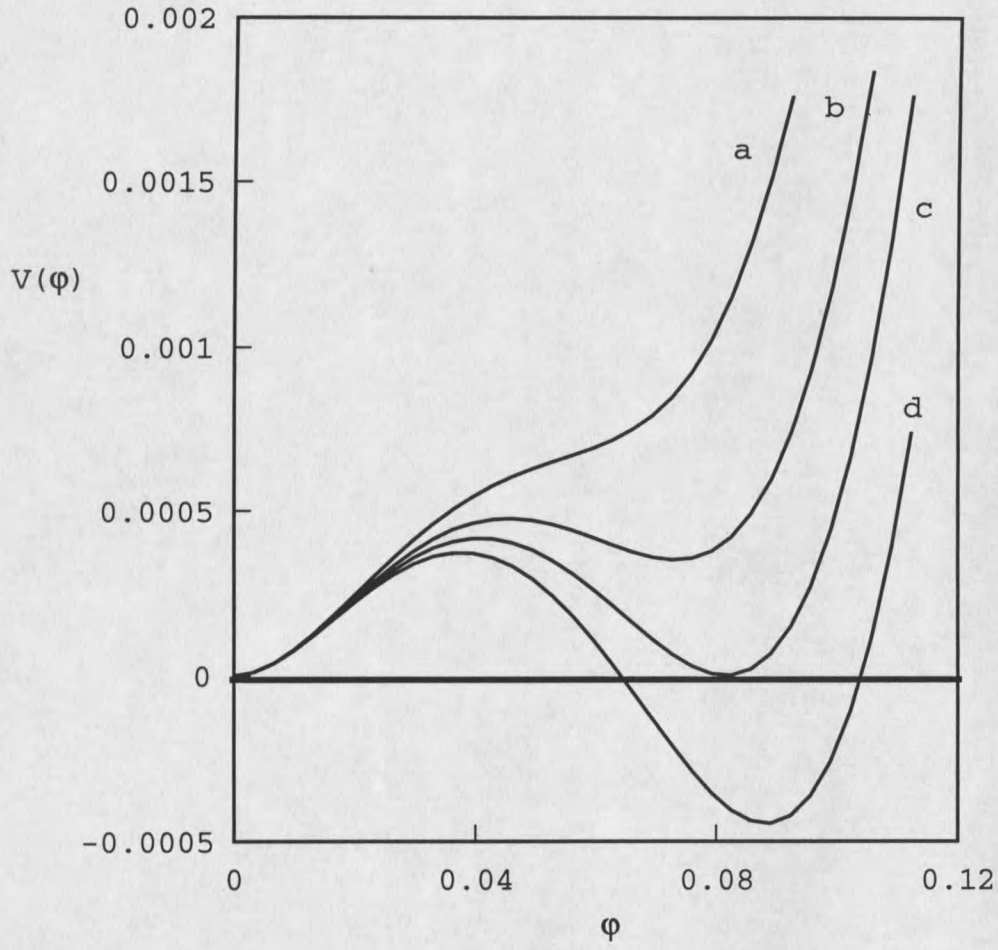

Figure 6. The 2-3-4 potential. Curves a, b, c and d have ξ = 0.42, 0.47, 0.50, 0.53 respectively. Λ = 300 for all four curves. Note that they are nearly indistinguishable near σ = 0.

The primes denote differentiation by x. The two Einstein field equations are $G_t{}^t = 8\pi T_t{}^t$ and $G_r{}^r = 8\pi T_r{}^r$, viz.

$$\frac{A'}{xA^2} + \frac{1}{x^2}\left(1 - \frac{1}{A}\right) = \left(1 - \frac{\Omega^2}{B}\right)\sigma^2 - 2\eta^*\sigma^3 + \tfrac{1}{2}\Lambda\sigma^4 + \frac{1}{A}\left(\sigma'\right)^2 , \quad (3.18)$$

$$\frac{B'}{xAB} - \frac{1}{x^2}\left(1 - \frac{1}{A}\right) = \left(\frac{\Omega^2}{B} - 1\right)\sigma^2 + 2\eta^*\sigma^3 - \tfrac{1}{2}\Lambda\sigma^4 + \frac{1}{A}\left(\sigma'\right)^2 . \quad (3.19)$$

After configuring the system by setting values for ξ and Λ, I solve equations (3.17), (3.18) and (3.19) subject to a set of boundary conditions I will now describe. The central value of the field, $\sigma(0)$, is left as an unspecified constant. The value of the central field will distinguish solutions in a given family of solutions. The field must be nonsingular at the origin, so the central value of the first derivative, $\sigma'(0)$, must vanish. As x approaches infinity the limit of B(x) is unity. Physically, the dimensionless mass function $\mathcal{M}(x)$ of the spacetime

$$\mathcal{M}(x) = \tfrac{1}{2}x\left(1 - \frac{1}{A(x)}\right) \quad (3.20)$$

must vanish near the origin faster than x, since there is no mass inside a sphere of radius zero. This allows me to set A(0) to unity.

The asymptotic limit on B(x) does not, however, tell me what value of B(0) to use when starting the solution

algorithm. In the fourth-order Runge-Kutta scheme I use, I must actually specify the value of $\Omega^2/B(0)$. The way I resolved this puzzle was through the realization that B(0) is related to the central redshift of the star. In general, the redshift z(r) of a photon emitted at radius r and observed at infinity follows from analysis of the constants of the motion along null geodesics in a static spherical spacetime:[11]

$$\frac{\lambda(r)}{\sqrt{B(r)}} = \frac{\lambda(\infty)}{\sqrt{B(\infty)}} = \text{constant.} \qquad (3.21)$$

This allows one to calculate z(r),

$$z(r) \equiv \frac{\lambda(\infty) - \lambda(r)}{\lambda(r)} = \sqrt{\frac{B(\infty)}{B(r)}} - 1 \ . \qquad (3.22)$$

Therefore, no matter how the distant observer arranges his scale for B(r), as long as the quotient $B(\infty)/B(0)$ is constant, then he will make the same measurement of the central redshift. Thus I may set the scale at B(0) = 1 and proceed with the Runge Kutta procedure. The value I obtain for $B(\infty)$ will then allow me to rescale B(x), so that the rescaled B(x) approaches unity as x approaches infinity.

It is permissible to rescale B(x) by a constant C in order to fit the boundary condition at infinity. This has no effect on the system of equations. If one sets B(x) to

[11]Misner, Thorne and Wheeler, Gravitation , 659.

$C \cdot B(x)$, then the terms containing B'/B are unchanged. What about the terms containing Ω^2/B? This quotient remains the same when I rescale $B(x)$ by a constant C. Consider the invariant interval Δs taken along a timelike geodesic. If I rescale $B(x)$ by the constant C, I must rescale the time interval by a constant $C^{-1/2}$,

$$\Delta s = \sqrt{B(x)}\,\Delta t = \sqrt{C}\,\sqrt{B(x)}\left(\frac{\Delta t}{\sqrt{C}}\right) . \qquad (3.23)$$

Rescaling the time interval by $C^{-1/2}$ means that frequencies rescale by $C^{1/2}$. Thus the terms containing Ω^2/B remain unchanged by the rescaling.

If I set $B(0) = 1$ and rescale $B(x)$, I still must come up with the "correct" value for the Lagrange multiplier Ω. Before reviewing that task, I must present a set of good solutions for a typical boson star configuration. Comparing bad solutions against the good will show how to select Ω.

In figure 7, I show the plot of the field $\sigma(x)$ for a typical boson star configuration, with $\Lambda = 300$, $\xi = 0.52$ and $\sigma(0)=0.5\ \sigma_1$. With it is $\sigma'(x)$, the first derivative of σ with respect to x. The radius at which the σ field has fallen to 1% of its central value is approxi-mately 11.27. One might call this distance the radius of the boson star. Another method is to find the value x_{max} at which $A(x)$ is at its maximum, and calculate an effective radius, $\mathbb{X}_{eff}$:

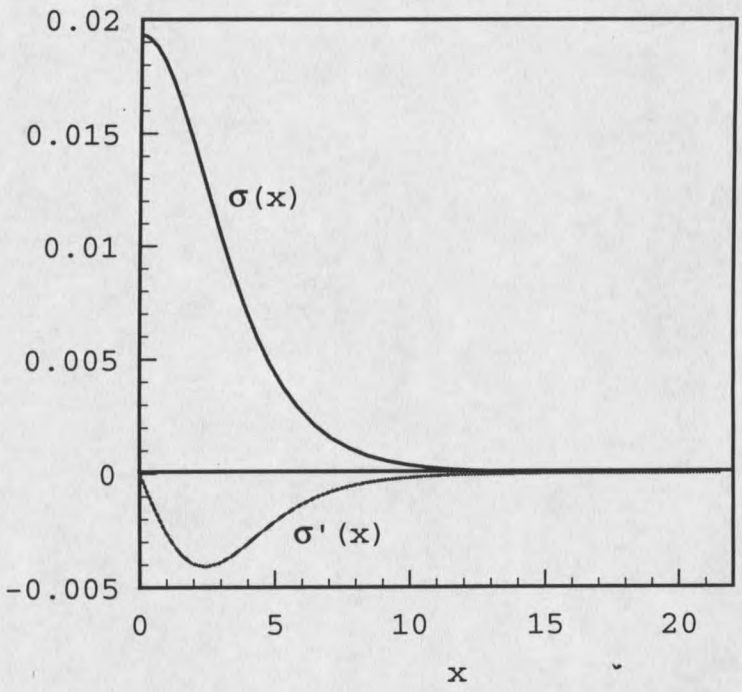

Figure 7. The upper curve is a typical solution for the field $\sigma(x)$; the lower curve is $\sigma'(x)$. $\Lambda = 300$, $\xi = 0.52$, and $\sigma(0) = 0.5\ \sigma_1$.

$$X_{eff} = \int_0^{x_{max}} \sqrt{A(x)}\, dx \ . \qquad (3.24)$$

This is the spatial distance along a path from x = 0 to x_{max}.

It is now apposite look at solutions for A(x) and B(x). In figure 8, I show the plot of the metric functions. B(x) has been rescaled so that B(∞) = 1. Figure 3.5 shows the plot of the mass function for the star, $\mathcal{M}(x)$. Note that, although B(x) and A(x) do not converge rapidly to their asymptotic limits, the mass function does converge rapidly to a limit. In this example, the mass of the star is 0.003459 in units of $(M_{Planck})^2/m$. If the scalar mass m = 100 GeV, then the mass of the star is 5.0×10^{33} GeV or about 9000 metric tons, the displacement of a fully loaded guided missile destroyer like DDG-993, the *USS Kidd*.

The evident failure of B(x) and A(x) to reach limiting values on the scale of the plot might lead the reader to complain: why not continue the plot to larger x-values where the asymptotic value for B(x) will be evident? The answer is that the solution inevitably diverges, either negatively or positively, due to very slight differences between the assumed value of the eigenfrequency, Ω^*, and the true value of Ω. Figures 10 and 11 show these two cases. The computer program uses an estimate, Ω^*, in order to calculate the trial solution for the field, σ^*. When Ω^* is slightly larger than

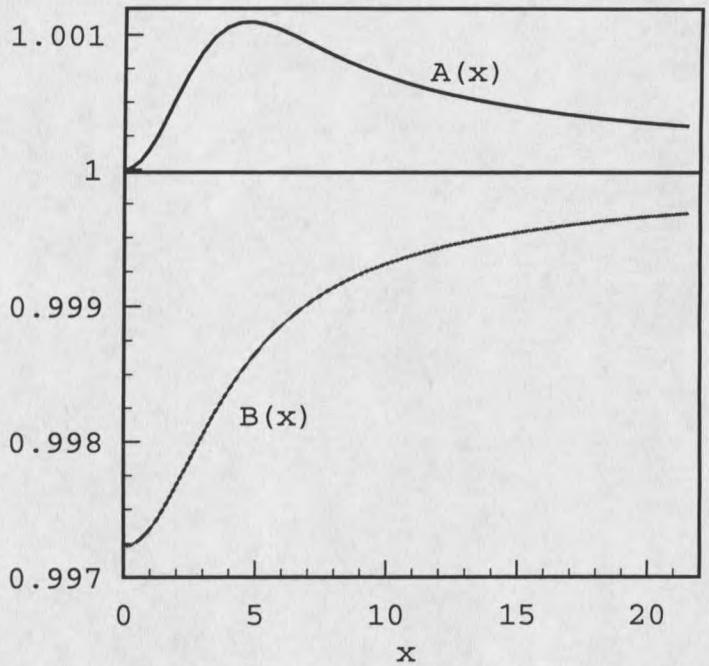

Figure 8. Metric functions for the example boson star.

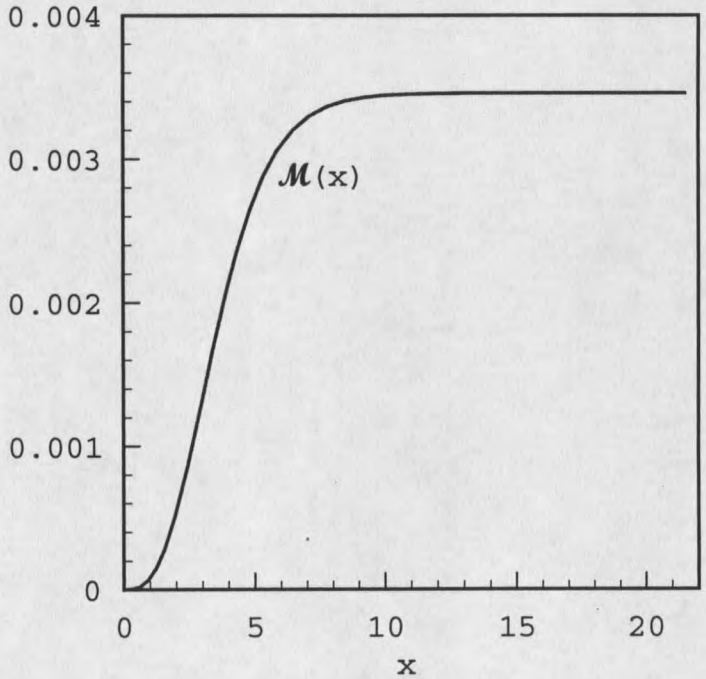

Figure 9. The mass function for the example boson star.

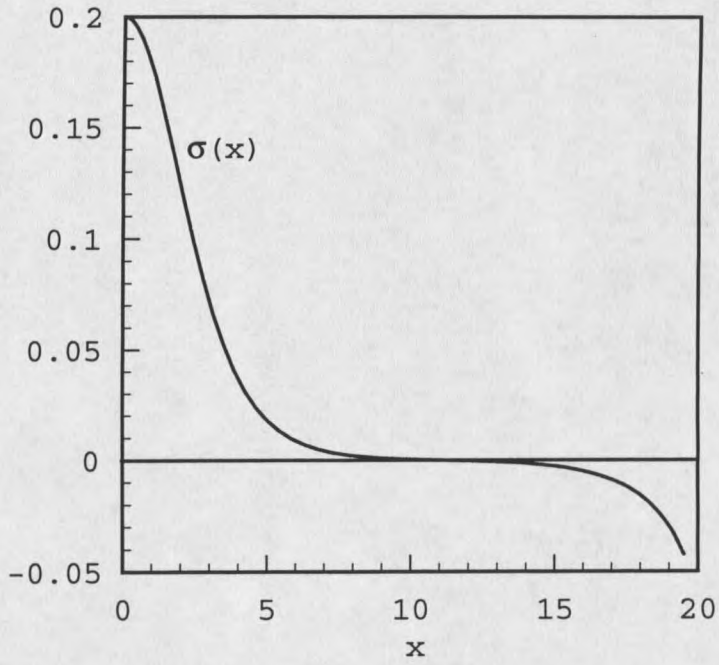

Figure 10. An example of a trial solution with Ω too large.

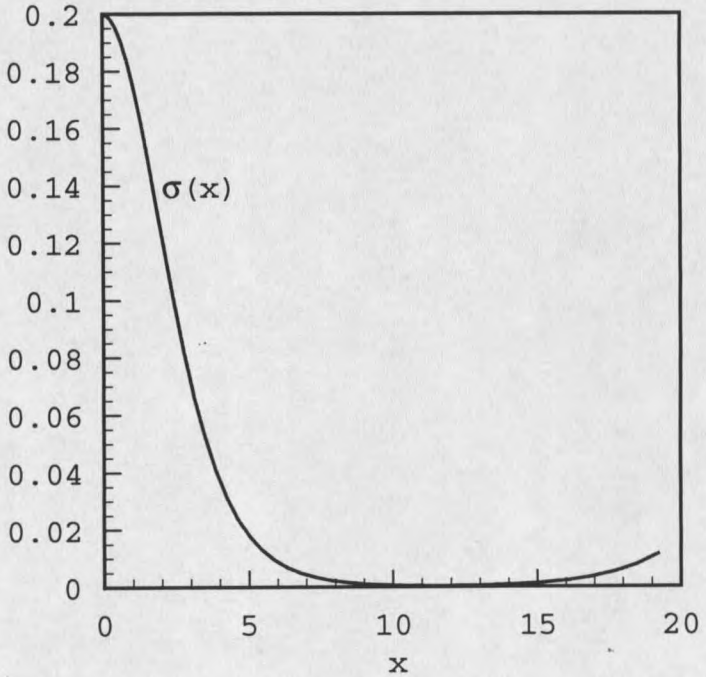

Figure 11. An example of a trial solution with Ω too small.

Ω, the trial solution, σ^*, eventually plunges across the x-axis and diverges in the negative direction. When Ω^* is slightly smaller than Ω, the trial solution turns away from the x-axis and diverges in the positive direction. Using a bisection algorithm, splitting the difference between the oversized Ω^* value and the undersized Ω^* value, one can rapidly settle on a good value of Ω. As the accuracy of the Ω value improves, the solution extends further and further along the x-axis before it diverges. The precision of the computer then limits the search for Ω, which is why the sample solution above does not extend into the region where the metric functions level off.

In summary: I solve the system (3.17), (3.18), (3.19) in accordance with boundary conditions

$$\begin{aligned} \sigma'(0) &= 0 \ , \\ A(0) &= 1 \ , \\ B(0) &= 1 \ , \end{aligned} \tag{3.25}$$

and I independently select a central field value in the range

$$0 < \sigma(0) < \sigma_1 \ . \tag{3.26}$$

I search for a value of Ω that gives a nodeless solution extending as far in x as possible. I interpret this value of Ω as the eigenenergy of the ground state. I extract an

asymptotic value for $B(\infty)$ and rescale the solution for $B(x)$ so that it fits the asymptotic condition $B(\infty) = 1$. The model of the boson star is now complete. One can then analyze it for various properties such as size and mass.

Now that I have spelled out the solution method for the boson star system, in figure 12 I present a collection of field configurations for a range of values of $\sigma(0)$, with $\sigma(0)$ expressed as a percentage of σ_1.

It is worth noting that the variation in shape of $\sigma(x)$ depends on the central field value. Speaking in terms of the 2-3-4 potential, this means that the spatial variation depends on how far up the "bump" one starts the solution. One can say that solutions starting near the top of the bump "roll" quickly back to $\sigma = 0$. Solutions that start down in the well, with $\sigma(0)$ closer to $\sigma = 0$, roll only very slowly back to $\sigma = 0$. This appeals to one's analogical thinking about a particle in a potential well.

In terms of spatial variation of the boson star configuration, one can say that relatively large values of $\sigma(0)$ generate solutions that are relatively small in spatial extent. Smaller values of $\sigma(0)$ generate solutions that are relatively large. This distinction will be of crucial importance in the next chapter where I consider the nucleation of vacuum phase transitions in the case of a small star and a large bubble.

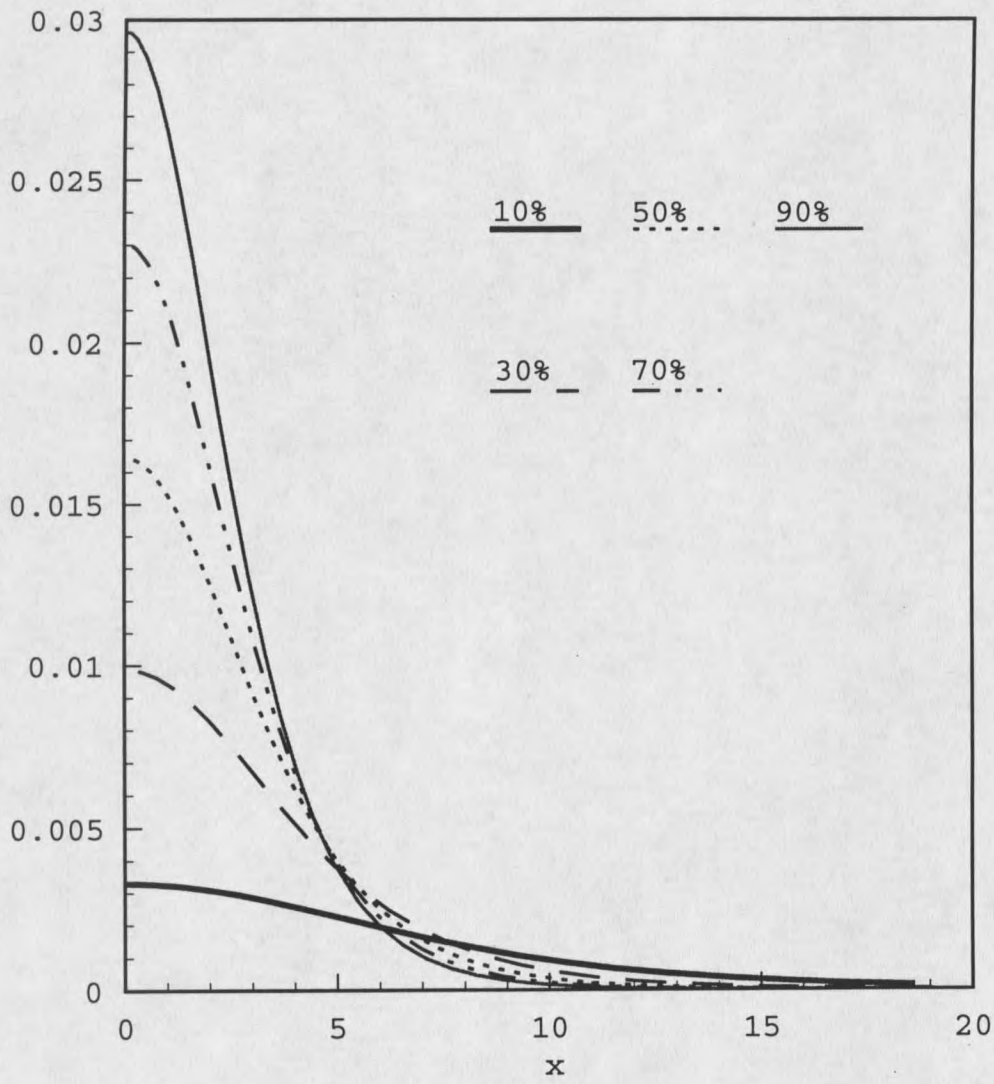

Figure 12. A gallery of solutions for the scalar field $\sigma(x)$ in the 2-3-4 potential, each solution with a different central value, $\sigma(0)$. For this set of solutions, $\Lambda = 300$ and $\xi = 0.60$. The central value for each solution is expressed as a percentage of the value of σ_1, as shown in the legend. Note how rapidly the 90% solution drops off and how broad the 10% solution is.

CHAPTER 4

HOW DO BOSON STARS AFFECT THE DECAY OF THE FALSE VACUUM?

In chapter 3, I showed how one models a boson star in the 2-3-4 potential. In this chapter, my objective is to use those models to study first order vacuum phase transitions as a boson star would nucleate them. To begin, I shall review concepts and techniques for studying vacuum phase transitions. Following that, I shall focus on a special case of "small" boson stars nucleating vacuum phase transitions. The chapter concludes with a summary of the effects in this special case.

The picture of what happens in a first order vacuum phase transition is relatively simple. It is similar to the formation of a bubble of steam in hot water. The scalar field φ is initially in the so-called false vacuum state, φ_{false}, everywhere. Due to quantum fluctuations, other perturbations to the system, or impurities, a bubble forms containing the field in the so-called true vacuum state, φ_{true}. Say that the change in volume energy density inside the bubble is $\mathcal{E}$, which will be negative since the true vacuum is at a lower energy density than the false. In addition, say that the bubble forms with a positive surface energy density $\mathcal{S}$. One can show, using conservation of energy, that

if the system's total energy change is zero, the bubble forms with radius $\mathcal{R}$ such that

$$\mathcal{R} = \frac{3S}{|\mathcal{E}|} \quad . \tag{4.1}$$

A bubble of at least this size will expand until all the false vacuum (or hot water) is converted to true vacuum (or steam).

It is important to distinguish between spontaneous decay of the false vacuum and induced decay. Here again, the example of water is useful. Consider the formation of cloud droplets. Although water droplets can form spontaneously in a mass of water vapor, they form more readily around atmospheric aerosol particles, called cloud condensation nuclei or CCN.[1] The CCN is an impurity in the vapor. Similarly, a vacuum phase transition can proceed spontaneously, or an impurity in the vacuum can nucleate a phase transition.[2] Boson stars can be such an impurity.

---

[1]A.S. Arnett, Weather Modification by Cloud Seeding (New York: Academic Press, 1980), 7, 31.

[2]D.A. Samuel and W.A. Hiscock, "Gravitationally compact objects as nucleation sites for first-order vacuum phase transitions," Physical Review D, 45, 4411 (1992); V.A. Berezin, V.A. Kuzmin and I.I. Tkachev, "Black holes initiate false-vacuum decay," Physical Review D 43, R3112 (1990); G. Mendell and W.A. Hiscock, "Gravitational nucleation of vacuum phase transitions by compact objects," Physical Review D 39, 1537 (1989); W.A. Hiscock, "Can black holes nucleate vacuum phase transitions?" Physical Review D 35, 1161 (1987).

Coleman's Theory of Decay of the False Vacuum

One can liken a first order phase transition in a quantum field to the penetration of a potential barrier by a particle. Consider a particle of mass μ in a potential $V(x)$ that has minima at $x = 0$ and $x = x_2$. See figure 13. In a classical theory, the point $x = 0$ is a stable equilibrium, but in a quantum theory it is not stable. The particle initially at $x = 0$ may tunnel through the potential barrier and emerge at $x = x_{out}$ with zero kinetic energy. From there it propagates classically toward x_2. The amplitude for this process in the semiclassical approximation is

$$\Gamma = A e^{-B}\left[1 + O(\hbar)\right] . \tag{4.2}$$

The quantity B is

$$B = \int_0^{x_{out}} \sqrt{2\mu V(x)}\, dx . \tag{4.3}$$

and A is a normalization constant. Banks, Bender and Wu constructed[3] the amplitude (4.2) as a path integral. The dominant contribution to the total amplitude comes from the region near the path that extremizes B,

---

[3]T. Banks, C.M. Bender, T.T. Wu, "Coupled Anharmonic Oscillators. I. Equal-Mass Case," Physical Review D, 8, 3346 (1973).

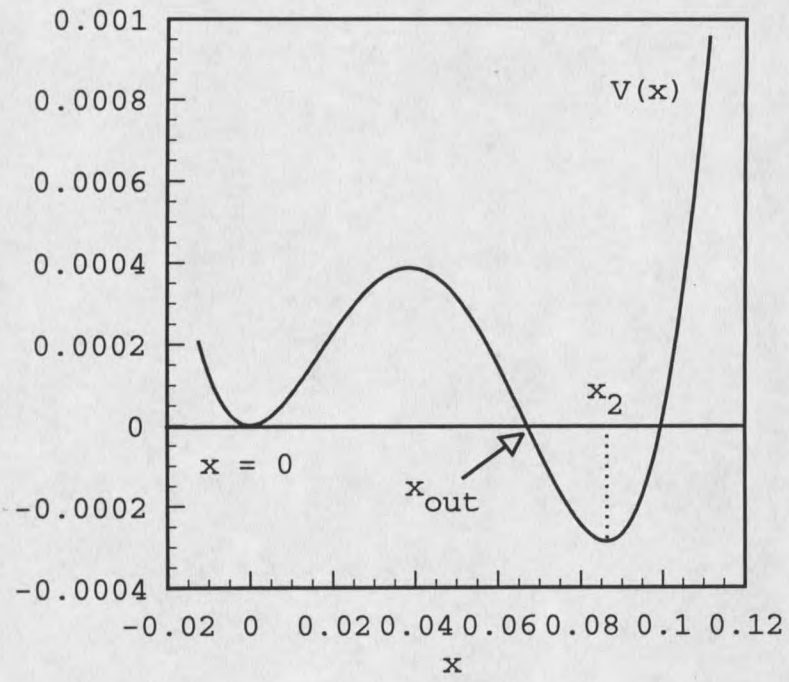

Figure 13. Potential with unstable equilibrium at x = 0. A particle can tunnel quantum mechanically away from x = 0.

$$\delta B = 0 \ . \tag{4.4}$$

Equation (4.4) is a special case of the more general variational problem,

$$\delta \int \sqrt{2\mu\,(E - V(x))}\, dx = 0 \ , \tag{4.5}$$

for the motion of a particle of mass μ with total energy E, moving in the potential V(x). The equation of motion from (4.5) is

$$\mu \frac{d^2x}{dt^2} = -\frac{dV}{dx} \ . \tag{4.6}$$

The special variational problem (4.4), however, corresponds to a particle of mass μ with zero total energy, moving in an "upside-down potential," -V(x). The classical equation of motion for the tunneling problem has a very significant sign difference with respect to (4.6), viz.

$$\mu \frac{d^2x}{dt^2} = +\frac{dV}{dx} \ . \tag{4.7}$$

Coleman also interpreted this as the equation of motion for a particle in the potential V(x) but with a replacement of the

time t with an imaginary time, $\tau = it$, also known as the Euclidean time. The quantity B is the action, S_E, calculated in Euclidean space. The Lagrangian in the Euclidean space, L_E, is

$$L_E = \tfrac{1}{2}\mu\left(\frac{dx}{dt}\right)^2 + V(x) \ . \tag{4.8}$$

This concludes the first half of the analogy between particle tunneling and vacuum phase transitions.

The second half of the analogy focuses on the quantum field, φ. One calculates the amplitude for the phase transition. In general, one calculates the Euclidean action, S_E, for the field tunneling from the false vacuum at φ_{false} to the true vacuum at φ_{true}, as figure 14 shows. For a scalar field in flat space, the Euclidean action is

$$S_E = \int\left[\tfrac{1}{2}\left(\nabla\varphi\right)^2 + V\left(\varphi\right)\right]d^4x \ . \tag{4.9}$$

There are several ways[4] to calculate S_E. One can solve the Euclidean equations of motion exactly for the bubble solution, φ. If one assumes that the bubble solution has O(4) symmetry, then it is useful to transform to an O(4) radial coordinate, $\rho^2 = \tau^2 + r^2$, with τ defined as the

---

[4]D.A. Samuel and W.A. Hiscock, "'Thin-wall' approximations to vacuum decay rates," Physics Letters B261, 251 (1991).

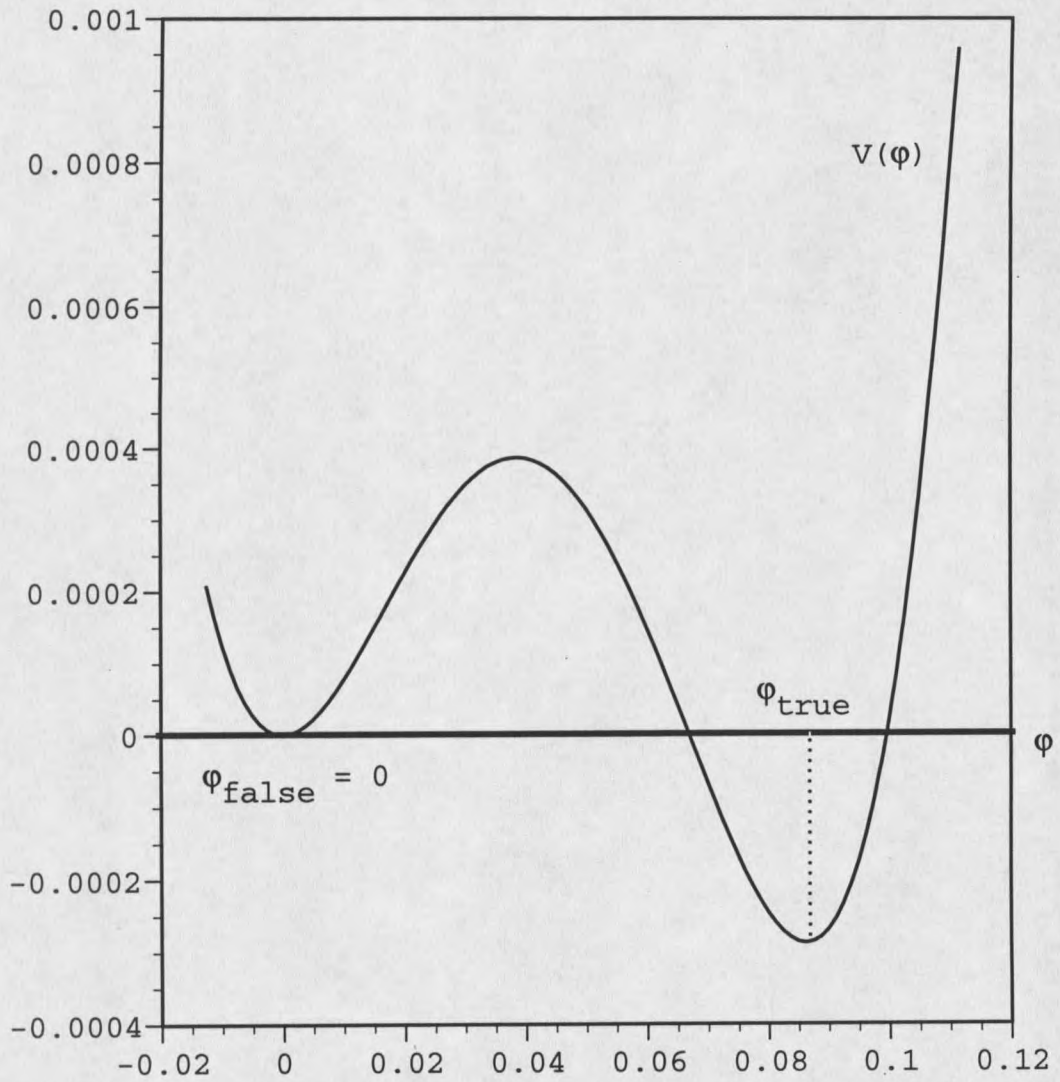

Figure 14. Potential in which a first order phase transition is possible. The field φ can tunnel from the false vacuum at φ_{false} to the true vacuum at φ_{true}.

Euclidean time. After that transformation, the Euclidean equation of motion for the field becomes

$$\frac{d^2\varphi}{d\rho^2} + \frac{3}{\rho}\frac{d\varphi}{d\rho} = \frac{dV}{d\varphi} \quad . \tag{4.10}$$

Once one has obtained a solution, either analytically or numerically, one can calculate the S_E integral in a straightforward manner.

Coleman invented another way[5] to calculate S_E. He devised an approximation scheme for getting a solution to (4.10) under a special condition. This condition was that the potential is nearly degenerate. To state this limit more precisely, if one defines ε as the energy difference between the vacua, $\varepsilon = V(\varphi_{false}) - V(\varphi_{true})$, then his approximation is legitimate in the small-ε limit. Coleman's scheme has the added advantage of giving a closed-form expression for S_E. He named this scheme the thin-wall approximation. It is the approximation scheme I will use, so it is appropriate to examine it closely.

The key idea is to interpret (4.10) in an analogy to particle motion. Let the reader beware: this is a different analogy from that used at the beginning of this section. To clariify the particle analogy for equation (4.10), Coleman wrote:

---

[5]Coleman, "Fate of the false vacuum," 2932.

> If we interpret φ as a particle position and ρ as a time, Eq. (3.9) is the mechanical equation for a particle, moving in a potential *minus U* and subject to a somewhat peculiar viscous damping force with Stoke's law coefficient inversely proportional to the time.[6]

The tunnelling problem becomes a trip from peak to peak in the upside down potential, $-V(\varphi)$, which figure 15 shows.

In order to get a more intuitive grasp of this interpretation of equation (4.10), consider for a moment that it is an ordinary classical mechanics equation of particle motion. That is, substitute x for φ and t for ρ, viz.

$$\frac{d^2x}{dt^2} + \left(\frac{3}{t}\right)\frac{dx}{dt} = \frac{dV}{dx} \quad . \tag{4.11}$$

The first term in (4.11) is the particle's acceleration. The second term contains the velocity dx/dt, and it has a coefficient that is time-dependent, 3/t. The right-hand side of (4.11) has usual the potential gradient, except that the sign is opposite the customary usage, hence the upside-down potential's name. The sign of the velocity's coefficient is important; since it is positive, it corresponds to a force that opposes the motion of the particle. That force slows the particle's speed. So there are two forces: a gradient force from $-V(x)$, the upside-down potential, and a damping force opposing the motion and slowing down the particle. One

---

[6]Ibid. N.b. In Coleman's notation $U(\varphi)$ is the potential; his equation (3.9) is my equation (4.10).

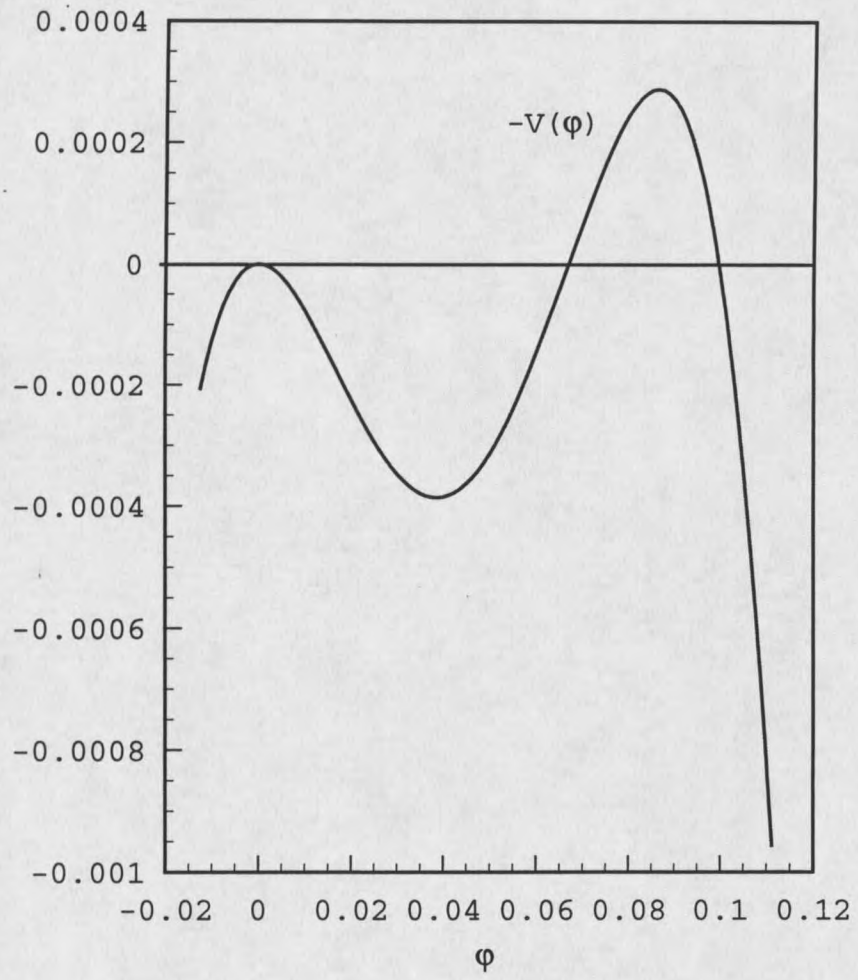

Figure 15. The upside-down potential, $-V(\varphi)$.

can conceive of different motions of the particle for different sets of initial conditions. For example, there is a critically damped system, in which the particle starts with an initial velocity at time t_0, from the top of the highest "hill" in the upside down potential, moves slowly to the left and comes to a halt exactly at the bottom of the "valley" between the two hills. Since the damping force diminishes with time, one can conceive another kind of motion. After some amount of time, T_1, the damping force will be so small as to be negligible. After that time, the particle would respond only to the gradient force. If one starts the particle very near the top of the highest hill, the damping force will keep it near the top until about time T_1, when it starts to move across the valley as if there were no damping. In this motion, the particle will shoot over the top of the smaller hill and keep going. Between these two cases is a third kind of motion. One starts the particle near the top of the highest hill, and it loiters there amid the damping for an amount of time, $T < T_1$. After that amount of time has elapsed, the particle begins to move rapidly across the valley, but it does not shoot over, but coasts perfectly to a stop at the top of the smaller hill as t approaches infinity.

Taking this intuitive grasp of the problem of a particle in an upside-down potential, one can apply it to the field theory problem at hand. With suitably chosen initial "position," $\varphi(0)$ near the top of the highest hill, and with

initial speed $\varphi'(0)=0$, the "particle" can be released at "time" $\rho = 0$ and it will loiter near the top (at φ_{true}) for some amount of time ρ^*. After that amount of time has elapsed, the "damping force" has diminished enough to allow the particle to make a "rapid" transition through the valley and reach the secondary peak at φ_{false} as ρ approaches infinity. The tunnelling process from φ_{false} to φ_{true} is just the "time-reversal" of this process. Figure 16 shows an example of a tunnelling solution for $\varphi(\rho)$.

In terms of the scalar field φ, the solution has a nearly constant value, $\varphi(\rho) \approx \varphi_{true}$, for $\rho < \rho^*$. When $\rho \approx \rho^*$, the field changes value rapidly to φ_{false}. Then for $\rho > \rho^*$, $\varphi(\rho) \approx \varphi_{false}$. This solution corresponds to a "bubble" of true vacuum inside a "wall" of radius approximately ρ^*. Far beyond this wall, the false vacuum is still present at $\rho >> \rho^*$. The wall is thin in that the field changes rapidly from φ_{false} to φ_{true} in a relatively brief interval of "time."

The method that Coleman employed to get a closed form for S_E took advantage of the behavior of $\varphi(\rho)$ near the bubble wall at $\rho = \rho^*$. In the limit of small ε, he substituted a degenerate potential $V_+(\varphi)$ for the actual potential, $V(\varphi)$. As long as the minima of $V_+(\varphi)$ are very close to φ_{false} and φ_{true}, and as long as ε is small, this substitution is legitimate. Since the "time" has already run out long enough, the viscous damping term in (4.10) may be neglected. The result is that the solution near the wall, $\varphi_{wall}(\rho)$ obeys an equation that is

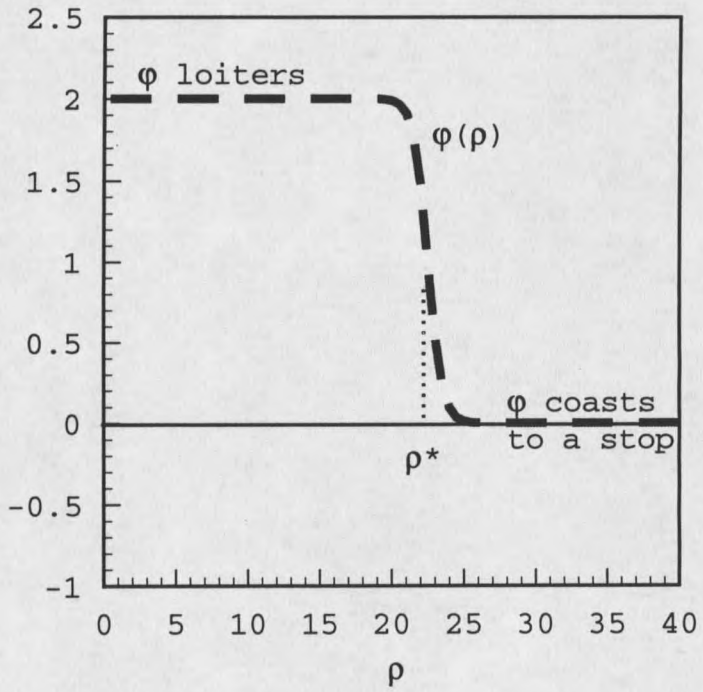

Figure 16. Shape of a typical solution $\varphi(\rho)$ in the thin-wall approximation. I used a hyperbolic tangent function to plot this curve. $\varphi_{true}= 2$, $\varphi_{false}= 0$. Most of the change in $\varphi(\rho)$ occurs near ρ^*.

slightly different from (4.10), viz.

$$\frac{d^2\varphi_{wall}}{d\rho^2} = \frac{dV_+}{d\varphi_{wall}} \quad . \tag{4.12}$$

Coleman showed that the action, S_E^{wall}, of this solution φ_{wall} has a simple relationship to the total bubble action, $S_E^{Coleman}$:

$$S_E^{Coleman} = \frac{27\,\pi^2 \left(S_E^{wall}\right)^4}{2\varepsilon^3} \quad , \tag{4.13}$$

with

$$S_E^{wall} = \int_{\varphi_{true}}^{\varphi_{false}} \sqrt{2V_+}\, d\varphi \quad . \tag{4.14}$$

Also, Coleman showed that the radius which minimizes the bubble action is

$$R = \frac{3S_E^{wall}}{\varepsilon} \quad . \tag{4.15}$$

Therefore one considers R to be the radius of the bubble of true vacuum at the moment of formation. The bubble forms at τ=0 with radius R. The wall of the bubble then moves along a circular trajectory in Euclidean space, $\tau^2 + r^2 = R^2$. The analytic continuation of this motion back to Lorentzian space indicates that the bubble wall will form at time t = 0 with

radius R, followed by expansion of the bubble wall along a hyperbolic trajectory $-t^2 + r^2 = R^2$. Figure 17 shows the two trajectories in one combination graph. Note that the bubble wall speed approaches the speed of light in this approximation. .This completes the review of concepts and techniques for studying vacuum phase transitions.

Before going on, I summarize: I shall borrow from Coleman his procedure for calculating the quantuty B in the thin-wall approximation. Specifically, I shall use dimensionless versions of thin-wall formulas (4.13), (4.14) and (4.15). The actions contain dimensionless potential $V(\sigma)$ and $V_+(\sigma)$:

$$S_E^{\text{Coleman}} = 27\pi \left(\frac{M_{\text{Planck}}}{m}\right)^2 \frac{\left[S_E^{\text{Wall}}\right]^4}{\left[-V(\sigma_2)\right]^3} , \qquad (4.16)$$

$$S_E^{\text{wall}} = \int_{\sigma_2}^{0} \sqrt{2V_+}\, d\sigma . \qquad (4.17)$$

For $V_+(\sigma)$, I use the degenerate 2-3-4 potential, which means I set ξ to a value of 1/2. The dimensionless bubble radius is $\mathbb{X} = mR$:

$$\mathbb{X} = \frac{6\, S_E^{\text{Wall}}}{\left[-V(\sigma_2)\right]} . \qquad (4.18)$$

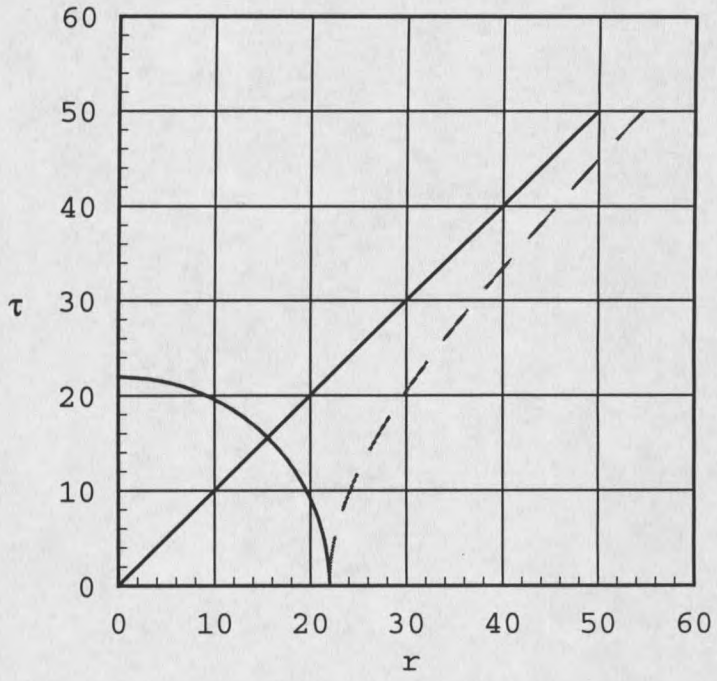

Figure 17. Trajectory of the bubble wall. The solid curve is a circle, $\tau^2 + r^2 = R^2$. The dashed curve is an hyperbola, $-\tau^2 + r^2 = R^2$. R = 22. The 45° diagonal line is the trajectory of a photon, for reference. For convenience, I have identified t and τ in this graph only.

As in chapter 3, σ_2 is the location of the true vacuum in the dimensionless potential $V(\sigma)$. I shall use the formula for the circular trajectory of the bubble wall, but in a dimensionless version,

$$\beta^2 + x^2 = \mathbb{X}^2 \ , \tag{4.19}$$

with a dimensionless time, $\beta = m\tau$.

"Adding" a Boson Star to the Spacetime

This nucleation process with a boson star serving as the nucleation site or "seed," is not a simple process compared to spontaneous decay in an empty spacetime. The objective is to calculate a tunnelling rate for a decay process involving bubble nucleation by a boson star. In formula (4.2) for the tunnelling rate, $\Gamma = Ae^{-B}[1+O(\hbar)]$, the quantity A contains a difficult functional determinant[7]. When I change the parameters of the potential, there will be a change in A. However, since small changes in the argument of an exponential function can overwhelm small changes in almost any other function, it is customary to concentrate on changes in B and neglect smaller changes in A.

It is necessary to revise B to reflect the presence of

[7]C.G. Callan and S. Coleman, "Fate of the False Vacuum. II. First Quantum Corrections," Physical Review D, 16, 1762 (1977).

the boson star. The quantity B for this process is not, in general, a simple one to calculate. As Coleman and De Luccia pointed out,[8] the quantity B is the difference between the action, S_E^{bubble}, for a spacetime containing a bubble which a boson star has nucleated, and the action, $S_E^{\text{no bubble}}$, for a spacetime containing no bubble. Here, the "no bubble" configuration of the spacetime is not empty, as in the earlier case: it contains a boson star.

$$B = S_E^{\text{bubble}} - S_E^{\text{no bubble}} \quad . \tag{4.20}$$

To compare the induced nucleation process with spontaneous formation of bubbles in empty space, I shall compute a ratio, B/B_0, with B_0 equal to the Euclidean action in (4.16), the bubble action in Coleman's thin wall approximation. One might fancy this to be like taking two equal four volumes, one that is empty of boson stars and another that has a boson star in it. Which four-volume will produce a bubble of true vacuum more readily, the empty one or the one with the boson star impurity? If $B/B_0 < 1$, then the second four-volume, with the boson star impurity, wins the bubble production race.

Since I am using the thin-wall approximation as a comparison, which is appropriate only in the limit of small ε, I must restrict my boson star models to the same limit, with

[8] S. Coleman and F. De Luccia, "Gravitational effects on and of vacuum decay," Physical Review D 21, 3305 (1980).

potentials "near" the degenerate potential with $\xi = 1/2$. At the end of this chapter I shall make this concept of "nearness" to degeneracy more precise.

Going toward $\xi = 1/2$, however, does not guarantee the boson star will nucleate a thin-wall bubble. Remember that the thin-wall approximation described spontaneous decay in an empty, flat spacetime. If a boson star is at the center of a bubble, then the spacetime is definitely not empty, and it might not be flat. One must ask if it is legitimate to use the thin-wall approximation for this process. Under what conditions might the thin-wall approximation be legitimate? One can give an answer to these questions after taking a look at the field profiles of the bubble solution and the no-bubble solutions. I will refer to the bubble solution as $\sigma(x)$ and to the star solution as $\sigma_*(x)$, for clarity.

The Euclidean space version of the full boson star solution changes only in that the imaginary time $\tau = it$ replaces the real time t. Recall that the time and spatial dependences separate in the ground state. If one calls the full solution for the star $\Sigma_*(t,x)$, then

$$\Sigma_*(t,x) = e^{-i\omega t}\,\sigma_*(x) \ . \qquad (4.21)$$

The analytic continuation of this full solution to Euclidean space simply changes the oscillating behavior of the complex exponential to that of a decaying exponential. After replacing τ with its dimensionless version, β, the solution

has the form

$$\Sigma_*(\beta,x) = e^{-\Omega\beta}\,\sigma_*(x) \quad . \tag{4.22}$$

With increasing time β, the solution $\Sigma_*(\beta,x)$ decays exponentially from its value at $\beta=0$. This exponential decay will be important in the next section when I consider the notion of "small" boson stars.

The bubble profile will, in general, start out near the true vacuum at σ_2. That is, $\sigma(0) \approx \sigma_2$. It will dip downward toward the false vacuum at zero, perhaps in a gradual curve or perhaps in a sharp curve. For instance, in the extreme thin-wall limit, the bubble profile will have the shape of a step-function. Other shapes are possible outside the thin-wall limit. Figure 16 shows a function whose shape is nearly that of a step-function.

If a boson star nucleates a thin-wall bubble, the interior will contain true vacuum $\sigma = \sigma_{true}$. Outside the wall of the bubble, the spacetime is not filled with false vacuum -- it is filled with the boson star solution, $\sigma_*(x)$, which asymptotically approaches the false vacuum. It is a subtle difference. Instead of approaching the false vacuum along a curve like that in figure 16, now the bubble solution $\sigma(x)$ approaches the star solution $\sigma_*(x)$, and $\sigma_*(x)$ approaches the false vacuum at zero. The asymptotic limit of $\sigma(x)$ is $\sigma_*(x)$, and the asymptotic limit of $\sigma_*(x) = 0$. Figure 18 shows an example of what the exact solution should look like. It is

not easy to make an exact calculation of a bubble solution which, outside $\mathbb{X}$, will smoothly tend toward the star solution as x approaches infinity. To handle this difficulty, I will make an approximation to $\sigma(x)$ with the following working assumptions.

(i) The interior and wall portions of the bubble solution will vary just as if the boson star were not there. I denote this part of the solution as $\sigma_0(x)$, which might not have a thin-wall shape.

(ii) At $x = x_t$, the bubble solution changes over to the star solution $\sigma_*(x)$ in a continuous if not smooth manner.

In mathematical terms, these two assumptions mean that

$$\begin{aligned} &\exists x_t\colon \sigma_0(x_t) = \sigma_*(x_t) \\ &\qquad \sigma(x) = \sigma_0(x), \quad x < x_t \\ &\qquad \sigma(x) = \sigma_*(x), \quad x > x_t \ . \end{aligned} \tag{4.23}$$

Figures 19 and 20 show solutions $\sigma_*(x)$ and $\sigma_0(x)$, respectively. Figure 21 shows how the assumptions (i) and (ii) allow one to graft the tail of $\sigma_*(x)$ onto $\sigma_0(x)$, forming my approximation to the bubble solution, $\sigma(x)$.

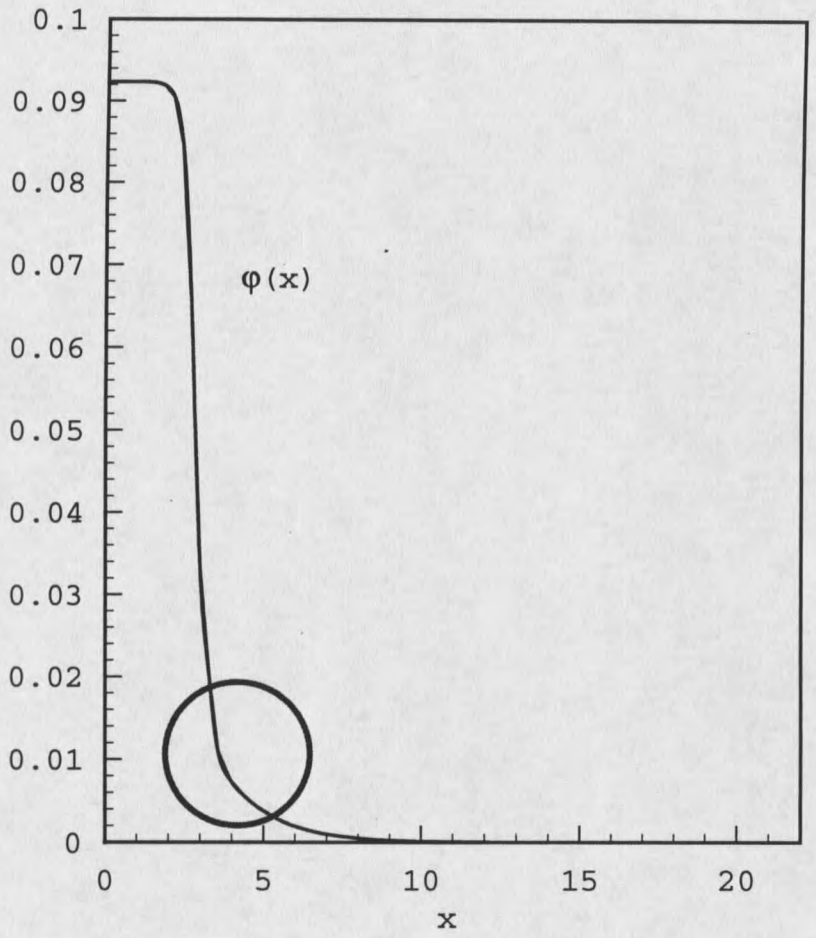

Figure 18. The shape of a smoothly varying bubble solution. Inside the circle, the standard bubble shape (as in figure 16) smoothly changes toward a star solution, which then approaches the false vacuum at $\sigma = 0$ as x approaches infinity.

This nucleation process changes the endpoints of the tunnelling "path." The field σ begins tunnelling into the potential barrier at σ_t instead of zero, as I mentioned in chapter 1. It still tunnels out to the true vacuum at σ_2. Figure 22 shows this subtle but important change. The boson star solution $\sigma_*(x)$ reaches zero as x approaches infinity. Therefore, the value of σ_t will be zero only when the radius of the bubble is infinite, when the potential becomes degenerate. For a potential with $\xi > 1/2$, the value of σ_t will be positive. It now apposite to use σ_t to construct a supplementary parameter, the ratio $\chi \equiv \sigma_t/\sigma_2$. In one way, χ is more useful than ξ. The two limits $\xi \to 1/2$ and $\chi \to 0$ both describe the approach to a degenerate potential. The latter, however, has explicit information about the nucleation by the boson star and about the bubble; the former knows nothing of any boson star.

* * * * * * *

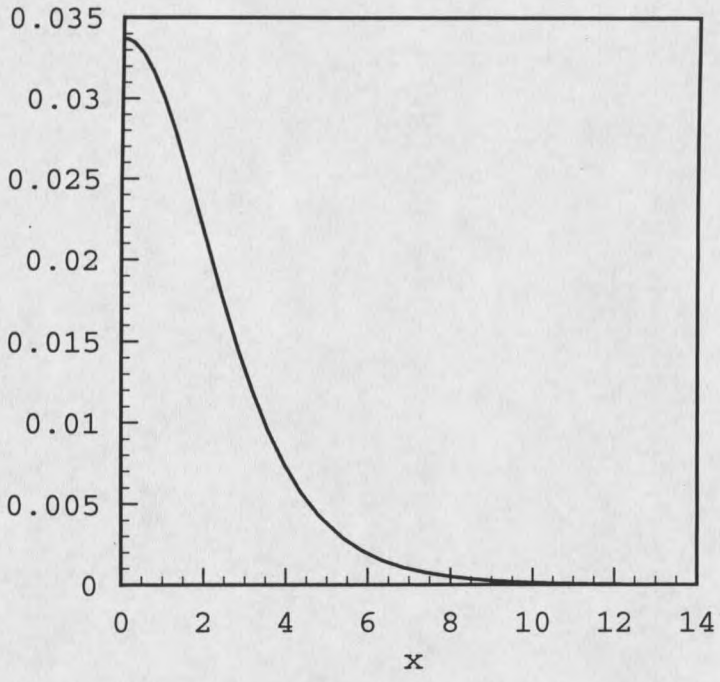

Figure 19. A typical boson star solution $\sigma_*(x)$. This is the shape of the field at $\beta = 0$. At later times, $\beta > 0$, the field will have the same shape but it will have been shrunk by a factor of $\exp(-\Omega\beta)$.

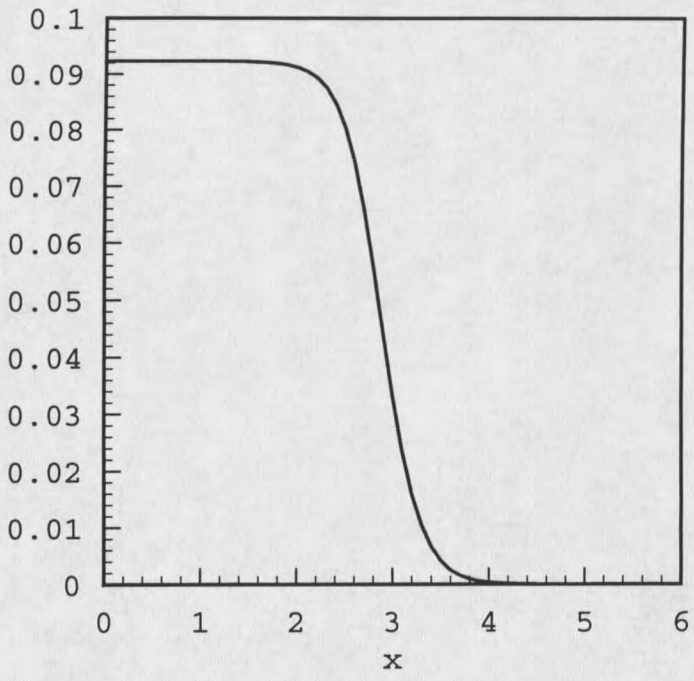

Figure 20. Shape of a bubble profile that is neither thick- nor thin-wall. The dimensionless bubble radius, $\mathbb{X} = 2.882$, is where the curve is at half of its original height.

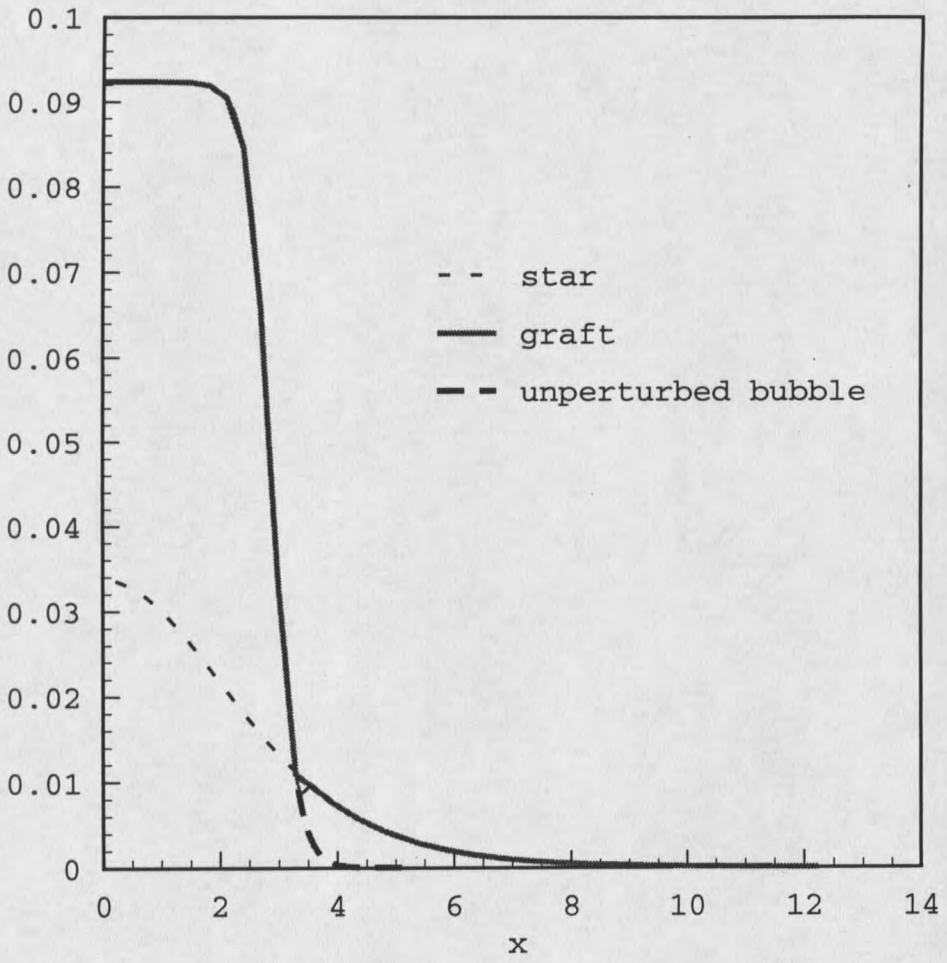

Figure 21. Graft of a star solution onto an unperturbed bubble solution. The solid line represents the generic shape, according to assumption (i) and (ii), for an approximate bubble solution $\sigma(x)$ when a boson star has nucleated the bubble. The boson star solution $\sigma_*(x)$ replaces the empty space bubble solution $\sigma_0(x)$, for this example, at about $x_t = 3.29$. Note that this is slightly larger than $\mathbb{X} = 2.882$, because the bubble solution $\sigma_0(x)$ is not an extreme thin-wall bubble solution.

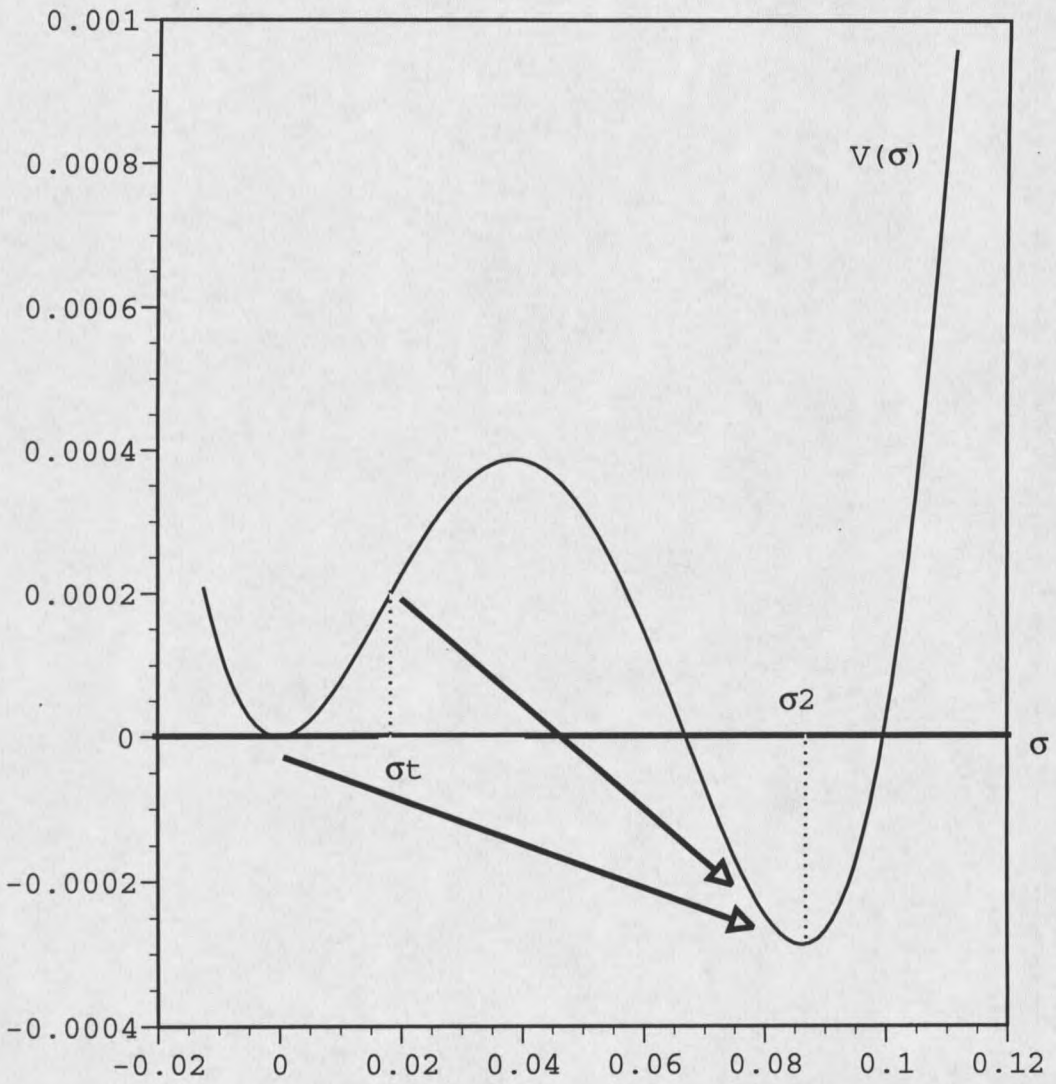

Figure 22. Tunnelling endpoint changes. The upper arrow shows the change that a boson star impurity produces. The lower arrow shows the vacuum-to-vacuum tunnelling process.

The Case of a Small Star Nucleating a Large Bubble

It is interesting to work out the case of a "small" star that nucleates a "large" bubble. In the case of small star-large bubble (SSLB), "small" means that the star's effective radius is much less than $\mathbb{X}$, the bubble radius. This is equivalent to a small value for χ, as I shall now explain.

Star solutions that meet this criterion are easy to find. I pointed out at the conclusion of chapter 3, commenting on figure 12, that relatively large values of $\sigma_*(0)$ generate solutions that correspond to relatively small boson stars. If one has the bubble radius, then one must simply compare it with the effective radius of the star.

With some potentials, nearly all in their family of star solutions meet the SSLB criterion. That is, solutions with $\sigma_*(0) = 0.99\ \sigma_1$ meet the criterions but so do the broad-shouldered solutions with $\sigma_*(0) = 0.10\ \sigma_1$ and smaller. The reasons for this are the following. In general, the bubble radius increases without bound as $\xi \rightarrow 1/2$. When the hills of the upside-down potential are nearly equal in height, the viscous damping force must be waited out, for longer "times," before the "particle" can journey across the valley. This larger "time" means the bubble has a larger radius $\mathbb{X}$. Even the heftiest star, as long as it is localized and has a finite effective radius, will be "small" compared to

degeneracy will always have many SSLB combinations with small values of χ.

One can also run into the opposite problem: with other potentials, none in their family of star solutions meets the SSLB criterion of small-χ. For instance, the bubble solution in figure 21 has $\chi \approx 1/9$. I would not consider that star-bubble combination to meet the SSLB criterion. In general, as ξ increases from 1/2, the bubble radius decreases. When the peaks of the upside-down potential are of significantly different heights, the "particle" needs to start across the valley quickly, while there is still enough viscous damping to slow it down before it overshoots the lower peak. Therefore, stars in a potential far from degeneracy might fail the small χ test. I will briefly discuss star-bubble combinations like this in chapter 5.

The last check for smallness is in the time behavior of the full star solution. In general, the bubble wall trajectory in the Euclidean x-β plane will not necessarily be a circular one, as it is for the bubble formed in empty space. Assume at least that the Euclidean sector trajectory of the bubble wall, $\beta = \Theta(x)$, is bounded on the β-axis by $\mathbb{T}$.

$$\exists \mathbb{T} : \forall x \in \left(0, \mathbb{X}\right), \Theta(x) < \mathbb{T} \ . \qquad (4.24)$$

In other words, one can pencil the trajectory $\Theta(x)$ into a

box, centered at the origin, with dimensions $2\mathbb{X}$ by $2\mathbb{T}$. (If the bubble wall oscillates with period $2\mathbb{T}$ in Euclidean space, then the trajectory is not bounded, but one can make a similar argument for a box that bounds the first full cycle, $0 \leq \beta \leq 2\mathbb{T}$.) Recall that the full solution has the time dependence $\exp(-\Omega\beta)$. This factor is largest when $\beta = 0$. At $\beta = \mathbb{T}$, this factor has diminished. To check the "smallness" of the full solution over time, the quantities to compare are Ω^{-1} and $\mathbb{T}$. If $\mathbb{T} >> \Omega^{-1}$, then $\Sigma_*(\mathbb{T},0)$ will be small. In practice, I found the ratio $\theta \equiv \Sigma_*(\mathbb{T},0)/\sigma_2$ to be very small indeed for the SSLB case, smaller than χ. For example, the star-bubble combination in figure 23 has $\chi = 0.002434$, but it also has $\theta = 0.0001931$. Over a large range of parameters in the 2-3-4 potential, I found that θ was never more than about one percent of χ. Table 1 shows some specific values of both χ and θ for a range of boson star solutions.

Because χ and θ are not necessarily the same, however, there is some asymmetry between the β- and the x-axes in the SSLB configuration. This means that O(4) symmetry would not be a legitimate symmetry of the bubble solution. Samuel and Hiscock alluded to the notion of gravity "pulling in" the bubble wall, deforming it from O(4) symmetry, when the spacetime is not exactly flat.[9] The trajectory of the bubble in the x-β plane deforms to an ellipse; the bubble has only

[9]Samuel and Hiscock, "Compact Objects," 4416.

O(3) symmetry. A similar deformity might occur in the SSLB case due to asymmetry in surface tension. Classically, surface tension in a stretched membrane depends upon a difference in the energy density between its equilibrium state and the stretched state.[10] In bubble nucleation the surface tension is due to the difference in the scalar field between bubble exterior and bubble interior. If $\chi > \theta$, then the difference in field values at $(0,\mathbb{X})$ will be greater than the difference at $(\mathbb{T},0)$. Thus, the surface tensions at those two points will be different, and the bubble will not enjoy O(4) symmetry. However, if χ and θ are both small compared to unity, then the surface tensions at $(0,\mathbb{X})$ and at $(\mathbb{T},0)$ will not be substantially different from the tension in the empty space case. Therefore they can each be neglected, even though the asymmetry is still formally present. In the SSLB case, then, an O(4) bubble will be a good approximation to the actual bubble, and the circular trajectory of the bubble wall in Euclidean space will be appropriate.

One final mention of the ratio χ: The integrals for the wall action, (4.14) and (4.17), depend on the endpoints of tunnelling. Although I shall use the Coleman wall action integral, whose limits are σ_2 and zero, when a boson star nucleates the bubble, the wall action is actually an integral from σ_2 to σ_t, even in the SSLB case.

---

[10]A.L. Fetter and J.D. Walecka, Theoretical Mechanics of Particles and Continua (New York: McGraw-Hill, 1980), 271.

$$S_E^{wall} = \int_{\sigma_2}^{\sigma_t} \sqrt{2V_+}\, d\sigma \ . \qquad (4.25)$$

If one rescales the variable of integration to $u = \sigma/\sigma_2$, then the wall action limits of integration are from unity to χ, viz.

$$S_E^{wall} = \int_1^{\chi} \sqrt{2V_+\left(\sigma_2 u\right)}\, du \ . \qquad (4.26)$$

In the limit of small χ, the upper limit will be close to zero. Thus, in the SSLB case, the change in the wall action due to the boson star will be negligible. This is another useful result, for the wall action is identified as the surface tension of the bubble. Introduction of the boson star does not change the surface tension of the O(4) bubble appreciably in the SSLB case, so the bubble will be the same size as the bubble that forms spontaneously in an empty spacetime, equation (4.18). (A greater surface tension might have shrunk the bubble symmetrically, while preserving its O(4) symmetry.) This partially justifies the use of working assumption (i).

* * * * * * *

Summary of Simplifications in the Small-χ Limit

In summary, the small-χ limit describes the SSLB type of nucleation event. In the SSLB case, it is appropriate to use Coleman's thin-wall approximation for the bubble which has been nucleated by the boson star.

The small-χ limit allows a simpler construction of the bubble solution, $\sigma(x)$: graft the tail of the boson star solution, $\sigma_*(x)$, onto a step function, the shape of $\sigma_0(x)$ in the extreme thin-wall limit, doing so precisely at $x = \mathbb{X}$, not at some value $x_t > \mathbb{X}$ as in figure 21. Figure 23 shows the small-χ SSLB limit on the shape of the bubble solution.

The SSLB simplifies the form of the quantity B. The two integrals are both integrations over all space, but outside the bubble wall, $\sigma(x) = \sigma_*(x)$, by construction. To take advantage of this construction, one divides up $S_E(\sigma)$ into an integral over the inside of the bubble (including the bubble wall) and an integral over the outside of the bubble, viz.

$$\begin{aligned} S_E(\sigma) &= \int d^4x \; \mathcal{L}_E(\sigma) \\ &= \int_{x \le \mathbb{X}} d^4x \, \mathcal{L}_E(\sigma) + \int_{x > \mathbb{X}} d^4x \, \mathcal{L}_E(\sigma) \\ &= \int_{x \le \mathbb{X}} d^4x \, \mathcal{L}_E(\sigma_0) + \int_{x > \mathbb{X}} d^4x \; \mathcal{L}_E(\sigma_*) \; . \end{aligned} \tag{4.27}$$

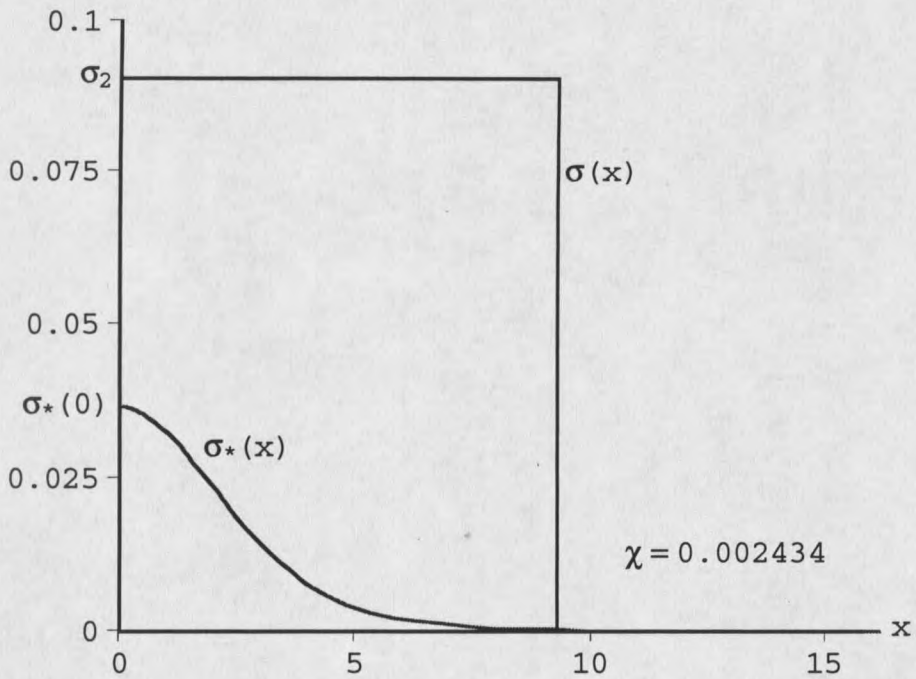

Figure 23. A good SSLB combination, with χ = 0.002434 and θ = 1x10^{-6}. This is an example of the small-χ limit of the more general star-bubble combination in figure 21.

Here, the parameters of the potential are ξ = 0.54 and Λ = 300, with the "bump" at σ_1 = 0.03687 and the true vacuum at σ_2 = 0.09041. The bubble radius is $\mathbb{X}$ = 9.268.

The star solution $\sigma_*(x)$ has $\sigma_*(0)$ = 0.03650, which is 99% of σ_1. The eigenfrequency is $\Omega \approx$ 0.827.

Similarly, one can divide $S_E(\sigma_*)$ into a pair of integrals, although the integrand is just $\sigma_*(x)$ in both pieces, viz.

$$\begin{aligned} S_E(\sigma_*) &= \int d^4x\, \mathcal{L}_E(\sigma_*) \\ &= \int_{x\le\mathbb{X}} d^4x\, \mathcal{L}_E(\sigma_*) + \int_{x>\mathbb{X}} d^4x\, \mathcal{L}_E(\sigma_*) \ . \end{aligned} \tag{4.28}$$

When subtracting $S_E(\sigma_*)$ from $S_E(\sigma)$, the two integrals over the region outside the bubble cancel exactly in the SSLB case. Therefore, the calculation of the quantity B requires only the integrals inside and including the bubble wall.

$$B = \int_{in} d^4x\, \mathcal{L}(\sigma_0) - \int_{in} d^4x\, \mathcal{L}(\sigma_*) = S_E^{Coleman} - S_E^* \ . \tag{4.29}$$

(The reader should understand S_E^* to be an integral over the bubble interior only.) The calculation of S_E^* is simple: the range of integration on the x-β plane is just the interior of the circle of radius $\mathbb{X}$. The form of B/B_0 is also simple:

$$\frac{B}{B_0} = \frac{S_E^{Coleman} - S_E^*}{S_E^{Coleman}} = 1 - \frac{S_E^*}{S_E^{Coleman}} \ . \tag{4.30}$$

This concludes the summary of simplifications one gains from using the small-χ SSLB case.

Methods of Calculation of B

Now I shall explain the details of the calculation of the quantity B for the SSLB case. The bubble action is easy to calculate, using (4.16). Given only the values of parameters Λ and ξ in $V(\sigma)$, one can make all calculations of the bubble action, $S_E(\sigma)$. There is some latitude is in the selection of a degenerate potential $V_+(\sigma)$. I selected the 2-3-4 potential with ξ=1/2 as the degenerate potential, viz.

$$V_+(\sigma) = \sigma^2(1 - \eta^*\sigma)^2 \quad . \tag{4.31}$$

This simplifies the wall action nicely. With explicit σ_t included, that integral is

$$S_E^{wall} = \int_{\sigma_2}^{\sigma_t} (\sigma - \eta^*\sigma^2)\,d\sigma = \sqrt{2}\ \sigma_2{}^2\left[\tfrac{1}{2}(\chi^2-1) - \tfrac{1}{3}\eta^*\sigma_2(\chi^3-1)\right] \quad . \tag{4.32}$$

In the SSLB case, I will set χ to zero in this integral, since it is significantly smaller than unity. This is legitimate because χ^2 is the lowest order of χ in the integral (4.32). Then substitution of (4.32) into (4.16) completes the calculation of $S_E(\sigma)$. One can also calculate $\mathbb{X}$ from S_E^{wall} and $V(\sigma_2)$ as in (4.18).

The calculation of S_E^* is a bit trickier, since it

requires numerical integration over a two-dimensional region of Euclidean space. The full Lagrangian for the boson is

$$\mathcal{L}_E^* = \left(\frac{m^2 M_{Planck}^{\ 2}}{8\pi}\right)\left[\frac{\Omega^2}{B}\sigma_*^{\ 2} + \frac{1}{A}\left(\frac{d\sigma_*}{dx}\right)^2 + V(\sigma_*)\right] . \qquad (4.33)$$

Because the gravity of the boson star is so weak in the SSLB combinations I found, with B(r) different from unity by no more than a few percent in most SSLB combinations, I decided to streamline the S_E^* calculation by setting A and B to unity. This is equivalent to making a flat space calculation.

I integrate $\mathcal{L}_E^*$ over a finite region of the x–β plane, the inside of a circle of radius $\mathbb{X}$, using $x(\beta) = (\mathbb{X}^2 - \beta^2)^{1/2}$ to describe the circular boundary of the region. Performing the angular integration leaves a factor of 4π; converting to dimensionless β and x integrals supplies a factor of m^{-4}. The integral for S_E^* is

$$S_E^* = \left(\frac{1}{2}\frac{M_{Planck}^{\ 2}}{m^2}\right)\int_0^{\mathbb{X}} d\beta \int_0^{x(\beta)} dx\, x^2\left[\Omega^2\sigma_*^{\ 2} + v_*^{\ 2} + V(\sigma_*)\right] . \qquad (4.34)$$

Notice the common factor of $(M_{planck})^2/m^2$ in the expressions for $S_E^{Coleman}$ and S_E^*. This common factor will cancel from the ratio B/B_0, making the results, as expressed in this ratio, independent of m, the mass of the scalar field in question.

The gist of my computer calculation[11] of S_E^* is as follows. First, I calculate a star solution. My main program for calculating star solutions is bxrevise.bas. I rescale the star solutions and format them for numerical integration in the program ez_sys.bas. The integration program is actntrap.bas uses a simple trapezoidal algorithm. The listings of these three programs are in appendix A.

In some of these calculations, the star solution began to diverge before reaching the bubble wall, as I mentioned in chapter 2. Where this occurred, far out along the x-axis, it ought to have been in its asymptotic approach to $\sigma = 0$. In those regions, I substituted zero for the value of the solution. I judged that the action calculation would not change significantly under this substitution.

Boson Stars Efficiently Nucleate First Order Phase Transitions, in the SSLB Limit.

Having calculated the ratio B/B_0 for a large range of star-bubble combinations, I found that the SSLB nucleation process is more efficient at nucleating bubbles of true vacuum than is the spontaneous formation process of Coleman. There are two ways to show this increase in efficiency.

---

[11]W.H. Press et al., Numerical Recipes in FORTRAN: The Art of Scientific Computing, 2nd ed. (New York: Cambridge University Press, 1992), 704, 708, 130.

One way to express the increase in efficiency is by comparing a set of SSLB combinations at fixed ξ and Λ, computing B/B_0 for a family of star solutions. Figure 24 displays this comparison with $\sigma_*(0)$ up to 99% of σ_1. For that figure, I used star-bubble combinations that met the SSLB criterion. The curves in figure 24 show that B/B_0 decreases as the ratio $\sigma_*(0)/\sigma_1$ increases. The nucleation of the phase transition is more efficient by stars with larger values of $\sigma_*(0)$. These tend to be smaller stars, with steeper field profiles. This is one of the reasons I concentrated on small stars: they are better at nucleating vacuum phase transitions. However, for ξ = 0.51, the decrease is less than one percent; for ξ = 0.52, the decrease is less than three percent. Thus, the gain in efficiency near the thin wall limit, ξ=1/2, is measurable, and B differs from B_0 by a few percent. That decrease by a few percent might seem unremarkable until one realizes that B belongs in the exponential part of Γ, and a few percent in an exponential can make for a large effect. For example, consider a star-bubble combination for which B/B_0 is 97%, and consider the coefficient A to be approximately the same for the SSLB process and the empty space process (i.e., $A \approx A_0$.). Let the value of B_0 be 2; then B is 1.94. The ratio of the nucleation rates is

$$\frac{\Gamma}{\Gamma_0} = \frac{Ae^{-B}}{A_0 e^{-B_0}} \approx e^{B_0 - B} = e^{0.06} = 1.06 \ . \qquad (4.35)$$

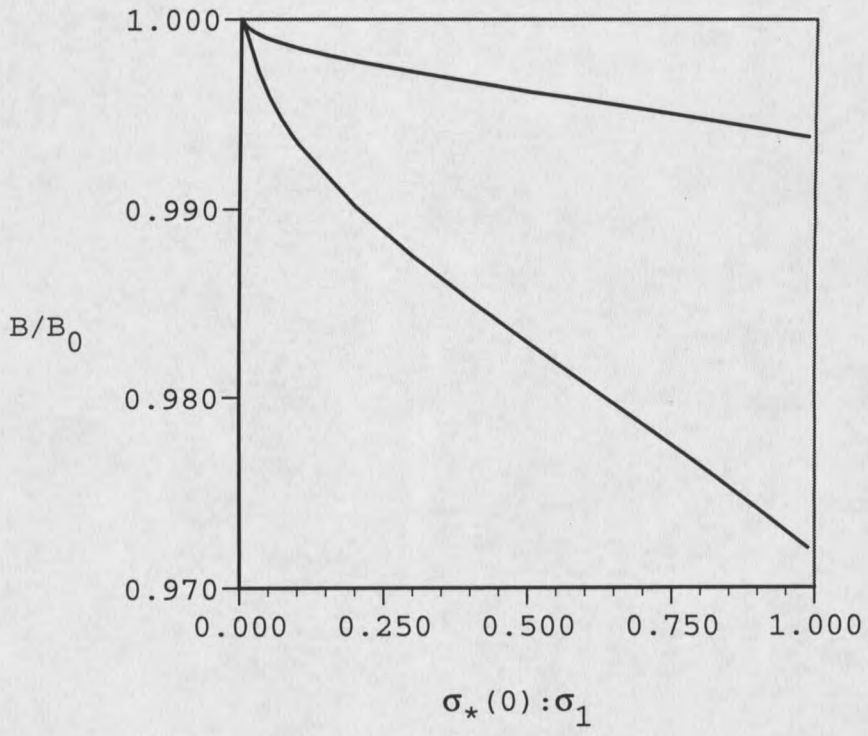

Figure 24. The relative gain in efficiency for SSLB vs. the Coleman process. The upper curve is for star-bubble combinations in a potential with $\xi = 0.51$ and $\Lambda = 300$, the lower curve, for a potential with $\xi = 0.52$ and $\Lambda = 300$.

That means that star-bubble combination induces a mere 6% gain in the nucleation rate. However, let the value of B_0 be 200. Then the ratio Γ/Γ_0 is about 403, a gain in the nucleation rate of over forty thousand percent!

Both curves in figure 24 tend toward $B/B_0 = 1$, as $\sigma_*(0)$ tends to zero, as one might expect. When $\sigma_*(0) = 0$, one no longer has a boson star, per se; the tunnelling is from false to true vacuum -- the Coleman process. Therefore, in the limit of $\sigma_*(0) = 0$, one ought to expect that B/B_0 reaches unity.

Notice that in both curves in figure 24, the biggest decrease in B/B_0 occurs for higher values of $\sigma_*(0)/\sigma_1$ and for higher values of ξ. This pattern is true over a large range in ξ and Λ, so I decided to look only at star-bubble combinations with large fixed values of $\sigma_*(0)/\sigma_1$; I selected $\sigma_*(0) = 0.99\ \sigma_1$, although some star-bubble combinations with $\sigma_*(0)$ values lower than that can meet the SSLB criterion. I wanted to see if B/B_0 decreased as ξ increased. I found that this is true. This is the second way of showing the increase in the bubble nucleation rate. Figure 25 shows a pair of curves of B/B_0 versus increasing ξ, for two values of Λ. As ξ increases the ratio B/B_0 decreases significantly from unity. The boson star wins the bubble production race.

Recall that one limited way to interpret the parameter ξ is as an inverse temperature. In this interpretation, increasing ξ from 1/2 corresponds physically to a decrease in

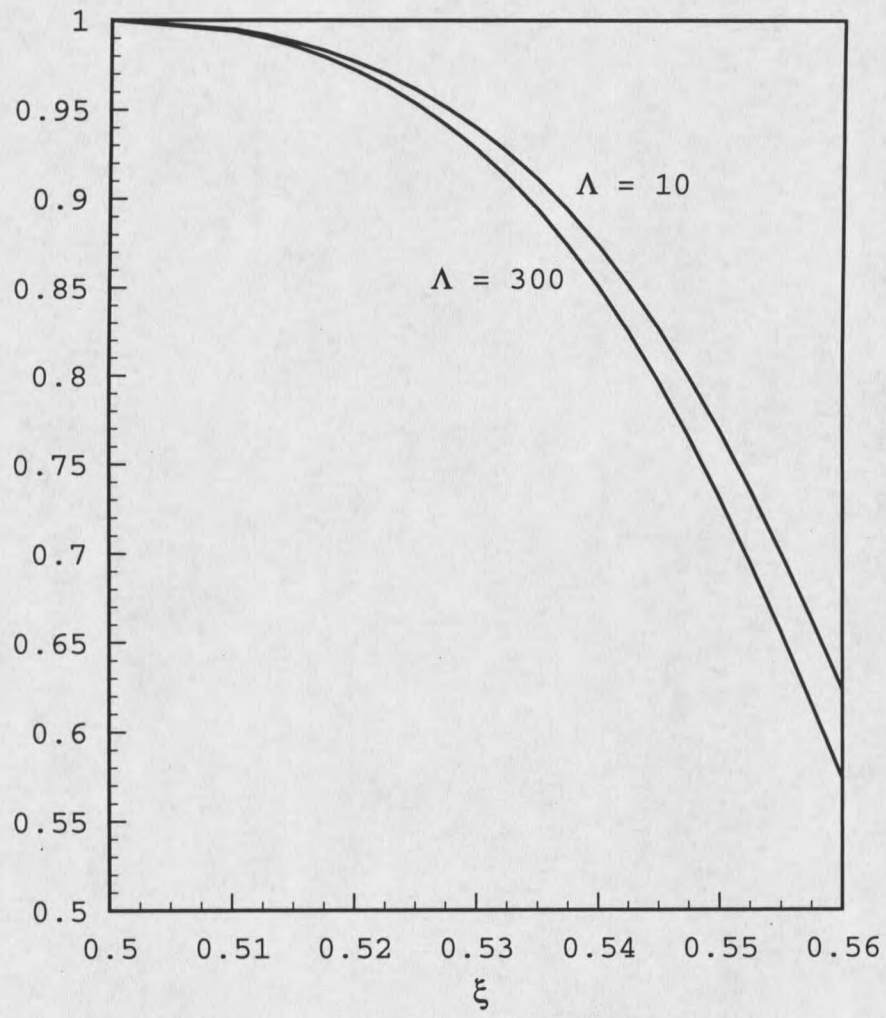

Figure 25. The ratio B/B_0 for two different values of Λ. The efficiency of the SSLB nucleation process is significantly greater than spontaneous bubble formation in empty space.

the temperature of the early universe. As the universe cools below the critical temperature, nucleation of a phase transition by a boson star increases in likelihood.

Before going on, I must rate the star-bubble combinations that I used to produce figure 25. Was the value of χ sufficiently small? What about the value of θ? Table 1 shows the value of χ and θ for several of the solutions from which I plotted figure 25.

Table 1. Values of χ and θ for several SSLB combinations.

	$\Lambda = 10$		$\Lambda = 300$	
ξ	χ	θ	χ	θ
0.51	$< 6 \times 10^{-6}$	$< 10^{-24}$	$< 8 \times 10^{-6}$	$< 10^{-22}$
0.52	$< 2 \times 10^{-5}$	$< 10^{-13}$	$< 9 \times 10^{-5}$	$< 10^{-12}$
0.53	9×10^{-5}	7×10^{-7}	1.6×10^{-4}	2×10^{-9}
0.54	1.7×10^{-3}	6×10^{-7}	2.4×10^{-3}	1×10^{-6}
0.55	0.01	3×10^{-5}	0.013	5×10^{-5}
0.56	0.034	4×10^{-4}	0.04	6×10^{-4}

In figure 25, I ended the range of ξ at 0.56, since this corresponds to a value of χ equal to a few percent. There is a way to judge whether χ is sufficiently small to justify the use of the approximations in the SSLB limit. Consider the integral for the wall action, (4.26). I explicitly included χ as the upper limit, so I denote that integral as $S_E^{wall}(\chi)$.

If I had set the upper limit to zero, the integral would be the wall action for the empty space bubble formation process. I denote this action as $S_E^{wall}(0)$ The ratio of these two integrals, $S_E^{wall}(\chi)/S_E^{wall}(0)$, should approach unity in the small-χ limit. I calculated this ratio for each of the star-bubble combinations in table 1. For none of those combinations is the ratio less than 0.9912. Most of the combinations have a ratio larger than 0.9999, with the ξ = 0.51 ratios being the closest to unity. Therefore, the use of the thin wall bubble in the SSLB limit is justified.

Table 2 shows the dimensionless energy difference between the vacua, $-V(\sigma_2)$, for the same solutions as in Table 1. This dimensionless energy difference is the conventional measure of approach to degeneracy of the potential. Coleman also showed[12] that when $\mathbb{X} >> 1$, his thin-wall approximation process is valid. Therefore, table 2 also shows the dimensionless bubble radius, $\mathbb{X}$.

Notice in table 2 that $-V(\sigma_2)$ is not larger than 0.03 for any of the combinations. This verifies that the potentials in use are fairly close to degeneracy, as indeed they must be for the use of the thin-wall approximation. One minor caveat: Samuel and Hiscock called the robustness of the thin-wall approximation into question,[13] comparing Coleman's

---

[12]Coleman, "Fate of the false vacuum," 2933.

[13]Samuel, "Thin-wall approximation," 254.

approximate bubble action to the action of the exact bubble solution. They found the thin-wall approximation to be rather unsatisfactory for $-V(\sigma_2)$ greater than about 0.02. That caveat is not a major cause for worry here, though, for $-V(\sigma_2)$ is larger than 0.02 in only two of the combinations at $\Lambda = 10$. In the $\Lambda = 300$ case, the thin-wall approximation is quite good.

Table 2. Conventional validity measures for Coleman's thin-wall approximation, over a range of SSLB combinations.

	$\Lambda = 10$		$\Lambda = 300$	
ξ	$\mathbb{X}$	$-V(\sigma_2)$	$\mathbb{X}$	$-V(\sigma_2)$
0.51	46.93	4.2×10^{-3}	46.93	1.4×10^{-4}
0.52	21.87	8.6×10^{-3}	21.87	2.9×10^{-4}
0.53	13.48	0.013	13.48	4.5×10^{-4}
0.54	9.268	0.018	9.268	6.2×10^{-4}
0.55	6.728	0.024	6.728	8.0×10^{-4}
0.56	5.026	0.030	5.026	9.8×10^{-4}

Summary and Conclusions

I have used the 2-3-4 scalar potential to model finite-temperature effective potentials in which first order phase transitions are possible. I examined the process of nucleation of a phase transition by a boson star, a non-vacuum configuration of the scalar field, when the potential is fairly close to degeneracy. I focused on a special subset of all possible combinations of boson star and vacuum bubble; I call this subset the "small-star-large bubble" limit. For this limit, I crafted an approximation scheme that had several convenient simplifications. In that limit I calculated the quantity B in the bubble formation rate per unit four-volume, Γ/V. I have shown that the nucleation of vacuum phase transitions by boson stars is more efficient than the empty space bubble formation process of Coleman. In fact, when the system is supercooled below the critical temperature, the increase in the bubble formation rate is significant when boson stars are present.

It is reasonable to have found a significant increase in the bubble nucleation rate for boson stars in the SSLB limit. As I mentioned earlier in this chapter, other scientists have found that "impurities" in the form of other astrophysical objects have an enhancing effect on the nucleation rate. The boson star is the latest addition to that list of exotic

astrophysical objects.

Another reasonable result is that this increase in nucleation rate is more pronounced for larger values of ξ, which are equivalent to potentials with a deeper well. That is, one would expect the field to tunnel more easily when either a deep well is present or a low barrier is present.

One can also say that the presence of the boson star is a way of making the potential barrier smaller. Since $\sigma_t > 0$, the field tunnels from part way up the potential barrier, instead of from the bottom of the potential well at $\sigma = 0$. For this reason, one can also say that the results in figure 25 are reasonable. In fact, for a very small investment in χ, climbing the potential barrier a very small amount, one gains a windfall of enhancement in the nucleation rate. In chapter 5, I will have more to say about other star-bubble configurations with greater values of χ.

However, the windfall enhancement of the nucleation rate only occurs for potentials farther and farther removed from degeneracy. The potential moves away from degeneracy as the temperature of the universe drops below the critical temperature of the field theory in question. Will the universe cool more rapidly than the field will tunnel? Using the 2-3-4 potential only as a model, and without a particular field theory (e.g., electroweak), it is not possible to calculate the exact nucleation rate. (One needs to calculate the coefficient A, which is a thorny matter indeed.)

Nonetheless, the boson star's enhancement of the nucleation rate presents an interesting effect. For once the temperature of the system dips past the critical temperature, any boson stars present will have acquired a decided advantage in the race to produce bubbles of true vacuum.

The SSLB limit describes only a subset of all the possible bubble-star combinations. There are several interesting classes of star-bubble combinations outside the SSLB limit. Also, there are several refinements one can also make to the SSLB calculations I have done. In chapter 5 I will discuss these topics briefly.

CHAPTER 5

WHAT ADDITIONAL TASKS REMAIN FOR THE FUTURE?

This thesis covers the SSLB limit, which is only one subset of all possible star-bubble combinations. Several other interesting types of star-bubble combination exist.

The first type is nucleation of a vacuum phase transition by a boson star that is much larger than the bubble. If the bubble is small enough, then the star solution will be nearly constant over the interior of the bubble. Figure 26 shows a closeup view of such a star-bubble combination. The bubble wall will be small compared to the star for potentials very far from degeneracy, where the Coleman thin-wall approximation loses validity. Therefore, the alternate thin-wall approximation of Samuel and Hiscock might be acceptable. If that approximation turns out to be unacceptable, one must calculate the bubble solution exactly, by integrating (4.9). This type of nucleation event may be approximated by $\sigma_*(x) \approx \sigma_*(0)$ over the inside of the bubble, making the calculation of the star action quite easy. With-out contributions from the $d\sigma_*/dx$ term in the Lagrangian, the star action inside the bubble will diminish markedly compared to the SSLB star action, which was calculated over most of the spatial extent of the star. Therefore, this type of star-bubble combination

might yield a very significant decrease in B, and a significant increase in the bubble formation rate.

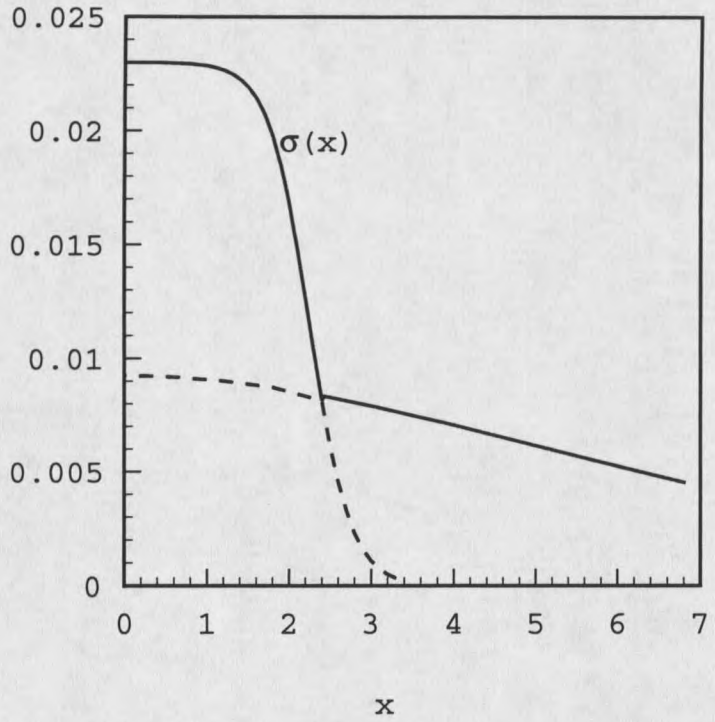

Figure 26. Star bubble combination in which the bubble is much smaller than the star. The solid line shows the bubble solution $\sigma(x)$; the dashed lines show the star solution $\sigma_*(x)$ inside the bubble and the remainder of $\sigma_0(x)$ outside the bubble. Notice that the tunnelling will begin from $\sigma = \sigma_t$ quite close to $\sigma_*(0)$, so χ will not be small as in combinations of the SSLB type.

Another interesting type of star-bubble combination is one in which the star and the bubble are roughly the same size. As Samuel and Hiscock showed,[1] gravitationally compact objects enhance the bubble nucleation rate when the object and the bubble are of comparable size. This kind of

[1]Samuel and Hiscock, "Compact objects," 4416.

nucleation, with star and bubble roughly the same size, does not require a potential with a drastic departure from degeneracy. Inside the bubble, the star solution will change value significantly, unlike the previous type. Tunnelling will occur from $\sigma = \sigma_t$, which will be somewhere between $\sigma_*(0)$ and zero. In figure 27, I show a star-bubble combination of this kind. The reservations about approximations for the large star-small bubble combination also apply for the case of a star of roughly the same size as the bubble..

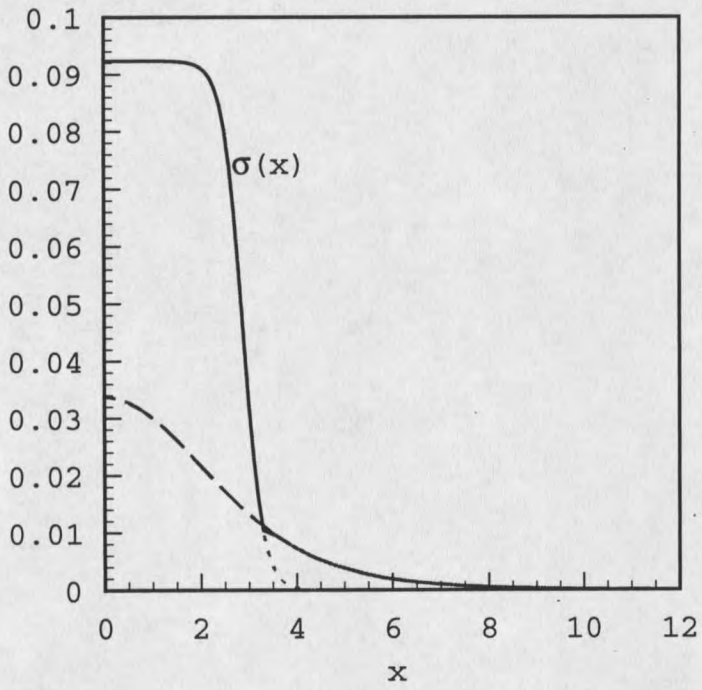

Figure 27. A bubble-star combination in which the star and the bubble are of comparable size.

In both types of nucleation events, one will have to make a serious modification to the shape of the bubble wall trajectory in the x-β plane. The reason for this is that the surface tension asymmetry will <u>not</u> be negligible in these two types of nucleation events. Thus, one must expect the bubble to deform significantly from the O(4) symmetry that was so useful in the SSLB limit. If the bubble wall trajectory is only elliptical on the x-β plane, then the bubble will not expand as rapidly, and the bubble wall will not asymptotically approach the speed of light but some smaller terminal velocity. The bubble wall trajectory might be even more complicated -- for instance,it might be periodic on the x-β plane. In any case, one must develop a quantitative method to handle the surface tension asymmetry and its effect on the bubble wall trajectory.

* * * * * * *

This concludes my thesis, in which I have shown how boson stars efficiently nucleate vacuum phase transitions. However, I hope it is not the end of the study of this small but interesting problem. For cosmology and astrophysics are small parts in the general scientific enterprise, the noble quest for understanding of the wide world which God created.

REFERENCES CITED

Alpher, R.A., and Herman, R. "Evolution of the Universe," Nature, 162, 774 (1948).

Arnett, A.S., Weather Modification by Cloud Seeding. New York: Academic Press, 1980.

Banks, T., Bender,C.M., and Wu, T.T., "Coupled Anharmonic Oscillators. I. Equal-Mass Case," Physical Review D, 8, 3346 (1973).

Berezin, V.A., Kuzmin, V.A., and Tkachev, I.I., "Black holes initiate false-vacuum decay," Physical Review D 43, R3112 (1990).

Callan, C.G., and Coleman, S., "Fate of the False Vacuum. II. First Quantum Corrections," Physical Review D, 16, 1762 (1977).

Coleman, S., "Fate of the false vacuum: Semiclassical theory," Physical Review D, 15, 2929 (1977).

Coleman, S., and De Luccia, F., "Gravitational effects on and of vacuum decay," Physical Review D 21, 3305 (1980).

Colpi, M., Shapiro, S.L., Wasserman, I., "Boson Stars: Gravitational Equilibria of Self-Interacting Scalar Fields," Physical Review Letters, 57, 2485 (1986).

Dicke, R.H., et al., "Cosmic Black-body Radiation," Astrophysical Journal, 142, 414 (1965).

Fetter, A.L., and Walecka, J.D., Theoretical Mechanics of Particles and Continua. New York: McGraw-Hill, 1980.

Hiscock, W.A., "Can black holes nucleate vacuum phase transitions?" Physical Review D 35, 1161 (1987).

Hubble, E.P., "A Relation between Radial Distance and Velocity among Extra-Galactic Nebulae," Proceedings of the National Academy of Sciences, 15, 168 (1929).

Jetzer, P., "Boson stars," Physics Report, 220, 163 (1992)

Kaup, D.J., "Klein-Gordon Geon," Physical Review, 172, 1331 (1968).

Landau, L.D., and Lifshitz, E.M., Statistical Physics (Part I). trans. J.B. Sykes and M.J. Kearsley, 3rd ed. Oxford: Pergamon Press, 1980.

Lee, T.D., and Pang, Y., "Nontopological solitons," Physics Reports, 221, 251 (1992).

Linde, A., Particle Physics and Inflationary Cosmology. New York: Harwood Academic Publishers, 1990.

Mendell, G., and Hiscock, W.A., "Gravitational nucleation of vacuum phase transitions by compact objects," Physical Review D 39, 1537 (1989).

Misner, C.W., Thorne, K.S., and Wheeler, J.A., Gravitation. San Francisco: Freeman, 1973.

Oppenheimer, R., and Volkoff, G.M., "On Massive Neutron Cores," Physical Review, 55, 374 (1939).

Peebles, P.J.E., Principles of Physical Cosmology. Princeton: Princeton University Press, 1993.

Penzias, A.A., and Wilson, R.W., "A Measurement of Excess Antenna Temperature at 4080 Mc/s," Astrophysical Journal, 142, 419 (1965).

Press, W.H., et al., Numerical Recipes in FORTRAN: The Art of Scientific Computing, 2nd ed. New York: Cambridge University Press, 1992.

Ruffini,R., and Bonazzola, S., "Systems of Self-Gravitating Particles in General Relativity and the Concept of an Equation of State," Physical Review, 187, 1767 (1969).

Samuel, D.A., and Hiscock, W.A., "Gravitationally compact objects as nucleation sites for first-order vacuum phase transitions," Physical Review D, 45, 4411 (1992).

Samuel, D.A., and Hiscock, W.A., "'Thin-wall' approximations to vacuum decay rates," Physics Letters B, 261, 251 (1991).

Wald, R.M., General Relativity. Chicago: University of Chicago Press, 1984.

Wheeler, J.A., "Geons," Physical Review, 97, 511 (1955).

APPENDIX

COMPUTER PROGRAMS

I wrote these programs in the Quick Basic language. The first listing is for bxrevise.bas, the principal program I used for calculating boson star solutions. The second listing is ez_sys.bas, which I used to rescale the boson star solutions and format them for numerical integration. The third listing is for actntrap.bas, which calculated the action integrals. The specifications of a particular boson star solution, i.e., eigenfrequency Ω and $B(\infty)$, are output from bxrevise.bas and input for ez_sys.bas. Data files constructed by ez_sys.bas, containing boson star solutions, were input for actntrap.bas.

```
'bxrevise.bas
DECLARE SUB headr (eta#, LAMBDA#, OMEGA#, s0#, pass#)
DECLARE FUNCTION Sbar1# (s0#, eta#, LAMBDA#)
DECLARE FUNCTION BubbleX# (s0#, eta#, LAMBDA#)
DECLARE FUNCTION Vbar# (s#, eta#, LAMBDA#)
DECLARE FUNCTION F# (x#)
DECLARE FUNCTION epsilon# (eta#, LAMBDA#)
DECLARE FUNCTION Rbubble# (eta#, LAMBDA#)
DECLARE FUNCTION bump# (eta#, LAMBDA#)
DECLARE FUNCTION truevac# (eta#, LAMBDA#)
DECLARE FUNCTION DVAC# (LAMBDA#, eta#)
DECLARE SUB vps2 (xx#(), ss#(), size#)
DECLARE SUB SORTN (aa#(), n#)
DECLARE SUB vps (xx#(), ss#(), size#)
DECLARE SUB SORT4 (d#())
DECLARE FUNCTION S41# (x#, s#, v#, A#, B#, OMEGA#, eta#, LAMBDA#, sk31#,
sk32#, sk33#, sk34#, h#)
DECLARE FUNCTION S42# (x#, s#, v#, A#, B#, OMEGA#, eta#, LAMBDA#, s0#,
B0#, sk31#, sk32#, sk33#, sk34#, h#)
DECLARE FUNCTION S43# (x#, s#, v#, A#, B#, OMEGA#, eta#, LAMBDA#, sk31#,
sk32#, sk33#, sk34#, h#)
DECLARE FUNCTION S44# (x#, s#, v#, A#, B#, OMEGA#, eta#, LAMBDA#, sk31#,
sk32#, sk33#, sk34#, h#)
DECLARE FUNCTION S31# (x#, s#, v#, A#, B#, OMEGA#, eta#, LAMBDA#, sk21#,
sk22#, sk23#, sk24#, h#)
DECLARE FUNCTION S32# (x#, s#, v#, A#, B#, OMEGA#, eta#, LAMBDA#, s0#,
B0#, sk21#, sk22#, sk23#, sk24#, h#)
DECLARE FUNCTION S33# (x#, s#, v#, A#, B#, OMEGA#, eta#, LAMBDA#, sk21#,
sk22#, sk23#, sk24#, h#)
DECLARE FUNCTION S34# (x#, s#, v#, A#, B#, OMEGA#, eta#, LAMBDA#, sk21#,
sk22#, sk23#, sk24#, h#)
```

```
DECLARE FUNCTION S21# (x#, s#, v#, A#, B#, OMEGA#, eta#, LAMBDA#, sk11#,
sk12#, sk13#, sk14#, h#)
DECLARE FUNCTION S22# (x#, s#, v#, A#, B#, OMEGA#, eta#, LAMBDA#, s0#,
B0#, sk11#, sk12#, sk13#, sk14#, h#)
DECLARE FUNCTION S23# (x#, s#, v#, A#, B#, OMEGA#, eta#, LAMBDA#, sk11#,
sk12#, sk13#, sk14#, h#)
DECLARE FUNCTION S24# (x#, s#, v#, A#, B#, OMEGA#, eta#, LAMBDA#, sk11#,
sk12#, sk13#, sk14#, h#)
DECLARE FUNCTION S11# (x#, s#, v#, A#, B#, OMEGA#, eta#, LAMBDA#, h#)
DECLARE FUNCTION S12# (x#, s#, v#, A#, B#, OMEGA#, eta#, LAMBDA#, s0#,
B0#, h#)
DECLARE FUNCTION S13# (x#, s#, v#, A#, B#, OMEGA#, eta#, LAMBDA#, h#)
DECLARE FUNCTION S14# (x#, s#, v#, A#, B#, OMEGA#, eta#, LAMBDA#, h#)
DECLARE FUNCTION DV# (x#, s#, v#, A#, B#, OMEGA#, eta#, LAMBDA#, s0#,
B0#)
DECLARE FUNCTION DS# (x#, s#, v#, A#, B#, OMEGA#, eta#, LAMBDA#)
DECLARE FUNCTION DB# (x#, s#, v#, A#, B#, OMEGA#, eta#, LAMBDA#)
DECLARE FUNCTION DA# (x#, s#, v#, A#, B#, OMEGA#, eta#, LAMBDA#)
DEFDBL A-Z

'The several arrays for my Runge-Kutta adaptive step size procedure.
DIM SHARED xout(0 TO 500): DIM SHARED xdata(0 TO 500)
DIM SHARED x1out(0 TO 500): DIM SHARED x2out(0 TO 500)

DIM SHARED sout(0 TO 500): DIM SHARED sdata(0 TO 500)
DIM SHARED s1out(0 TO 500): DIM SHARED s2out(0 TO 500)

DIM SHARED vout(0 TO 500): DIM SHARED vdata(0 TO 500)
DIM SHARED v1out(0 TO 500): DIM SHARED v2out(0 TO 500)

DIM SHARED Aout(0 TO 500): DIM SHARED Adata(0 TO 500)
DIM SHARED A1out(0 TO 500): DIM SHARED A2out(0 TO 500)

DIM SHARED Bout(0 TO 500): DIM SHARED Bdata(0 TO 500)
DIM SHARED B1out(0 TO 500): DIM SHARED B2out(0 TO 500)

DIM SHARED Mdata(0 TO 500)
DIM SHARED d(1 TO 4)
DIM SHARED dd(1 TO 500): DIM SHARED cc(1 TO 500)
DIM SHARED xx(1 TO 500): DIM SHARED ss(1 TO 500)
DIM SHARED aa(1 TO 500)

CLS

'File #1 holds entire solutions for one or mere passes across s0 values.
ff$ = "a:\dxx26.prn"
OPEN ff$ FOR APPEND AS #1
PRINT #1, ff$, DATE$, TIME$
PRINT #1, "parameters = {eps, scales, scalev, scaleA, scaleB, OMEGAtol,
passes}"
PRINT #1, "             {OMEGA, eta, LAMBDA, xi, bump, s(0):bump, X}"
```

```
PRINT #1, "data =       {x, s(x), v(x), 1 - A(x), 1 - B(x), M(x), 1 -
B(infinity)}"

'File #2 holds solution parameters and the target OMEGA value.
gg$ = "a:\nudata26.prn"
OPEN gg$ FOR APPEND AS #2
PRINT #2, gg$, "data summary from bxrevise.bas", DATE$, TIME$
PRINT #2,

'energy parameters {OMEGA,eta,LAMBDA}
CONST LAMBDA = 100
FOR q = 0 TO 20 'q counts the number of levels of eta of the solutions.
eta = SQR(LAMBDA * (.51# + q * .0025))
'Setting eta = 0 will compare with Colpi, et al., Fig.(3)
'Setting LAMBDA = 0 will compare with Ruffini and Bonazzola figures.

'BOUNDARY CONDITIONS: s(0),v(0),A(0),B(0).
'Central redshift is OMEGA^2/B(0); adjust so that B("infinity") -> 1.
ss1 = bump(eta, LAMBDA): ss2 = truevac(eta, LAMBDA)
FOR r = 0 TO 0 STEP 1  'r counts the number of s0 values between 0 and
ss1.
s0 = (.99# + .1# * r) * ss1: B0 = 1
v0 = 0: A0 = 1: x0 = 0

'Runge-Kutta adaptive step size parameters.
CONST safety = .9: CONST eps = .000002#
OMEGAtol = .0000000000000002#

h = .2: maxsteps = 300
minshrink = .1: minboost = 1.05: maxboost = 5
scales = s0: scalev = -.7: scaleA = 4: scaleB = .1

PRINT #1, TIME$
'OMEGA bisection parameters.
OMEGA1 = .01: OMEGA2 = 1.2
OMEGA = OMEGA2

FOR p = 1 TO 60          'p counts the number of OMEGA bisection passes.
OMEGACOPY = OMEGA
x = x0: s = s0: v = v0: A = A0: B = B0

headr eta, LAMBDA, OMEGA, s0, p

FOR i = 1 TO maxsteps    'i counts out the Runge Kutta solution steps,
                         'including "false" steps.
```

```
'================================================
'======== RUNGE KUTTA SOLUTION SECTION ========
'
'
'The U(i,j) are the solution parts after one full step.
U11 = S11(x, s, v, A, B, OMEGA, eta, LAMBDA, h)
U12 = S12(x, s, v, A, B, OMEGA, eta, LAMBDA, s0, B0, h)
U13 = S13(x, s, v, A, B, OMEGA, eta, LAMBDA, h)
U14 = S14(x, s, v, A, B, OMEGA, eta, LAMBDA, h)


U21 = S21(x, s, v, A, B, OMEGA, eta, LAMBDA, U11, U12, U13, U14,
h)
U22 = S22(x, s, v, A, B, OMEGA, eta, LAMBDA, s0, B0, U11, U12,
U13, U14, h)
U23 = S23(x, s, v, A, B, OMEGA, eta, LAMBDA, U11, U12, U13, U14,
h)
U24 = S24(x, s, v, A, B, OMEGA, eta, LAMBDA, U11, U12, U13, U14,
h)

U31 = S31(x, s, v, A, B, OMEGA, eta, LAMBDA, U21, U22, U23, U24,
h)
U32 = S32(x, s, v, A, B, OMEGA, eta, LAMBDA, s0, B0, U21, U22,
U23, U24, h)
U33 = S33(x, s, v, A, B, OMEGA, eta, LAMBDA, U21, U22, U23, U24,
h)
U34 = S34(x, s, v, A, B, OMEGA, eta, LAMBDA, U21, U22, U23, U24,
h)

U41 = S41(x, s, v, A, B, OMEGA, eta, LAMBDA, U31, U32, U33, U34,
h)
U42 = S42(x, s, v, A, B, OMEGA, eta, LAMBDA, s0, B0, U31, U32,
U33, U34, h)
U43 = S43(x, s, v, A, B, OMEGA, eta, LAMBDA, U31, U32, U33, U34,
h)
U44 = S44(x, s, v, A, B, OMEGA, eta, LAMBDA, U31, U32, U33, U34,
h)

'The arrays s1out(), etc. are the solutions after one full step.
s1out(i) = s + (U11 + 2 * U21 + 2 * U31 + U41) / 6
v1out(i) = v + (U12 + 2 * U22 + 2 * U32 + U42) / 6
A1out(i) = A + (U13 + 2 * U23 + 2 * U33 + U43) / 6
B1out(i) = B + (U14 + 2 * U24 + 2 * U34 + U44) / 6
x1out(i) = x + h

'The Y(i,j) are the solution parts after one half-step.
Y11 = S11(x, s, v, A, B, OMEGA, eta, LAMBDA, h / 2)
Y12 = S12(x, s, v, A, B, OMEGA, eta, LAMBDA, s0, B0, h / 2)
Y13 = S13(x, s, v, A, B, OMEGA, eta, LAMBDA, h / 2)
Y14 = S14(x, s, v, A, B, OMEGA, eta, LAMBDA, h / 2)
```

```
        Y21 = S21(x, s, v, A, B, OMEGA, eta, LAMBDA, Y11, Y12, Y13, Y14,
h / 2)
        Y22 = S22(x, s, v, A, B, OMEGA, eta, LAMBDA, s0, B0, Y11, Y12,
Y13, Y14, h / 2)
        Y23 = S23(x, s, v, A, B, OMEGA, eta, LAMBDA, Y11, Y12, Y13, Y14,
h / 2)
        Y24 = S24(x, s, v, A, B, OMEGA, eta, LAMBDA, Y11, Y12, Y13, Y14,
h / 2)

        Y31 = S31(x, s, v, A, B, OMEGA, eta, LAMBDA, Y21, Y22, Y23, Y24,
h / 2)
        Y32 = S32(x, s, v, A, B, OMEGA, eta, LAMBDA, s0, B0, Y21, Y22,
Y23, Y24, h / 2)

        Y33 = S33(x, s, v, A, B, OMEGA, eta, LAMBDA, Y21, Y22, Y23, Y24,
h / 2)
        Y34 = S34(x, s, v, A, B, OMEGA, eta, LAMBDA, Y21, Y22, Y23, Y24,
h / 2)

        Y41 = S41(x, s, v, A, B, OMEGA, eta, LAMBDA, Y31, Y32, Y33, Y34,
h / 2)
        Y42 = S42(x, s, v, A, B, OMEGA, eta, LAMBDA, s0, B0, Y31, Y32,
Y33, Y34, h / 2)
        Y43 = S43(x, s, v, A, B, OMEGA, eta, LAMBDA, Y31, Y32, Y33, Y34,
h / 2)
        Y44 = S44(x, s, v, A, B, OMEGA, eta, LAMBDA, Y31, Y32, Y33, Y34,
h / 2)

        'The values shalf, etc. are the solution after one half-step.
        shalf = s + (Y11 + 2 * Y21 + 2 * Y31 + Y41) / 6
        vhalf = v + (Y12 + 2 * Y22 + 2 * Y32 + Y42) / 6
        Ahalf = A + (Y13 + 2 * Y23 + 2 * Y33 + Y43) / 6
        Bhalf = B + (Y14 + 2 * Y24 + 2 * Y34 + Y44) / 6
        xhalf = x + h / 2

        'The W(i,j) are the solution parts after another half-step.
        W11 = S11(xhalf, shalf, vhalf, Ahalf, Bhalf, OMEGA, eta, LAMBDA,
h / 2)
        W12 = S12(xhalf, shalf, vhalf, Ahalf, Bhalf, OMEGA, eta, LAMBDA,
s0, B0, h / 2)
        W13 = S13(xhalf, shalf, vhalf, Ahalf, Bhalf, OMEGA, eta, LAMBDA,
h / 2)
        W14 = S14(xhalf, shalf, vhalf, Ahalf, Bhalf, OMEGA, eta, LAMBDA,
h / 2)

        W21 = S21(xhalf, shalf, vhalf, Ahalf, Bhalf, OMEGA, eta, LAMBDA,
W11, W12, W13, W14, h / 2)
        W22 = S22(xhalf, shalf, vhalf, Ahalf, Bhalf, OMEGA, eta, LAMBDA,
s0, B0, W11, W12, W13, W14, h / 2)
        W23 = S23(xhalf, shalf, vhalf, Ahalf, Bhalf, OMEGA, eta, LAMBDA,
W11, W12, W13, W14, h / 2)
```

```
        W24 = S24(xhalf, shalf, vhalf, Ahalf, Bhalf, OMEGA, eta, LAMBDA,
W11, W12, W13, W14, h / 2)

        W31 = S31(xhalf, shalf, vhalf, Ahalf, Bhalf, OMEGA, eta, LAMBDA,
W21, W22, W23, W24, h / 2)
        W32 = S32(xhalf, shalf, vhalf, Ahalf, Bhalf, OMEGA, eta, LAMBDA,
s0, B0, W21, W22, W23, W24, h / 2)
        W33 = S33(xhalf, shalf, vhalf, Ahalf, Bhalf, OMEGA, eta, LAMBDA,
W21, W22, W23, W24, h / 2)
        W34 = S34(xhalf, shalf, vhalf, Ahalf, Bhalf, OMEGA, eta, LAMBDA,
W21, W22, W23, W24, h / 2)

        W41 = S41(xhalf, shalf, vhalf, Ahalf, Bhalf, OMEGA, eta, LAMBDA,
W31, W32, W33, W34, h / 2)
        W42 = S42(xhalf, shalf, vhalf, Ahalf, Bhalf, OMEGA, eta, LAMBDA,
s0, B0, W31, W32, W33, W34, h / 2)

        W43 = S43(xhalf, shalf, vhalf, Ahalf, Bhalf, OMEGA, eta, LAMBDA,
W31, W32, W33, W34, h / 2)
        W44 = S44(xhalf, shalf, vhalf, Ahalf, Bhalf, OMEGA, eta, LAMBDA,
W31, W32, W33, W34, h / 2)

        'The values s2, etc. are the solutions after another half-step.
        s2 = shalf + (W11 + 2 * W21 + 2 * W31 + W41) / 6
        v2 = vhalf + (W12 + 2 * W22 + 2 * W32 + W42) / 6
        A2 = Ahalf + (W13 + 2 * W23 + 2 * W33 + W43) / 6
        B2 = Bhalf + (W14 + 2 * W24 + 2 * W34 + W44) / 6

        '================================================
        '======== ADAPTIVE STEP SIZE SUBSECTION ========
        '
        '
        'error estimates scaled by s0, maximum slope in Ruffini and
Bonazzola
        'Fig.(6), 2 * A(0), and B("infinity") = 1.

        d(1) = ABS((s2 - s1out(i)) / scales)
        d(2) = ABS((v2 - v1out(i)) / scalev)
        d(3) = ABS((A2 - A1out(i)) / scaleA)
        d(4) = ABS((B2 - B1out(i)) / scaleB)

        SORT4 d()
        delta = d(4)

        IF delta / eps > 1 THEN
                hnew = h * safety * (delta / eps) ^ (-.25)
                xout(i) = -1
                IF delta / eps > (safety / minshrink) ^ 4 THEN
                        hnew = minshrink * h
                END IF
        ELSE
```

```
        IF delta / eps > (safety / minboost) ^ 5 THEN
                hnew = minboost * h
                x = x1out(i)
                s = s1out(i): v = v1out(i)
                A = A1out(i): B = B1out(i)
        ELSEIF delta / eps < (safety / maxboost) ^ 5 THEN
                hnew = maxboost * h
                x = x1out(i)
                s = s1out(i): v = v1out(i)
                A = A1out(i): B = B1out(i)
        ELSE
                hnew = h * safety * (delta / eps) ^ (-.2)
                x = x1out(i)
                s = s1out(i): v = v1out(i)
                A = A1out(i): B = B1out(i)
        END IF

        xout(i) = x
        sout(i) = s: vout(i) = v
        Aout(i) = A: Bout(i) = B

END IF

        PRINT "h':h = ";
PRINT USING "##.#### "; hnew / h; x; s
h = hnew

'
'
'======== END OF ADAPTIVE STEP SIZE SUBSECTION ========
'======== AND THE RUNGE KUTTA SOLUTION SECTION ========
'=====================================================

'=================================================
'======== OMEGA BISECTION REDIRECT SECTION ========
'
'This section short circuits Runge Kutta when it becomes clear
'that OMEGA fails either low or high.
IF v > 0 THEN
        'low failure for OMEGA
        OMEGA1 = OMEGA
        OMEGA = (OMEGA1 + OMEGA2) / 2
        imax = i
        gogo = -1
        EXIT FOR
END IF
IF s < 0 THEN
        'high failure for OMEGA
        OMEGA2 = OMEGA
        OMEGA = (OMEGA1 + OMEGA2) / 2
        imax = i
```

```
                gogo = 1
                EXIT FOR
        END IF
        '
        '======== END OF OMEGA BISECTION REDIRECT SECTION ========
        '=========================================================

NEXT i          'Continue Runge Kutta solution.

PRINT "gogo = "; gogo

'Test whether successive OMEGA values meet the tolerance setting,
OMEGAtol.
'Short circuit the bisection process if tolerance test is met.
IF ABS(OMEGACOPY - OMEGA) < OMEGAtol THEN
        makepeace = p
        PRINT "makepeace @ "; p
        EXIT FOR
END IF

NEXT p          'Continue OMEGA bisection search.


'================================
'======== DATA REARRANGE ========
'
k = 1
FOR j = 1 TO imax
        IF xout(j) > 0 THEN
                xdata(k) = xout(j)
                sdata(k) = sout(j)
                vdata(k) = vout(j)
                Adata(k) = Aout(j)
                Bdata(k) = Bout(j)
                Mdata(k) = .5 * xout(j) * (1 - 1 / Aout(j))
                k = k + 1
        END IF
NEXT j
kmax = k - 1
Binf = Adata(kmax) * Bdata(kmax)
PRINT "There are "; kmax; "data points.  ";
'
'======== END DATA REARRANGE ========
'====================================


'=============================================================
'======== GRAPH SCALAR FIELD s(x) AND MASS FUNCTION M(x) ========
'
'               vps xdata(), sdata(), kmax
'               vps2 xdata(), Mdata(), kmax
```

```
'
'======== END SCALAR FIELD AND MASS FUNCTION GRAPH ========
'===========================================================

'====================================
'======== DATA OUTPUT SECTION ========
'
'File #2 holds solution parameters and the target OMEGA value.
PRINT #2, USING "##.######    "; eta;
PRINT #2, CHR$(9);
PRINT #2, USING "####.###### "; LAMBDA;
PRINT #2, CHR$(9);
PRINT #2, USING "##.####      "; eta * eta / LAMBDA;
PRINT #2, CHR$(9);
PRINT #2, USING "##.####      "; s0 / ss1;
PRINT #2, CHR$(9);
PRINT #2, USING "##.##^^^^    "; OMEGAtol;
PRINT #2, CHR$(9);
PRINT #2, USING "##.##################  "; OMEGA;
PRINT #2, CHR$(9);
PRINT #2, USING "##.###### "; Binf
PRINT #2, CHR$(9);
PRINT #2, USING "##.####^^^^ "; BubbleX(0, eta, LAMBDA)


'File #1 holds entire solutions.
PRINT #1, "bxrevise.bas output"
PRINT #1, USING "##.####^^^^ "; eps;
PRINT #1, CHR$(9);
PRINT #1, USING "##.####^^^^ "; CSNG(scales);
PRINT #1, CHR$(9);
PRINT #1, USING "##.####^^^^ "; CSNG(scalev);
PRINT #1, CHR$(9);
PRINT #1, USING "##.####^^^^ "; CSNG(scaleA);
PRINT #1, CHR$(9);
PRINT #1, USING "##.####^^^^ "; CSNG(scaleB);
PRINT #1, CHR$(9);
PRINT #1, USING "##.####^^^^ "; OMEGAtol;
PRINT #1, CHR$(9);
PRINT #1, USING "##.##        "; makepeace


PRINT #1, USING "##.##################    "; OMEGA;
PRINT #1, CHR$(9);
PRINT #1, USING "####.###### "; eta;
PRINT #1, CHR$(9);
PRINT #1, USING "####.###### "; LAMBDA;
PRINT #1, CHR$(9);
PRINT #1, USING "####.###### "; eta * eta / LAMBDA;
PRINT #1, CHR$(9);
```

```
PRINT #1, USING "##.####^^^^ "; ss1;
PRINT #1, CHR$(9);
PRINT #1, USING "##.####^^^^ "; s0 / ss1;
PRINT #1, CHR$(9);
PRINT #1, USING "##.####^^^^ "; BubbleX(0, eta, LAMBDA)


PRINT #1, USING "##.####^^^^ "; CSNG(x0);
PRINT #1, CHR$(9);
PRINT #1, USING "##.####^^^^ "; CSNG(s0);
PRINT #1, CHR$(9);
PRINT #1, USING "##.####^^^^ "; CSNG(v0);
PRINT #1, CHR$(9);
PRINT #1, USING "##.####^^^^ "; CSNG(A0);
PRINT #1, CHR$(9);
PRINT #1, USING "##.####^^^^ "; CSNG(B0);
PRINT #1, CHR$(9);
PRINT #1, USING "##.####^^^^ "; 0
LOCATE 1, 1: PRINT "  x           B(x)"
FOR k = 1 TO kmax
        PRINT USING "##.###      "; xdata(k); Bdata(k)
        PRINT #1, USING "##.####^^^^ "; CSNG(xdata(k));
        PRINT #1, CHR$(9);
        PRINT #1, USING "##.####^^^^ "; CSNG(sdata(k));
        PRINT #1, CHR$(9);
        PRINT #1, USING "##.####^^^^ "; CSNG(vdata(k));
        PRINT #1, CHR$(9);
        PRINT #1, USING "##.####^^^^ "; CSNG(Adata(k) - 1);
        PRINT #1, CHR$(9);
        PRINT #1, USING "##.####^^^^ "; CSNG(Bdata(k) - 1);
        PRINT #1, CHR$(9);
        PRINT #1, USING "##.####^^^^ "; CSNG(Mdata(k));
        PRINT #1, CHR$(9);
        PRINT #1, USING "##.####^^^^ "; CSNG((Adata(k) * Bdata(k)) - 1)
NEXT k
PRINT #1,
PRINT #1, "----------"
PRINT #1,


NEXT r          'Select another value of s0 for a new solution.
NEXT q          'Select another value of eta for a new range of
solutions.

CLOSE #1
CLOSE #2
END
```

```
'SUB PROCEDURES AND FUNCTIONS OF BXREVISE.BAS


FUNCTION BubbleX (s0, eta, LAMBDA)
'Dimensionless radius of the true vacuum bubble.
epsilon0 = Vbar(s0, eta, LAMBDA) + epsilon(eta, LAMBDA)
BubbleX = 6 * Sbar1(s0, eta, LAMBDA) / epsilon0
END FUNCTION

FUNCTION bump (eta, LAMBDA)
'Field value at the top of the bump in the potential Vbar.
xi = eta * eta / LAMBDA
IF xi >= .5 THEN
        bump = 1.5 * xi * (1 - SQR(1 - 4 / (9 * xi))) / eta
ELSE
        bump = 12.3
END IF
END FUNCTION

FUNCTION DA (x, s, v, A, B, OMEGA, eta, LAMBDA)
'First derivative of A(x)
IF x = 0 THEN
        DA = 0
ELSE
        DA1 = A * (1 - A) / x
        DA2 = (OMEGA * OMEGA / B + 1) * x * A * A * s * s
        DA3 = -2 * eta * x * A * A * s * s * s
        DA4 = LAMBDA * x * A * A * s * s * s * s / 2
        DA = DA1 + DA2 + DA3 + DA4 + x * v * v * A
END IF
END FUNCTION


FUNCTION DB (x, s, v, A, B, OMEGA, eta, LAMBDA)
'First derivative of B(x)
IF x = 0 THEN
        DB = 0
ELSE
        DB1 = B * (A - 1) / x
        DB2 = (-1 + OMEGA * OMEGA / B) * x * A * B * s * s
        DB3 = 2 * eta * x * A * B * s * s * s
        DB4 = -LAMBDA * x * A * B * s * s * s * s / 2
        DB = DB1 + DB2 + DB3 + DB4 + x * v * v * B
END IF
END FUNCTION
```

```
FUNCTION DS (x, s, v, A, B, OMEGA, eta, LAMBDA)
'First derivative of the scalar field
DS = v
END FUNCTION

FUNCTION DV (x, s, v, A, B, OMEGA, eta, LAMBDA, s0, B0)
'Second derivative of the scalar field...the scalar wave equation!
IF x = 0 THEN
        DV1 = (1 - OMEGA * OMEGA / B0) * s0 / 3 - eta * s0 * s0
        DV = DV1 + LAMBDA * s0 * s0 * s0 / 3
ELSE
        DV2 = -(2 / x + DB(x, s, v, A, B, OMEGA, eta, LAMBDA) / (2 * A))
* v
        DV3 = DA(x, s, v, A, B, OMEGA, eta, LAMBDA) * v / (2 * A)
        DV4 = (1 - OMEGA * OMEGA / B) * A * s - 3 * eta * A * s * s
        DV = DV2 + DV3 + DV4 + LAMBDA * A * s * s * s
END IF
END FUNCTION

FUNCTION epsilon (eta, LAMBDA)
'This block defines the difference between the false and the true vacua,
'epsilon.  (In my notes it is epsilon with a tilde!)

xi = eta ^ 2 / LAMBDA

IF xi > .5 THEN
        epsilon = -Vbar(truevac(eta, LAMBDA), eta, LAMBDA)
ELSE
        epsilon = 3030
END IF

END FUNCTION

SUB headr (eta, LAMBDA, OMEGA, s0, pass)
PRINT "eta, LAMBDA and xi ";
PRINT USING "###.#### "; eta; LAMBDA; eta * eta / LAMBDA
PRINT "bump, truevac and s(0)/bump: ";
PRINT USING "##.#######  "; bump(eta, LAMBDA); truevac(eta, LAMBDA); s0
/ bump(eta, LAMBDA)
PRINT "Energy difference and bubble radius: ";
PRINT USING "##.#######  "; epsilon(eta, LAMBDA); BubbleX(0, eta,
LAMBDA)
PRINT "OMEGA = "; OMEGA, "pass "; pass

END SUB
```

```
FUNCTION S11 (x, s, v, A, B, OMEGA, eta, LAMBDA, h)
'The S(i,j) are various shots in the Runge Kutta calculation.
'j = 1 denotes shot for calculating s(x)
'j = 2 "       "    "   "          v(x)
'j = 3 "       "    "   "          A(x)
'j = 4 "       "    "   "          B(x)
S11 = h * DS(x, s, v, A, B, OMEGA, eta, LAMBDA)
END FUNCTION

FUNCTION S12 (x, s, v, A, B, OMEGA, eta, LAMBDA, s0, B0, h)
S12 = h * DV(x, s, v, A, B, OMEGA, eta, LAMBDA, s0, B0)
END FUNCTION

FUNCTION S13 (x, s, v, A, B, OMEGA, eta, LAMBDA, h)
S13 = h * DA(x, s, v, A, B, OMEGA, eta, LAMBDA)
END FUNCTION

FUNCTION S14 (x, s, v, A, B, OMEGA, eta, LAMBDA, h)
S14 = h * DB(x, s, v, A, B, OMEGA, eta, LAMBDA)
END FUNCTION

FUNCTION S21 (x, s, v, A, B, OMEGA, eta, LAMBDA, sk11, sk12, sk13,
sk14, h)
S21 = h * DS(x + h / 2, s + sk11 / 2, v + sk12 / 2, A + sk13 / 2, B +
sk14 / 2, OMEGA, eta, LAMBDA)
END FUNCTION

FUNCTION S22 (x, s, v, A, B, OMEGA, eta, LAMBDA, s0, B0, sk11, sk12,
sk13, sk14, h)
S22 = h * DV(x + h / 2, s + sk11 / 2, v + sk12 / 2, A + sk13 / 2, B +
sk14 / 2, OMEGA, eta, LAMBDA, s0, B0)
END FUNCTION

FUNCTION S23 (x, s, v, A, B, OMEGA, eta, LAMBDA, sk11, sk12, sk13,
sk14, h)
S23 = h * DA(x + h / 2, s + sk11 / 2, v + sk12 / 2, A + sk13 / 2, B +
sk14 / 2, OMEGA, eta, LAMBDA)
END FUNCTION

FUNCTION S24 (x, s, v, A, B, OMEGA, eta, LAMBDA, sk11, sk12, sk13,
sk14, h)
S24 = h * DB(x + h / 2, s + sk11 / 2, v + sk12 / 2, A + sk13 / 2, B +
sk14 / 2, OMEGA, eta, LAMBDA)
END FUNCTION
```

```
FUNCTION S31 (x, s, v, A, B, OMEGA, eta, LAMBDA, sk21, sk22, sk23,
sk24, h)
S31 = h * DS(x + h / 2, s + sk21 / 2, v + sk22 / 2, A + sk23 / 2, B +
sk24 / 2, OMEGA, eta, LAMBDA)
END FUNCTION

FUNCTION S32 (x, s, v, A, B, OMEGA, eta, LAMBDA, s0, B0, sk21, sk22,
sk23, sk24, h)
S32 = h * DV(x + h / 2, s + sk21 / 2, v + sk22 / 2, A + sk23 / 2, B +
sk24 / 2, OMEGA, eta, LAMBDA, s0, B0)
END FUNCTION

FUNCTION S33 (x, s, v, A, B, OMEGA, eta, LAMBDA, sk21, sk22, sk23,
sk24, h)
S33 = h * DA(x + h / 2, s + sk21 / 2, v + sk22 / 2, A + sk23 / 2, B +
sk24 / 2, OMEGA, eta, LAMBDA)
END FUNCTION

FUNCTION S34 (x, s, v, A, B, OMEGA, eta, LAMBDA, sk21, sk22, sk23,
sk24, h)
S34 = h * DB(x + h / 2, s + sk21 / 2, v + sk22 / 2, A + sk23 / 2, B +
sk24 / 2, OMEGA, eta, LAMBDA)
END FUNCTION

FUNCTION S41 (x, s, v, A, B, OMEGA, eta, LAMBDA, sk31, sk32, sk33,
sk34, h)
S41 = h * DS(x + h, s + sk31, v + sk32, A + sk33, B + sk34, OMEGA, eta,
LAMBDA)
END FUNCTION

FUNCTION S42 (x, s, v, A, B, OMEGA, eta, LAMBDA, s0, B0, sk31, sk32,
sk33, sk34, h)
S42 = h * DV(x + h, s + sk31, v + sk32, A + sk33, B + sk34, OMEGA, eta,
LAMBDA, s0, B0)
END FUNCTION

FUNCTION S43 (x, s, v, A, B, OMEGA, eta, LAMBDA, sk31, sk32, sk33,
sk34, h)
S43 = h * DA(x + h, s + sk31, v + sk32, A + sk33, B + sk34, OMEGA, eta,
LAMBDA)
END FUNCTION

FUNCTION S44 (x, s, v, A, B, OMEGA, eta, LAMBDA, sk31, sk32, sk33,
sk34, h)
S44 = h * DB(x + h, s + sk31, v + sk32, A + sk33, B + sk34, OMEGA, eta,
LAMBDA)
END FUNCTION
```

```
FUNCTION Sbar1 (s0, eta, LAMBDA)
'Bounce action
bb2 = truevac(eta, LAMBDA)
Sbar1 = -.5 * (s0 ^ 2 - bb2 ^ 2) + (eta / 3) * (s0 ^ 3 - bb2 ^ 3)

END FUNCTION

SUB SORT4 (d())
FOR j = 2 TO 4
        dd = d(j)
        FOR i = j - 1 TO 1 STEP -1
                IF d(i) <= dd THEN
                        kk = 1
                        EXIT FOR
                ELSE
                        d(i + 1) = d(i)
                END IF
        NEXT i
        IF kk < 1 THEN i = 0
        d(i + 1) = dd
NEXT j
END SUB

SUB SORTN (aa(), n)

FOR j = 2 TO n
        dd = aa(j)
        FOR i = j - 1 TO 1 STEP -1
                IF aa(i) <= dd THEN
                        kk = 1
                        EXIT FOR
                ELSE
                        aa(i + 1) = aa(i)
                END IF
        NEXT i
        IF kk < 1 THEN i = 0
        aa(i + 1) = dd
NEXT j
END SUB

FUNCTION truevac (eta, LAMBDA)
'Field value at the true vacuum
xi = eta * eta / LAMBDA
IF xi >= .5 THEN
        truevac = 1.5 * xi * (1 + SQR(1 - 4 / (9 * xi))) / eta
ELSE
        truevac = 99
END IF

END FUNCTION
```

```
FUNCTION Vbar (s, eta, LAMBDA)
'Dimensionless 2-3-4 potential
Vbar = s ^ 2 - 2 * eta * s ^ 3 + .5 * LAMBDA * s ^ 4
END FUNCTION

SUB vps (xx(), ss(), size)
'Graphs the arrays (xx(), ss()) in the upper right corner.
FOR i = 1 TO size
      dd(i) = xx(i): cc(i) = ss(i)
NEXT i

SORTN dd(), size
SORTN cc(), size

Lx = dd(1): Ux = dd(size)
Ly = cc(1): Uy = cc(size)
ww = Ux - Lx: hh = Uy - Ux

CLS
SCREEN 2

VIEW (300, 5)-(600, 80), , 0

IF Ly < 0 THEN
        WINDOW (0, Ly)-(1.05 * Ux, 1.05 * Uy)
ELSE
        WINDOW (0, 0)-(1.05 * Ux, 1.05 * Uy)
END IF

LINE (0, 0)-(Ux, 0)
FOR i = 1 TO size
        PSET (xx(i), ss(i))
NEXT i

END SUB

SUB vps2 (xx(), ss(), size)
'Graphs the arrays (xx(), ss()) in lower right.
FOR i = 1 TO size
        dd(i) = xx(i): cc(i) = ss(i)
NEXT i

SORTN dd(), size
SORTN cc(), size

Lx = dd(1): Ux = dd(size)
Ly = cc(1): Uy = cc(size)
ww = Ux - Lx: hh = Uy - Ux


VIEW (300, 105)-(600, 180), , 0
```

```
IF Ly < 0 THEN
        WINDOW (0, Ly)-(1.05 * Ux, 1.05 * Uy)
ELSE
        WINDOW (0, 0)-(1.05 * Ux, 1.05 * Uy)
END IF

LINE (0, 0)-(Ux, 0)
FOR i = 1 TO size
        PSET (xx(i), ss(i))
NEXT i

END SUB
'end of bxrevise.bas
```

```
'ez_sys.bas
DECLARE FUNCTION Vbar# (s#, eta#, LAMBDA#)
DECLARE FUNCTION Sbar1# (s0#, eta#, LAMBDA#)
DECLARE FUNCTION BubbleX# (s0#, eta#, LAMBDA#)
DECLARE FUNCTION F# (x#)
DECLARE FUNCTION epsilon# (eta#, LAMBDA#)
DECLARE FUNCTION Rbubble# (eta#, LAMBDA#)
DECLARE FUNCTION bump# (eta#, LAMBDA#)
DECLARE FUNCTION truevac# (eta#, LAMBDA#)
DECLARE FUNCTION DVAC# (LAMBDA#, eta#)
DECLARE SUB vps2 (xx#(), ss#(), size#)
DECLARE SUB SORTN (aa#(), n#)
DECLARE SUB vps (xx#(), ss#(), size#)
DECLARE SUB SORT4 (d#())
DECLARE FUNCTION S41# (x#, s#, v#, A#, B#, OMEGA#, eta#, LAMBDA#, sk31#,
sk32#, sk33#, sk34#, h#)
DECLARE FUNCTION S42# (x#, s#, v#, A#, B#, OMEGA#, eta#, LAMBDA#, s0#,
B0#, sk31#, sk32#, sk33#, sk34#, h#)
DECLARE FUNCTION S43# (x#, s#, v#, A#, B#, OMEGA#, eta#, LAMBDA#, sk31#,
sk32#, sk33#, sk34#, h#)
DECLARE FUNCTION S44# (x#, s#, v#, A#, B#, OMEGA#, eta#, LAMBDA#, sk31#,
sk32#, sk33#, sk34#, h#)
DECLARE FUNCTION S31# (x#, s#, v#, A#, B#, OMEGA#, eta#, LAMBDA#, sk21#,
sk22#, sk23#, sk24#, h#)
DECLARE FUNCTION S32# (x#, s#, v#, A#, B#, OMEGA#, eta#, LAMBDA#, s0#,
B0#, sk21#, sk22#, sk23#, sk24#, h#)
DECLARE FUNCTION S33# (x#, s#, v#, A#, B#, OMEGA#, eta#, LAMBDA#, sk21#,
sk22#, sk23#, sk24#, h#)
DECLARE FUNCTION S34# (x#, s#, v#, A#, B#, OMEGA#, eta#, LAMBDA#, sk21#,
sk22#, sk23#, sk24#, h#)
DECLARE FUNCTION S21# (x#, s#, v#, A#, B#, OMEGA#, eta#, LAMBDA#, sk11#,
sk12#, sk13#, sk14#, h#)
DECLARE FUNCTION S22# (x#, s#, v#, A#, B#, OMEGA#, eta#, LAMBDA#, s0#,
B0#, sk11#, sk12#, sk13#, sk14#, h#)
DECLARE FUNCTION S23# (x#, s#, v#, A#, B#, OMEGA#, eta#, LAMBDA#, sk11#,
sk12#, sk13#, sk14#, h#)
DECLARE FUNCTION S24# (x#, s#, v#, A#, B#, OMEGA#, eta#, LAMBDA#, sk11#,
sk12#, sk13#, sk14#, h#)
DECLARE FUNCTION S11# (x#, s#, v#, A#, B#, OMEGA#, eta#, LAMBDA#, h#)
DECLARE FUNCTION S12# (x#, s#, v#, A#, B#, OMEGA#, eta#, LAMBDA#, s0#,
B0#, h#)
DECLARE FUNCTION S13# (x#, s#, v#, A#, B#, OMEGA#, eta#, LAMBDA#, h#)
DECLARE FUNCTION S14# (x#, s#, v#, A#, B#, OMEGA#, eta#, LAMBDA#, h#)
DECLARE FUNCTION DV# (x#, s#, v#, A#, B#, OMEGA#, eta#, LAMBDA#, s0#,
B0#)
DECLARE FUNCTION DS# (x#, s#, v#, A#, B#, OMEGA#, eta#, LAMBDA#)
DECLARE FUNCTION DB# (x#, s#, v#, A#, B#, OMEGA#, eta#, LAMBDA#)
DECLARE FUNCTION DA# (x#, s#, v#, A#, B#, OMEGA#, eta#, LAMBDA#)
DEFDBL A-Z
```

```
'The several arrays for my Runge-Kutta procedure.
DIM SHARED x1out(0 TO 500)
DIM SHARED s1out(0 TO 500)
DIM SHARED v1out(0 TO 500)
DIM SHARED A1out(0 TO 500)
DIM SHARED B1out(0 TO 500)
DIM SHARED Mdata(0 TO 500)

DIM SHARED dd(1 TO 500): DIM SHARED cc(1 TO 500)
DIM SHARED xx(1 TO 500): DIM SHARED ss(1 TO 500)
DIM SHARED aa(1 TO 500)

ff$ = "a:\ezss284.pr"
'This file will be used for graphing on Power Mac/Clarisworks
gg$ = "a:\sys284.pp"
'This file will be input for actntrap.bas

OPEN ff$ FOR OUTPUT AS #1
OPEN gg$ FOR OUTPUT AS #2

PRINT #1, ff$
PRINT #1, "Tab delimited output from ez-sys.bas", DATE$, TIME$
PRINT #1,

PRINT #2, gg$
PRINT #2, "Straight output from ez-sys.bas", DATE$, TIME$
PRINT #2,


'These data will come from newdata().prn summary.
OMEGAbar = .8672246631207673#
Binf = 1.167474#

'energy parameters {OMEGA,eta,LAMBDA}
CONST LAMBDA = 10
eta = SQR(LAMBDA * (.5600000000000001#))
'Setting eta = 0 will compare with Colpi, et al., Fig.(3)
'Setting LAMBDA = 0 will compare with Ruffini and Bonazzola figures.

'BOUNDARY CONDITIONS: s(0),v(0),A(0),B(0).
'Central redshift is OMEGA^2/B(0); adjust so that B("infinity") -> 1.
ss1 = bump(eta, LAMBDA): ss2 = truevac(eta, LAMBDA)

s0 = .99# * ss1: B0 = 1 / Binf
v0 = 0: A0 = 1: x0 = 0

'Runge-Kutta fixed step size parameters.
h = BubbleX(0, eta, LAMBDA) / 100
'h = .070644#
scales = s0: scalev = -.7: scaleA = 4: scaleB = .1
```

```
x = x0: s = s0: v = v0: A = A0: B = B0
x1out(0) = x0: s1out(0) = s0: v1out(0) = v0
A1out(0) = A0: B1out(0) = B0
OMEGA = OMEGAbar / SQR(Binf)

CLS

sratio = s0 / ss1
PRINT "eta, LAMBDA and xi ";
PRINT USING "###.#### "; eta; LAMBDA; eta * eta / LAMBDA
PRINT "bump, truevac and s(0)/bump: ";
PRINT USING "##.#######  "; ss1; ss2; sratio
PRINT "Energy difference and bubble radius: ";
PRINT USING "##.#######  "; epsilon(eta, LAMBDA); BubbleX(0, eta,
LAMBDA)
PRINT "OMEGA = "; OMEGA
i = 0
'FOR i = 1 TO maxsteps
DO UNTIL s < 0 OR v > 0 OR i = 100
        i = i + 1

        'The U(i,j) are the parts of the Runge Kutta procedure
        U11 = S11(x, s, v, A, B, OMEGA, eta, LAMBDA, h)
        U12 = S12(x, s, v, A, B, OMEGA, eta, LAMBDA, s0, B0, h)
        U13 = S13(x, s, v, A, B, OMEGA, eta, LAMBDA, h)
        U14 = S14(x, s, v, A, B, OMEGA, eta, LAMBDA, h)

        U21 = S21(x, s, v, A, B, OMEGA, eta, LAMBDA, U11, U12, U13, U14,
h)
        U22 = S22(x, s, v, A, B, OMEGA, eta, LAMBDA, s0, B0, U11, U12,
U13, U14, h)
        U23 = S23(x, s, v, A, B, OMEGA, eta, LAMBDA, U11, U12, U13, U14,
h)
        U24 = S24(x, s, v, A, B, OMEGA, eta, LAMBDA, U11, U12, U13, U14,
h)

        U31 = S31(x, s, v, A, B, OMEGA, eta, LAMBDA, U21, U22, U23, U24,
h)
        U32 = S32(x, s, v, A, B, OMEGA, eta, LAMBDA, s0, B0, U21, U22,
U23, U24, h)
        U33 = S33(x, s, v, A, B, OMEGA, eta, LAMBDA, U21, U22, U23, U24,
h)
        U34 = S34(x, s, v, A, B, OMEGA, eta, LAMBDA, U21, U22, U23, U24,
h)

        U41 = S41(x, s, v, A, B, OMEGA, eta, LAMBDA, U31, U32, U33, U34,
h)
        U42 = S42(x, s, v, A, B, OMEGA, eta, LAMBDA, s0, B0, U31, U32,
U33, U34, h)
        U43 = S43(x, s, v, A, B, OMEGA, eta, LAMBDA, U31, U32, U33, U34,
h)
```

```
        U44 = S44(x, s, v, A, B, OMEGA, eta, LAMBDA, U31, U32, U33, U34,
h)

        'The arrays s1out(), etc. are the solutions.
        s1out(i) = s + (U11 + 2 * U21 + 2 * U31 + U41) / 6
        v1out(i) = v + (U12 + 2 * U22 + 2 * U32 + U42) / 6
        A1out(i) = A + (U13 + 2 * U23 + 2 * U33 + U43) / 6
        B1out(i) = B + (U14 + 2 * U24 + 2 * U34 + U44) / 6
        x1out(i) = x + h


        x = x1out(i)
        s = s1out(i)
        v = v1out(i)
        A = A1out(i)
        B = B1out(i)
        PRINT i, x
'NEXT i
LOOP
maxsteps = i - 1
PRINT "Maxsteps = "; maxsteps, gg$
Mdata(0) = 0
FOR j = 1 TO maxsteps
        Mdata(j) = .5 * x1out(j) * (1 - 1 / A1out(j))
NEXT j

FOR i = maxsteps + 1 TO 100
        'This loop pads out the data files with ones and zeros.
        x1out(i) = h * i
        s1out(i) = 0
        v1out(i) = 0
        A1out(i) = 1
        B1out(i) = 1
        Mdata(i) = Mdata(maxsteps)
NEXT i

PRINT #1, eta; CHR$(9); LAMBDA; CHR$(9); sratio; CHR$(9); OMEGA;
CHR$(9);
PRINT #1, maxsteps

FOR k = 0 TO 100
        PRINT #1, USING "##.###       "; x1out(k);
        PRINT #1, CHR$(9);
        PRINT #1, USING "##.#####^^^^ "; CSNG(s1out(k));
        PRINT #1, CHR$(9);
        PRINT #1, USING "##.#####^^^^ "; CSNG(v1out(k));
        PRINT #1, CHR$(9);
        PRINT #1, USING "##.######### "; A1out(k);
        PRINT #1, CHR$(9);
        PRINT #1, USING "##.######### "; B1out(k);
        PRINT #1, CHR$(9);
```

```
        PRINT #1, USING "##.#####^^^^ "; CSNG(Mdata(k))
NEXT k

PRINT #2, eta, LAMBDA, sratio, OMEGA, maxsteps

FOR k = 0 TO 100
        PRINT #2, USING "##.###        "; x1out(k);
        PRINT #2, USING "##.#####^^^^ "; CSNG(s1out(k));
        PRINT #2, USING "##.#####^^^^ "; CSNG(v1out(k));
        PRINT #2, USING "##.######### "; A1out(k);
        PRINT #2, USING "##.######### "; B1out(k);
        PRINT #2, USING "##.#####^^^^ "; CSNG(Mdata(k))
NEXT k

'vps x1out(), s1out(), maxsteps

END



'SUB PROCEDURES AND FUNCTIONS OF EZ_SYS.BAS



FUNCTION BubbleX (s0, eta, LAMBDA)
epsilon0 = Vbar(s0, eta, LAMBDA) + epsilon(eta, LAMBDA)
BubbleX = 6 * Sbar1(s0, eta, LAMBDA) / epsilon0
END FUNCTION

FUNCTION bump (eta, LAMBDA)
xi = eta * eta / LAMBDA
IF xi >= .5 THEN
        bump = 1.5 * xi * (1 - SQR(1 - 4 / (9 * xi))) / eta
ELSE
        bump = 12.3
END IF
END FUNCTION

FUNCTION DA (x, s, v, A, B, OMEGA, eta, LAMBDA)
IF x = 0 THEN
        DA = 0
ELSE
        DA1 = A * (1 - A) / x
        DA2 = (OMEGA * OMEGA / B + 1) * x * A * A * s * s
        DA3 = -2 * eta * x * A * A * s * s * s
        DA4 = LAMBDA * x * A * A * s * s * s * s / 2
        DA = DA1 + DA2 + DA3 + DA4 + x * v * v * A
END IF
END FUNCTION
```

```
FUNCTION DB (x, s, v, A, B, OMEGA, eta, LAMBDA)
IF x = 0 THEN
        DB = 0
ELSE
        DB1 = B * (A - 1) / x
        DB2 = (-1 + OMEGA * OMEGA / B) * x * A * B * s * s
        DB3 = 2 * eta * x * A * B * s * s * s
        DB4 = -LAMBDA * x * A * B * s * s * s * s / 2
        DB = DB1 + DB2 + DB3 + DB4 + x * v * v * B
END IF
END FUNCTION

FUNCTION DS (x, s, v, A, B, OMEGA, eta, LAMBDA)
DS = v
END FUNCTION


FUNCTION DV (x, s, v, A, B, OMEGA, eta, LAMBDA, s0, B0)
IF x = 0 THEN
        DV1 = (1 - OMEGA * OMEGA / B0) * s0 / 3 - eta * s0 * s0
        DV = DV1 + LAMBDA * s0 * s0 * s0 / 3
ELSE
        DV2 = -(2 / x + DB(x, s, v, A, B, OMEGA, eta, LAMBDA) / (2 * A))
* v
        DV3 = DA(x, s, v, A, B, OMEGA, eta, LAMBDA) * v / (2 * A)
        DV4 = (1 - OMEGA * OMEGA / B) * A * s - 3 * eta * A * s * s
        DV = DV2 + DV3 + DV4 + LAMBDA * A * s * s * s
END IF
END FUNCTION

FUNCTION epsilon (eta, LAMBDA)
'This block defines the difference between the false and the true vacua,
'epsilon.  (In my notes it is epsilon with a tilde!)
epsilon = -Vbar(truevac(eta, LAMBDA), eta, LAMBDA)
END FUNCTION

FUNCTION S11 (x, s, v, A, B, OMEGA, eta, LAMBDA, h)
S11 = h * DS(x, s, v, A, B, OMEGA, eta, LAMBDA)
END FUNCTION

FUNCTION S12 (x, s, v, A, B, OMEGA, eta, LAMBDA, s0, B0, h)
S12 = h * DV(x, s, v, A, B, OMEGA, eta, LAMBDA, s0, B0)
END FUNCTION

FUNCTION S13 (x, s, v, A, B, OMEGA, eta, LAMBDA, h)
S13 = h * DA(x, s, v, A, B, OMEGA, eta, LAMBDA)
END FUNCTION

FUNCTION S14 (x, s, v, A, B, OMEGA, eta, LAMBDA, h)
S14 = h * DB(x, s, v, A, B, OMEGA, eta, LAMBDA)
END FUNCTION
```

```
FUNCTION S21 (x, s, v, A, B, OMEGA, eta, LAMBDA, sk11, sk12, sk13,
sk14, h)
S21 = h * DS(x + h / 2, s + sk11 / 2, v + sk12 / 2, A + sk13 / 2, B +
sk14 / 2, OMEGA, eta, LAMBDA)
END FUNCTION

FUNCTION S22 (x, s, v, A, B, OMEGA, eta, LAMBDA, s0, B0, sk11, sk12,
sk13, sk14, h)
S22 = h * DV(x + h / 2, s + sk11 / 2, v + sk12 / 2, A + sk13 / 2, B +
sk14 / 2, OMEGA, eta, LAMBDA, s0, B0)
END FUNCTION

FUNCTION S23 (x, s, v, A, B, OMEGA, eta, LAMBDA, sk11, sk12, sk13,
sk14, h)
S23 = h * DA(x + h / 2, s + sk11 / 2, v + sk12 / 2, A + sk13 / 2, B +
sk14 / 2, OMEGA, eta, LAMBDA)
END FUNCTION


FUNCTION S24 (x, s, v, A, B, OMEGA, eta, LAMBDA, sk11, sk12, sk13,
sk14, h)
S24 = h * DB(x + h / 2, s + sk11 / 2, v + sk12 / 2, A + sk13 / 2, B +
sk14 / 2, OMEGA, eta, LAMBDA)
END FUNCTION

FUNCTION S31 (x, s, v, A, B, OMEGA, eta, LAMBDA, sk21, sk22, sk23,
sk24, h)
S31 = h * DS(x + h / 2, s + sk21 / 2, v + sk22 / 2, A + sk23 / 2, B +
sk24 / 2, OMEGA, eta, LAMBDA)
END FUNCTION

FUNCTION S32 (x, s, v, A, B, OMEGA, eta, LAMBDA, s0, B0, sk21, sk22,
sk23, sk24, h)
S32 = h * DV(x + h / 2, s + sk21 / 2, v + sk22 / 2, A + sk23 / 2, B +
sk24 / 2, OMEGA, eta, LAMBDA, s0, B0)
END FUNCTION

FUNCTION S33 (x, s, v, A, B, OMEGA, eta, LAMBDA, sk21, sk22, sk23,
sk24, h)
S33 = h * DA(x + h / 2, s + sk21 / 2, v + sk22 / 2, A + sk23 / 2, B +
sk24 / 2, OMEGA, eta, LAMBDA)
END FUNCTION

FUNCTION S34 (x, s, v, A, B, OMEGA, eta, LAMBDA, sk21, sk22, sk23,
sk24, h)
S34 = h * DB(x + h / 2, s + sk21 / 2, v + sk22 / 2, A + sk23 / 2, B +
sk24 / 2, OMEGA, eta, LAMBDA)
END FUNCTION
```

```
FUNCTION S41 (x, s, v, A, B, OMEGA, eta, LAMBDA, sk31, sk32, sk33,
sk34, h)
S41 = h * DS(x + h, s + sk31, v + sk32, A + sk33, B + sk34, OMEGA, eta,
LAMBDA)
END FUNCTION

FUNCTION S42 (x, s, v, A, B, OMEGA, eta, LAMBDA, s0, B0, sk31, sk32,
sk33, sk34, h)
S42 = h * DV(x + h, s + sk31, v + sk32, A + sk33, B + sk34, OMEGA, eta,
LAMBDA, s0, B0)
END FUNCTION

FUNCTION S43 (x, s, v, A, B, OMEGA, eta, LAMBDA, sk31, sk32, sk33,
sk34, h)
S43 = h * DA(x + h, s + sk31, v + sk32, A + sk33, B + sk34, OMEGA, eta,
LAMBDA)
END FUNCTION

FUNCTION S44 (x, s, v, A, B, OMEGA, eta, LAMBDA, sk31, sk32, sk33,
sk34, h)
S44 = h * DB(x + h, s + sk31, v + sk32, A + sk33, B + sk34, OMEGA, eta,
LAMBDA)
END FUNCTION

FUNCTION Sbar1 (s0, eta, LAMBDA)
dd2 = truevac(eta, LAMBDA)
Sbar1 = -.5 * (s0 ^ 2 - dd2 ^ 2) + (eta / 3) * (s0 ^ 3 - dd2 ^ 3)
END FUNCTION

SUB SORT4 (d())
FOR j = 2 TO 4
        dd = d(j)
        FOR i = j - 1 TO 1 STEP -1
                IF d(i) <= dd THEN
                        kk = 1
                        EXIT FOR
                ELSE
                        d(i + 1) = d(i)
                END IF
        NEXT i
        IF kk < 1 THEN i = 0
        d(i + 1) = dd
NEXT j
END SUB

SUB SORTN (aa(), n)

FOR j = 2 TO n
        dd = aa(j)
        FOR i = j - 1 TO 1 STEP -1
                IF aa(i) <= dd THEN
```

```
                        kk = 1
                        EXIT FOR
                ELSE
                        aa(i + 1) = aa(i)
                END IF
        NEXT i
        IF kk < 1 THEN i = 0
        aa(i + 1) = dd
NEXT j

END SUB

FUNCTION truevac (eta, LAMBDA)
xi = eta * eta / LAMBDA
IF xi >= .5 THEN
        truevac = 1.5 * xi * (1 + SQR(1 - 4 / (9 * xi))) / eta
ELSE
        truevac = 99
END IF

END FUNCTION

FUNCTION Vbar (s, eta, LAMBDA)
'Scalar potential
Vbar = s ^ 2 - 2 * eta * s ^ 3 + .5 * LAMBDA * s ^ 4
END FUNCTION

SUB vps (xx(), ss(), size)
FOR i = 1 TO size
        dd(i) = xx(i): cc(i) = ss(i)
NEXT i

SORTN dd(), size
SORTN cc(), size

Lx = dd(1): Ux = dd(size)
Ly = cc(1): Uy = cc(size)
ww = Ux - Lx: hh = Uy - Ux

CLS
SCREEN 2

VIEW (300, 5)-(600, 80), , 0

IF Ly < 0 THEN
        WINDOW (0, Ly)-(1.05 * Ux, 1.05 * Uy)
ELSE
        WINDOW (0, 0)-(1.05 * Ux, 1.05 * Uy)
END IF

LINE (0, 0)-(Ux, 0)
```

```
FOR i = 1 TO size
        PSET (xx(i), ss(i))
NEXT i

END SUB

SUB vps2 (xx(), ss(), size)
FOR i = 1 TO size
        dd(i) = xx(i): cc(i) = ss(i)
NEXT i
SORTN dd(), size
SORTN cc(), size
Lx = dd(1): Ux = dd(size)
Ly = cc(1): Uy = cc(size)
ww = Ux - Lx: hh = Uy - Ux
VIEW (300, 105)-(600, 180), , 0
IF Ly < 0 THEN
        WINDOW (0, Ly)-(1.05 * Ux, 1.05 * Uy)
ELSE
        WINDOW (0, 0)-(1.05 * Ux, 1.05 * Uy)
END IF
LINE (0, 0)-(Ux, 0)
FOR i = 1 TO size
        PSET (xx(i), ss(i))
NEXT i
END SUB
```

```
'actntrap.bas
DECLARE FUNCTION BubbleX# (ss0#, eta#, LAMBDA#)
DECLARE FUNCTION truevac# (eta#, LAMBDA#)
DECLARE FUNCTION Sbar1# (ss0#, eta#, LAMBDA#)
DECLARE FUNCTION epsilonbar# (ss0#, eta#, LAMBDA#)
DECLARE FUNCTION Vbar# (s#, eta#, LAMBDA#)
DEFDBL A-Z
CLS
maxcuts = 50
ff$ = "a:\sys102.pp"
OPEN ff$ FOR INPUT AS #1
INPUT #1, a$, b$, c$
INPUT #1, eta, LAMBDA, sratio, OMEGA, maxsteps

DIM x(0 TO 100): DIM s(0 TO 100): DIM v(0 TO 100)
DIM a(0 TO 100)
DIM b(0 TO maxcuts): DIM xq(0 TO maxcuts): DIM jj(0 TO maxcuts)

INPUT #1, x(0), s(0), v(0), a0, b0, m0
PRINT USING "###.###### "; x(0); s(0); v(0); a0; b0; m0

FOR i = 1 TO 100
        INPUT #1, x(i), s(i), v(i), aa, bb, mm
        PRINT USING "###.###### "; x(i); s(i); v(i)
NEXT i



'These two step size lines can be adjusted, the first being the
'standard default value of X/100.
hh = BubbleX(0, eta, LAMBDA) / 100
'hh = .070644#
FOR i = 0 TO 100
        a(i) = (x(i)) ^ 2 * (OMEGA ^ 2 * (s(i)) ^ 2 + (v(i)) ^ 2 +
Vbar(s(i), eta, LAMBDA))
NEXT i

xq(0) = hh * 100: jj(0) = 100
betastep = hh * 100 / maxcuts
FOR i = 1 TO maxcuts - 1
        beta = SQR((hh * 100) ^ 2 - (betastep * i) ^ 2)
        j = FIX(beta / hh)
        PRINT j;
        PRINT USING " ##.## "; x(j);
        PRINT "..";
        jj(i) = j
        xq(i) = x(j)
NEXT i
PRINT
FOR j = 0 TO maxcuts - 1
        q = jj(j)
```

```
        accumulate = hh * .5 * (a(0) + a(q))
        FOR i = 1 TO q - 1
                accumulate = accumulate + hh * a(i)
        NEXT i
        PRINT j; "Number of steps:"; q;
        PRINT USING "-->##.########## "; accumulate
        b(j) = accumulate
NEXT j

actionaccumulate = .5 * betastep * (b(0) + b(maxcuts - 1))
FOR j = 1 TO maxcuts - 2
        actionaccumulate = actionaccumulate + betastep * b(j)
NEXT j
PRINT a$
PRINT b$
PRINT c$
PRINT "specs: "; eta, LAMBDA, sratio
PRINT "       "; OMEGA, maxsteps
PRINT ff$
PRINT "Boson star action ="; actionaccumulate / 2
ratio1 = (epsilonbar(0, eta, LAMBDA)) ^ 3 / (Sbar1(0, eta, LAMBDA)) ^ 4
ratio = actionaccumulate * ratio1 / (216 * ATN(1))
PRINT "Bubble action:"; 108 * ATN(1) / ratio1
PRINT "Bounce action:"; Sbar1(0, eta, LAMBDA)
PRINT "Energy difference:"; epsilonbar(0, eta, LAMBDA)
PRINT "Action ratio:"; ratio
END



'SUB PROCEDURES AND FUNCTIONS FOR ACTNTRAP.BAS


FUNCTION BubbleX (ss0, eta, LAMBDA)
BubbleX = 6 * Sbar1(ss0, eta, LAMBDA) / epsilonbar(ss0, eta, LAMBDA)
END FUNCTION

FUNCTION epsilonbar (ss0, eta, LAMBDA)
epsilonbar = Vbar(ss0, eta, LAMBDA) - Vbar(truevac(eta, LAMBDA), eta,
LAMBDA)
END FUNCTION

FUNCTION Sbar1 (ss0, eta, LAMBDA)
ss2 = truevac(eta, LAMBDA)
Sbar1 = ABS(.5 * (ss0 ^ 2 - ss2 ^ 2) - (eta / 3) * (ss0 ^ 3 - ss2 ^ 3))
END FUNCTION
```

```
FUNCTION truevac (eta, LAMBDA)
xi = eta * eta / LAMBDA
IF xi >= .5 THEN
        truevac = 1.5 * xi * (1 + SQR(1 - 4 / (9 * xi))) / eta
ELSE
        truevac = 99
END IF

END FUNCTION
FUNCTION Vbar (s, eta, LAMBDA)
Vbar = s ^ 2 - 2 * eta * s ^ 3 + .5 * LAMBDA * s ^ 4
END FUNCTION
```